

## N O T I C E

THIS DOCUMENT HAS BEEN REPRODUCED FROM  
MICROFICHE. ALTHOUGH IT IS RECOGNIZED THAT  
CERTAIN PORTIONS ARE ILLEGIBLE, IT IS BEING RELEASED  
IN THE INTEREST OF MAKING AVAILABLE AS MUCH  
INFORMATION AS POSSIBLE

**BOEING**

# Solar Power Satellite System Definition Study

SPS FIBER OPTIC  
LINK ASSESSMENT  
FINAL REPORT

**BOEING**

NASA CR-  
160575

N80-22780

(NASA-CR-160575) SOLAR POWER SATELLITE  
(SPS) FIBER OPTIC LINK ASSESSMENT Final  
Report (Boeing Aerospace Co., Seattle,  
Wash.) 102 p HC A06/MF A01

CSCL 10A

Unclassified  
18029

G3/44

NAS9-15636-A



**D180-25888-1**

**SPS FIBER OPTIC LINK ASSESSMENT**

Prepared for the NASA Lyndon B. Johnson Space Center  
Houston, Texas 77058  
Under Contract No. NAS9-15636A  
Project Monitor: Jack W. Seyl

Project Engineer: Thomas A. Lindsay  
Project Manager: Ervin J. Nalos

BOEING AEROSPACE COMPANY  
P.O. Box 3999, Seattle, WA 98124  
31 January 1980

## TABLE OF CONTENTS

	<u>PAGE</u>
LIST OF FIGURES	iii
SUMMARY	v
 1.0 INTRODUCTION	1
1.1 SPS PHASE CONTROL SYSTEM	1
1.2 TECHNICAL OBJECTIVES	3
1.3 TASK ORGANIZATION	3
2.0 FIBER OPTIC COMPONENT INVESTIGATION	8
2.1 FIBER INVESTIGATION	8
2.1.1 Thermal Effects in Fibers	14
2.1.2 Fiber Selection	16
2.2 EMITTER INVESTIGATION	17
2.3 DETECTOR INVESTIGATION	19
3.0 60 MHz THERMAL PHASE SENSITIVITY TESTS	24
3.1 TEST RESULTS	27
4.0 980 MHz LINK DESIGN	32
4.1 EMITTER MODULE DESIGN	32
4.2 DETECTOR MODULE DESIGN	35
4.3 FIBER OPTIC CABLE AND CONNECTOR SELECTION	39
5.0 980 MHz ONE-WAY LINK TESTS	44
5.1 TEST RESULTS	44
6.0 980 MHz TWO-WAY LINK DEVELOPMENT	50
6.1 EMITTER OPERATING CONDITIONS	50
6.2 DETECTOR OPERATING CONDITIONS	52
6.3 980 MHz DUAL LINK PHASE MATCHING	61
7.0 980 MHz TWO-WAY LINK CHARACTERISTICS	63
7.1 INPUT AND OUTPUT LEVEL SPECIFICATIONS	63
7.2 PHASE MISMATCH VERSUS INPUT PARAMETERS	63
8.0 CONCLUSIONS AND RECOMMENDATIONS	70
 LIST OF REFERENCES	73
APPENDIX I	
APPENDIX II	

**D180-25888-1**

**LIST OF FIGURES**

<u>FIGURE #</u>	<u>TITLE</u>	<u>PAGE</u>
1.1	SPS Reference Phase Control System	2
1.2	Comparison of Coaxial and F/O Cables	4
1.3	SPS Fiber Optic Dual Link System	5
2.1	Fiber Optic Component Investigation Summary	9
2.2	Components Selected for Further Investigation	10
2.3	Summary of Manufacturer's Fiber Data	15
2.4	Injection Laser Diode Performance Data	20
2.5	Avalanche Photo Diode Performance Data	23
3.1	60 MHz Phase Test - Block Diagram	25
3.2	Photograph of 60 MHz Phase Test	26
3.3	Specifications of Test Fibers	24
3.4	60 MHz Phase Versus Temperature Tests	28
3.5	Phase Versus Temperature for Corning Fibers	29
4.1	980 MHz Module Schematic Diagrams	33
4.2	ILD Thermoelectric Cooler Schematic	36
4.3	Emitter Module - Frontal View	37
4.4	Emitter Module - Internal View	38
4.5	Detector Module - External View	40
4.6	Detector Module - Internal View	41
4.7	Siecor 2-Fiber Cable Specifications	42
5.1	Initial SPS 980 MHz Fiber Optic Link Test	45
5.2	980 MHz Phase Versus Temperature Test	46

LIST OF FIGURES (Continued)

<u>FIGURE #</u>	<u>TITLE</u>	<u>PAGE</u>
5.3	980 MHz Attenuation Versus Temperature Tests	
6.1	Injection Laser Diode Bias Curves	51
6.2	Avalanche Photodiode Bias Data	53
6.3	Detector Module Phase Test	55
6.4	Detector Module Phase Sensitivity	56
6.5	Phase Matching of 980 MHz Two-Way Link	57
7.1	Dual Link Characterization Test Setup	64
7.2	980 MHz Two-Way Link Operating Characteristics	65
7.3	Phase Mismatch Versus Emitter Bias	67
7.4	Phase Mismatch Versus Detector Bias	68
7.5	Phase Mismatch Versus Emitter RF Drive	69

SUMMARY

A feasibility demonstration of a 980 MHz Fiber Optic Link for the Solar Power Satellite Phase Reference Distribution System was accomplished. A dual fiber-optic link suitable for a phase distribution frequency of 980 MHz was built and tested. The major link components include single mode injection laser diodes, avalanche photodiodes, and multimode high bandwidth fibers. Signal throughput was demonstrated to be stable and of high quality in all cases. For a typical SPS link length of 200 meters, the transmitted phase at 980 MHz varies approximately 2.5 degrees for every °C of fiber temperature change. This rate is acceptable because of the link length compensation feature of the phase control design.

## 1.0 INTRODUCTION

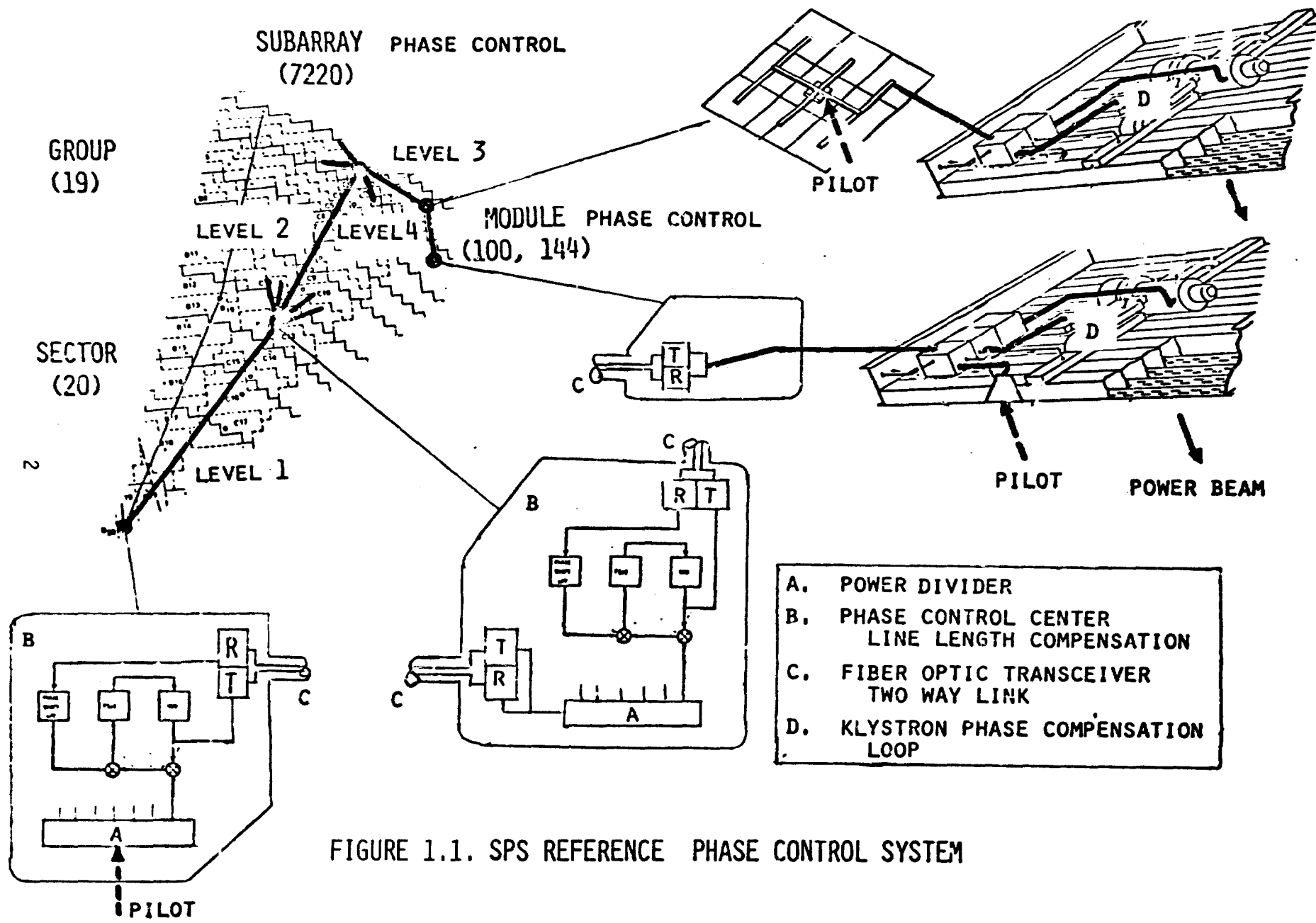
The purpose of the proposed Solar Power Satellite (SPS) is to convert solar energy to microwave energy which will be beamed down to an earth-based receiving station, converted, and fed to a power distribution grid. The downlink power transmission beam is formed by a phased array of microwave emitters, and the beam formation integrity is assured by the faithful distribution of a reference phase throughout the spaceborne array. One approach which offers possible advantages towards phase stability under large temperature variations, low EMI, low mass, and large length-bandwidth products, involves the use of fiber optic technology for phase signal distribution.

### 1.1 SPS PHASE CONTROL SYSTEM

The present approach for beam control is to form a phased array with approximately one hundred thousand microwave transmission modules. Figure 1.1 represents the proposed spaceborne configuration. The reference system has been configured by the LinCom Corporation. A pilot phase signal will be generated and injected into the phase reference distribution system as shown in the lower left corner of the figure. It is to be split and successively transmitted through four levels of distribution to each subarray. A control signal will be transmitted from the earth-based receiving station to the satellite, and each microwave module will detect the control signal phase as it is received, compare it with the reference phase, and simultaneously generate the power transmission signal with the conjugate phase angle. This scheme forces all of the modules' signals to be in phase towards the earth receiving station, regardless of the tilt of each satellite module.

Since each microwave module is to be phase-controlled to within  $\pm 10^\circ$ , the individual path lengths for each reference link must be well matched and stabilized if the proper phasing is to be maintained. Large thermal vari-

D180-25888-1



ations are expected across the SPS array, and thus, it is imperative that the phase distribution medium exhibits propagation properties that are highly predictable. The phase stability versus temperature for optical fibers approaches that of the highest quality phase-stable coaxial cable as is summarized in Figure 1.2.

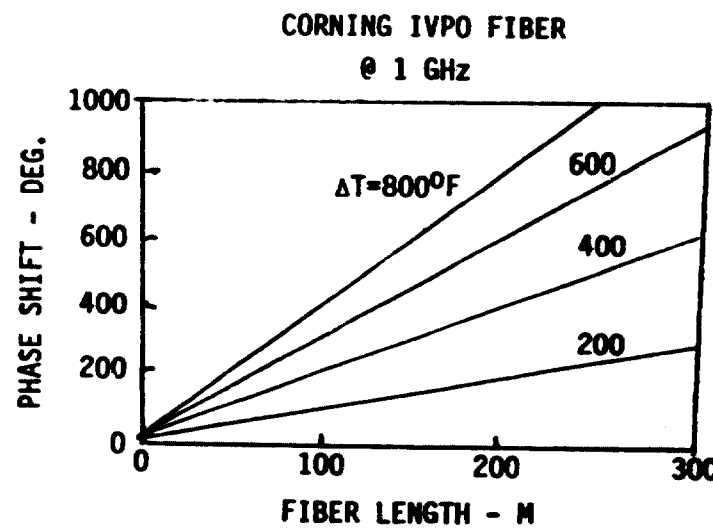
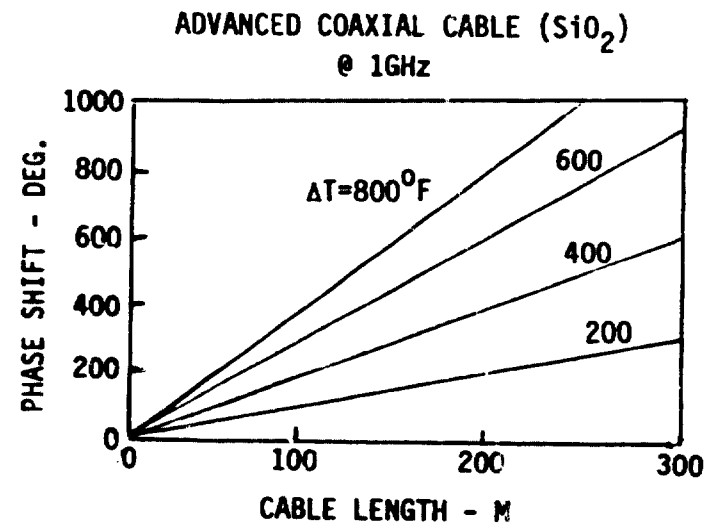
In the proposed configuration, a two-way link is to be built for each major distribution path such that any phase errors due to path length variations may be detected and compensated. Referring to Figures 1.1 and 1.3, it is shown that the transmitted phase is detected and returned to the source VCO for monitoring and correction, if required. Identical optical fibers are to be juxtaposed for the entire length of each phase link to provide accurate matching and tracking of the thermally induced phase effects. Figure 1.3 represents a NASA test setup geared towards investigating the validity of the SPS phase compensation system.

The outer level of the phase distribution network comprises over 90% of the network segments. At this level, the average link length is less than 10 meters, and since some tolerance is allowed, it may be possible to eliminate the return links as the phase shift will average less than 0.125 degrees per °C of fiber temperature.

The phase reference distribution system, in addition to being temperature stable, needs to be highly immune to EMI/RFI, which is expected to be severe in the vicinity of the SPS microwave array. Fiber optics are completely immune to EMI/RFI, and also offer theoretical length-bandwidth products of several gigahertz-kilometers, which is significant considering the proposed link lengths and frequencies involved. Fiber optics can also present savings in mass, physical size, and eventually, cost.

## 1.2 TECHNICAL OBJECTIVES

The purpose of this effort was to demonstrate the feasibility of a fiber optic link at 980 MHz for SPS application. The specific tasks were to:



ADVANTAGES

- o RADIATION PROOF

DISADVANTAGES

- o SEMI RIGID
- o WEIGHT

ADVANTAGES

- o EM. PROOF
- o LOW WEIGHT
- o LOW VOLUME
- o FLEXIBILITY

DISADVANTAGES

- o EXTRA COMPONENTS REQ'D

FIGURE 1.2. COMPARISON OF COAXIAL & FIBER OPTIC CABLES

D100-25888-1

D180-25888-1

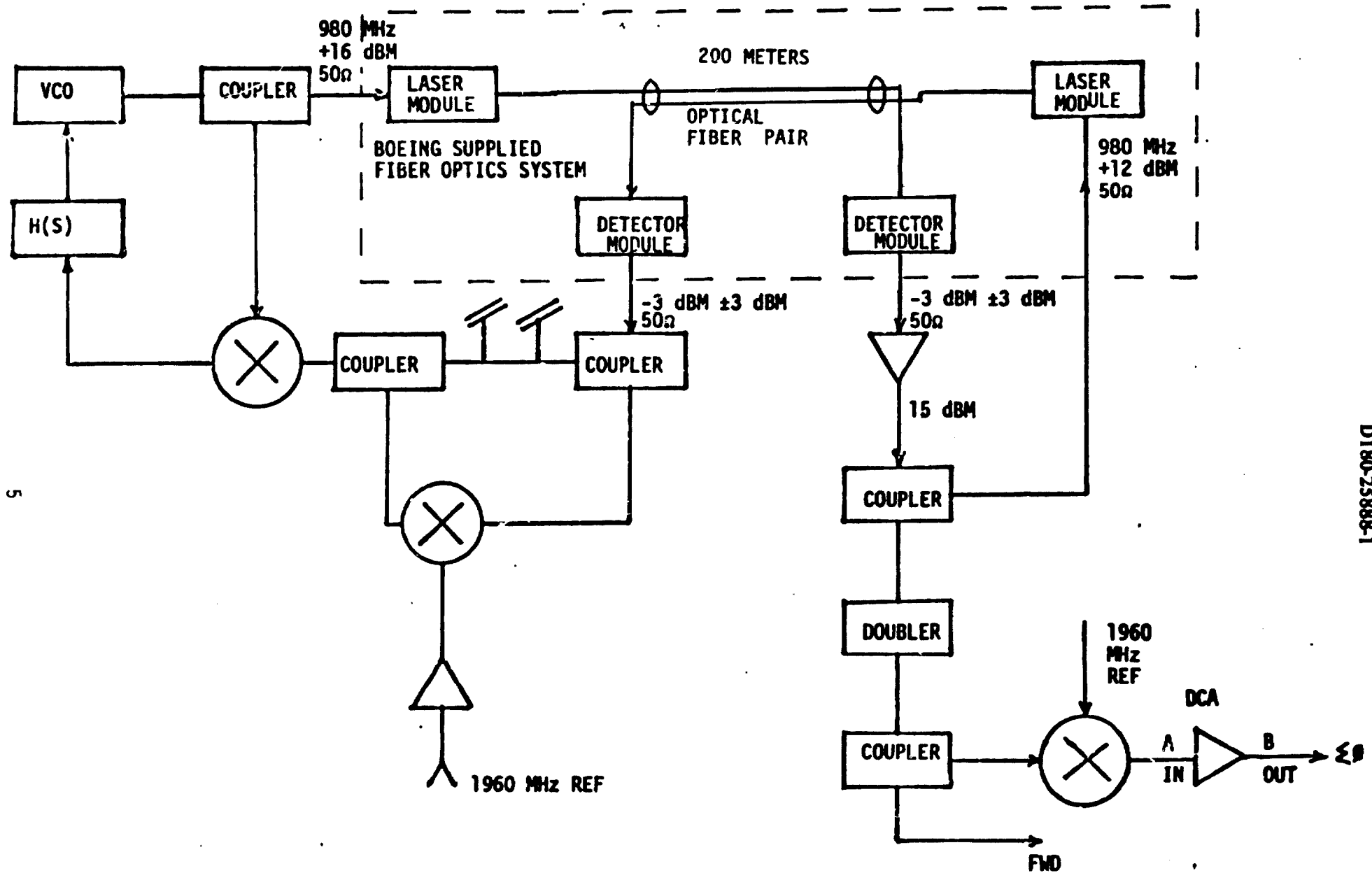


FIGURE 1.3. SPS FIBER OPTIC DUAL LINK SYSTEM

1. Analyze existing optical fibers for use in the phase distribution network with emphasis on thermal phase change effects, and the ability to transmit high frequency (980 MHz) signals.
2. Analyze optical emitters and detectors to determine their feasibility of operation for SPS usage at 980 MHz.
3. Test candidate fibers at 60 MHz to determine phase sensitivity to temperature variations.
4. Select and purchase optical emitters, detectors, and fibers for 980 MHz SPS link development.
5. Design and construct impedance matching systems for coupling the optical emitter and detector to laboratory equipment.
6. Assemble and test a two-way phase-matched link at 980 MHz consisting of similar emitters, detectors, and a two-fiber cable of minimum length of 200 meters.

### 1.3 TASK ORGANIZATION

Section 2 of this report discusses the investigation and selection of fiber optic components suitable for the SPS evaluation. Fibers, emitters, and detectors are discussed.

Section 3 presents data covering the results of phase angle versus temperature variation tests for four fibers selected as a result of the fiber investigation.

The design of a two-way 980 MHz fiber optic link is presented in Section 4. The design of suitable emitter and detector modules and the selection of a two-fiber cable and fiber optic connectors are discussed.

The results of initial testing at 980 MHz to demonstrate signal throughput and to further evaluate thermal effects on fibers are discussed in Section 5. Some discussion of fiber bandwidth is also presented in Section 5.

Section 6 covers the final development of the 980 MHz two-way link and includes the determination of the optimum operating conditions for the emitter and detector modules designed in Section 4. The discussion of the successful phase matching of the two similar links is also presented.

In Section 7, a complete characterization of the 980 MHz two-way link is performed. Information regarding phase variation for all input parameters, all suggested operating levels, and measured output data is given.

Suggestions for further study are presented in Section 8.

Appendices have also been included which present the test plans and the package drawings for the 980 MHz link modules.

## 2.0 FIBER OPTIC COMPONENT INVESTIGATION

For SPS application, optical fibers must be investigated with special attention given to their phase stability as a function of temperature, and their ability to transmit a 980 MHz signal with low attenuation and dispersion. Emitters and detectors must be investigated primarily with attention on their ability to be modulated by and to demodulate a 980 MHz signal with stable phase transmission properties. Figure 2.1 summarizes the various features of the fiber optic components that were investigated. Figure 2.2 lists the components chosen as a result of the task investigations for laboratory testing and further evaluation.

### 2.1 FIBER INVESTIGATION

Considering the requirements of the phase reference distribution system for the SPS, the objectives of this investigation were to determine the potential of modern fiber materials and fiber manufacturing techniques for minimizing the undesirable thermal path length variations, and also to determine the ability of present fibers to transmit a 980 MHz signal; i.e., low attenuation and adequate bandwidth.

Recently, work has begun on the effects of temperature on the optical length of fibers, and it appears that the effective path length variations for current fibers are comparable to the best of phase-stable coaxial cables.<sup>(1,2)</sup> As an outcome of this study, four types of optical fibers were evaluated, and Corning IVPO (Inside Vapor Phase Oxidation) fiber was recommended for the 980 MHz SPS link development.

FIGURE 2.1: FIBER OPTIC COMPONENT INVESTIGATION SUMMARY

Component	Type	Features
Emitter	GaAlAs Multi-Mode Injection Laser Diode	1. Moderate cost 2. High power 3. High modulation bandwidth
	GaAlAs Single-Mode Injection Laser Diode	1. High power        5. Low threshold 2. High coupling eff. 6. High reliability 3. High bandwidth    7. Narrow spectral width 4. Low distortion
	Light Emitting Diode (LED)	1. No threshold current 2. Low distortion 3. Low cost 4. Stable operating point
Detector	Silicon Avalanche Photodiode	1. Gain-BW product $\geq$ 80 GHz 2. High RCVR S/N 3. Moderate cost
	Silicon PIN Photo- diode	1. Low bias voltage 2. Stable operating point 3. Low cost
Fiber	Step-index glass multi-mode	1. Low cost 2. Low attenuation
	Graded-index glass multi-mode	1. Moderate cost 2. High bandwidth 3. Low attenuation
	Step-index glass single-mode	1. Extremely high bandwidth 2. Low attenuation 3. Poor coupling efficiency

COMPONENT	TYPE	MANUFACTURER	PART #
Emitter	Injection Laser Diode	Nippon Electric Co. (NEC)	NDL 3205P
Detector	Avalanche Photodiode	RCA	C30908E (hand-selected)
Fiber	IVPO Graded Index Lacquer Coated	Corning	Product Code #1514
	OVPO Graded-Index Lacquer Coated	Corning	Product Code #1504
	OVPO Graded-Index Fluorocarbon Coated	Times Wire & Cable	GA Series
	Double-Crucible Nylon Coated	Nippon Sheet Glass	"Selfoc" GI-60

FIGURE 2.2 COMPONENTS SELECTED FOR FURTHER INVESTIGATION

The initial investigation involved literature studies and contacts with manufacturers to gain knowledge of the relevant properties of various glasses. Modern fibers are drawn from extremely high purity doped fused silica. One significant exception is a Japanese product (Selloc) which is composed of multi-component glasses. Fused silica provides a pure material with highly predictable characteristics for proper control of index grading for high-bandwidth specifications, in addition to the potential of very low attenuation. At this point, no other materials are seriously being considered for fiber optics with the exception of the metallic halides for use with CO<sub>2</sub> lasers at 10.6 um. (3)

Several papers were found which dealt with the thermal properties of fused silica, including information on thermal expansion, thermal refractive index coefficients, wavelength effects, etc. Recently, some work has appeared on the thermal properties of optical fibers in particular. The remainder of the investigation involved discussions with several manufacturers of high-bandwidth fibers. Of particular interest, were the materials and the dopants used, and the manufacturing techniques involved.

Temperature can affect the phase of the reference signal transmitted through the fiber by two mechanisms: thermal expansion and thermal variation of refractive index. The following equation defines the relationship:

$$\Delta\theta^\circ = \frac{360 f n l}{c} \left( \frac{dn}{ndT} + \frac{dl}{TdT} \right) \Delta T$$

Where:      $\Delta\theta^\circ$  = change in transmitted phase, degrees  
 $\Delta T$  = change in temperature, °C  
 $f$  = frequency of transmitted signal  
 $n$  = nominal index of refraction of core  
 $l$  = nominal length of fiber  
 $c$  = speed of light (vacuum)

The results of an initial test<sup>(2)</sup> indicated that for a silica fiber at 820 nm, the effect due to a change in refractive index was significantly greater than the effect due to thermal expansion. For zero total effect, it is desirable that the refractive index coefficient be opposing in sign but equal in magnitude to the thermal expansion (length) coefficient. One of the tasks of the investigation was to determine if any fiber materials exhibited such characteristics.

Refractive index variations are caused by two distinct phenomena. As a fiber expands with temperature, its density will decrease, causing a negative refractive index coefficient. However, a phenomenon called electron polarizability will cause a positive refractive index coefficient.<sup>(4)</sup> Depending on the particular glass, the temperature range, or the wavelengths involved, either effect may dominate. Several common optical glasses do indeed exhibit negative index coefficients at longer wavelengths over some of the temperature range of our concern (-50°C to +150°C). It has been shown, however, that those glasses with the negative index coefficients also exhibit the greatest coefficients of thermal expansion.<sup>(5)</sup> The summed effects of both coefficients for any of the glasses surveyed show that no glass has significant "temperature hardness" improvement over fused silica. Although its index coefficient is positive (and essentially constant) for all wavelengths over which it is transparent,<sup>(6)</sup> the expansion coefficient of fused silica is extremely small, perhaps the lowest of all known materials. The expansion coefficients for other glasses are generally much greater.

For high silica fibers, two major manufacturing techniques are currently being used. The more common technique, called "inside vapor phase oxidation", involves the chemical vapor deposition of silica and the necessary dopants onto the inside of a large silica tube. Essentially, a "preform" is built up from the outside by deposition of core materials. Contaminants can be controlled down to one part per billion.<sup>(7)</sup> The alternate chemical vapor deposition technique is called "outside vapor phase oxidation" and involves the deposition of silica and dopants onto a mandrel from the outside.

The mandrel is then removed. In either case, the preform is then drawn through a furnace, collapsed and pulled into a fiber.

Several dopants may be used in the manufacture of fibers for an assortment of reasons, but the most significant are germanium, boron, and phosphorous. Germanium and phosphorous serve to increase the refractive index above that of pure silica; whereas, boron may be used to reduce the refractive index.

Selfoc is distinctly different from the high purity fused silica fibers discussed above. Not only is the fiber composition unique, the manufacturing technique utilizes a double crucible in which melted core material is held concentric with melted cladding material. As the fiber is drawn from the crucibles' nozzle, ions from the two melts tend to diffuse, creating a graded index profile.

Since linear thermal expansion and index of refraction variations are bulk properties of the glass which affect all modes of propagation identically, single-mode fibers would not offer any advantages and therefore were not thoroughly investigated. The use of single-mode fibers presents several difficulties in the coupling of sufficient optical power and with handling. If a single-mode fiber were chosen, a germanium-doped core fiber would be recommended because of the large cross-section of pure silica cladding.

Single mode fibers offer impressive bandwidth characteristics due to their inherent lack of intermodal dispersion, but in general, fiber bandwidth effects in multi-mode fibers should have little effect on the transmitted signal phase. Dispersion will cause the amplitudes of high frequency signals to diminish, and thus should always be avoided to maintain good signal-to-noise ratios. The phase should be stable under the effects of dispersion (if not excessive) unless the fiber's modal relationships are upset. Thermal variations could potentially cause such an upset (see Section 5.1), but the SPS two-way link compensation scheme should minimize these effects.

To summarize, modern high-bandwidth communications fibers are readily available with attenuation values of less than 10 db/Km and length-bandwidth products of several hundred megahertz-kilometers. Such fibers are more than adequate for the SPS application, and it is expected that limitations at 980 MHz would be due more to emitter and detector responses. Figure 2.3 summarizes the properties of presently available fibers (manufacturer-supplied data) suitable for consideration in the SPS application.

### 2.1.1 Thermal Effects in Fibers

Recent results of tests run on bulk glasses and on optical fibers in particular,<sup>(8,9)</sup> indicate that all of the high purity fused silica fibers will exhibit similar thermal characteristics, essentially identical to those of undoped fused silica.

The coefficient of thermal expansion,  $\frac{d\ell}{dT}$ , is expected to be close to, but slightly greater than that of undoped silica for all fibers, probably in the neighborhood of  $1 \times 10^{-6}$  per °C. The coefficient of refractive index,  $\frac{dn}{dT}$ , is expected to be typically 6 times greater, near  $6 \times 10^{-6}$  per °C. Germanium doping appears to have little effect on the thermal coefficients. Boron seems to increase the refractive index coefficient. However, it is usually not used in the core and thus, again, the effects will be small. Attenuation and dispersion properties of fibers should not be significantly affected by environmental temperature changes.<sup>(9, 10)</sup>

It is anticipated that the results from any testing of a high purity silica fiber should be similar to those of the initial test on Corning IVPO fibers. In that case, it was determined that:

$$\Delta\theta^\circ = 1.32 \times 10^{-11} \text{ per meter per Hz per } ^\circ\text{C}$$

It is further anticipated that the thermal phase variations will be greater for the Nippon multi-component fiber,<sup>(11)</sup> due mostly to a significantly larger thermal expansion coefficient and a nylon buffer. The refractive index coefficient may be smaller than that of fused silica, but it is

DIS00-25886-1

FIBER MANUFACTURER	CORNING GLASS WORKS	CORNING GLASS WORKS	TIMES WIRE AND CABLE	ITT E/O PROD.	NIPPON SHEET GLASS CO.	VALTEC	GALILEO
PRODUCT #	5101	5100	GA10-90	T-223	GI-60A	MG05	6000A-1
MINIMUM BANDWIDTH	1 GHz-Km	1 GHz-Km	300 MHz-Km	400 MKz-Km	200 MHz-Km	600 MHz-Km	400 MHz-Km
MAXIMUM ATTENUATION AT 820 nm	5 db/Km	5 db/Km	10 db/Km	5 db/Km	10 db/Km	5 db/Km	6 db/Km
MANUFAC. TECHNIQUE	CVD-IVPO	CVD-OVPO	CVD-OVPO	CVD-IVPO	DOUBLE CRUCIBLE	CVD-IVPO	CVD-IVPO
DOPANTS	Ge,B,P	Ge,B	B	Ge,B,P	B,Ge,??	Ge,B,P	Ge,B,P
HUMERICAL APERTURE	.21	.21	.21	.21	.16 ①	.21	.21
DIAMETERS mm	② 63,125,138	63,125,138	90,125,200	55,125,500	60,150,900	63,125,225	63,125,230
BUFFER COATING	LACQUER OR ACRYLATE	LACQUER OR ACRYLATE	FLUORO-CARBON	SILICONE RTV, HYTREL	SILICONE RTV, NYLON	SILICONE OR UV RESIN	UV RESIN
AVAILABLE (?)	YES	YES	YES	YES	YES	YES	YES
CHOSEN FOR TESTS	*	*	*		*		

① At 1 Km. All others measured on short lengths

② core, cladding, coating

FIGURE 2.3: SUMMARY OF MANUFACTURER'S FIBER DATA

expected that the thermal expansion will dominate to cause a greater total effect. The phase variations will most likely be greater for plastic-buffer fibers. Plastics are typically characterized by very large thermal expansion coefficients. It has been shown<sup>(9)</sup> that as the buffer expands (or contracts) it tends to linearly stretch (or compress) the internal fiber, creating a larger effective thermal expansion coefficient.

### 2.1.2 Fiber Selection

The following fibers were procured for purposes of thermal phase testing.

#### 1. Corning IVPO Graded Index

This is a high quality IVPO fiber and it represents the state-of-the-art for its type.

#### 2. Corning OVPO Graded Index

This fiber combines the outside vapor phase technique with dopants Ge, B.

#### 3. Times Wire and Cable OVPO Graded Index

This fiber is an OVPO fiber but is unique in that only B doping is used.

#### 4. Nippon Multi-component Graded Index

Of Japanese manufacture, this fiber is unique in its multi-component glass construction, as well as being drawn by the double-crucible technique.

All four of the fibers exhibit adequate bandwidth and attenuation characteristics for the SPS phase distribution task.

Most present fiber optic applications utilize wavelengths in the 800 nm to 900 nm range where GaAs emitters and silicon detectors provide adequate optical powers and detector sensitivities. However, it has been shown<sup>(11)</sup> that silica fibers reach their bandwidth peak and attenuation null in the 1200 nm to 1600 nm wavelength range, and it is expected that emitters and detectors in this range will become available in the early 1980's. The improvements in bandwidth and attenuation may be of some interest for SPS use, but it is expected that there would be little improvement, if any, in thermal phase effects due to the fact that the phase-affecting thermal coefficients are invariant by choice of wavelength. Further investigation is suggested, however, as the new technology matures.

## 2.2 EMITTER INVESTIGATION

The objectives of the emitter investigation were to determine the ability of various sources to be modulated at 980 MHz, and to determine optimum biasing, stabilization, physical configuration, and modulation techniques for use at 980 MHz. Suitable emitters were to be procured and evaluated in a 980 MHz fiber optic test link. A single mode injection laser diode was chosen for the tests for reasons of high power output, high bandwidth, and excellent linearity.

The most widely used optical sources for fiber optic systems are injection laser diodes (ILD) and light emitting diodes (LED) which emit in the 0.8 to 0.9 and 1.2 to 1.6  $\mu$  spectral ranges where the transmission properties of fibers are superior. Present technology dictates the use of devices in the 0.8 to 0.9 $\mu$  region due to progress made with GaAs devices<sup>(12)</sup>.

ILD's represent the widest possible system utility with high radiance, low loss coupling to fibers, ease of direct modulation to GHz rates, small size, and potential low cost. Temperature dependence of operating characteristics for ILD's is high, and thus temperature stabilization is normally required. Lifetimes are typically guaranteed to be greater than 10,000 hrs. for the 0.8 to 0.9 $\mu$  devices.

LED's may fulfill many system needs in relatively short or low bandwidth links with less restrictive operating conditions than those needed for ILD's. They are capable of coupling powers comparable to lasers into large-core, step-index, low-bandwidth fibers, modulation rates up to 100 MHz, are small in size, low cost, and offer excellent stability and linearity.

Recent advanced in InGaAsP have made it possible to construct both ILD's and LED's that operate in the  $1.3\mu$  spectral regions, where dispersion and attenuation both attain theoretical minima in silica fibers.<sup>(13)</sup> Reliability of these newer devices is presently poor, but future developments may allow the  $1.3\mu$  region to become extensively used.

The devices presently most appropriate for the SPS phase distribution network are GaAs ILD's, operating in the 0.8 to  $0.9\mu$  region. The choice is based on their high speed of response, high power output, and high coupling efficiency with high-bandwidth fibers. The longer wavelength region was rejected for this study because of the present reliability problems but should be considered in future investigations.

Although the impact of diode linearity on phase is not clear, devices which operate in a stable, single transverse mode should be selected because of their excellent linearity over a wide range of optical power. Linearity is required as the ILD's will be biased at an average value of current and linearly modulated about the bias point by the 980 MHz phase reference signal. Also, single mode lasers tend to have narrower emission spectra which allows higher fiber bandwidths due to reduced material dispersion.

ILD's typically exhibit sharp resonant peaks in modulation response around 1 GHz. Response above the peak rolls off very quickly, and thus it is imperative that operation be at or below the peak. Operation near the peak is not recommended because phase response is expected to change rapidly in this region. The ILD frequency response depends on the diode stripe width, dopant levels, and bias conditions and can be somewhat extended by an increase in the bias current.

It was difficult to determine the relative ability of various manufacturers' ILD's to operate at 980 MHz due to an inadequacy of manufacturers' data. Several manufacturers indicated that their devices had rise times guaranteed to be less than one nanosecond, but were not confident as to the performance at 980 MHz. The selection was also based on diode availability, cost and optical output (pigtail) compatible with high efficiency coupling to high bandwidth fibers.

Nippon Electric Co. (NEC) was selected as the supplier for the laser diodes. The devices (NDL-3205P) chosen were single mode, with attached pigtails, and were well packaged. The NEC diodes operate at 860 nm and additional performance data are included in Figure 2.4.

### 2.3 DETECTOR INVESTIGATION

The objectives of the detector investigation were to determine the response characteristics for various optical sensors at 980 MHz, and to determine the optimum biasing, stabilization, physical configuration and termination techniques for 980 MHz use. Those detectors which appeared worthy of further investigation were to be procured and evaluated in a 980 MHz fiber optic test link. An avalanche photodiode was chosen for the tests for reasons of high sensitivity, superior speed, and high signal responsivity. Hand-selected units were procured for the particular SPS 980 MHz requirements.

The four basic types of photosensors considered include photo-emissive, photovoltaic, photoconductive junction, and photoconductive bulk effect types. Practically all fiber optic sensors are of the photoconductive junction type, represented primarily by photodiodes and phototransistors in which the resistance across a semiconductor junction varies as a function of the incident light level, and with appropriate applied bias, a photocurrent is produced. They are generally the fastest in response, and quite linear.

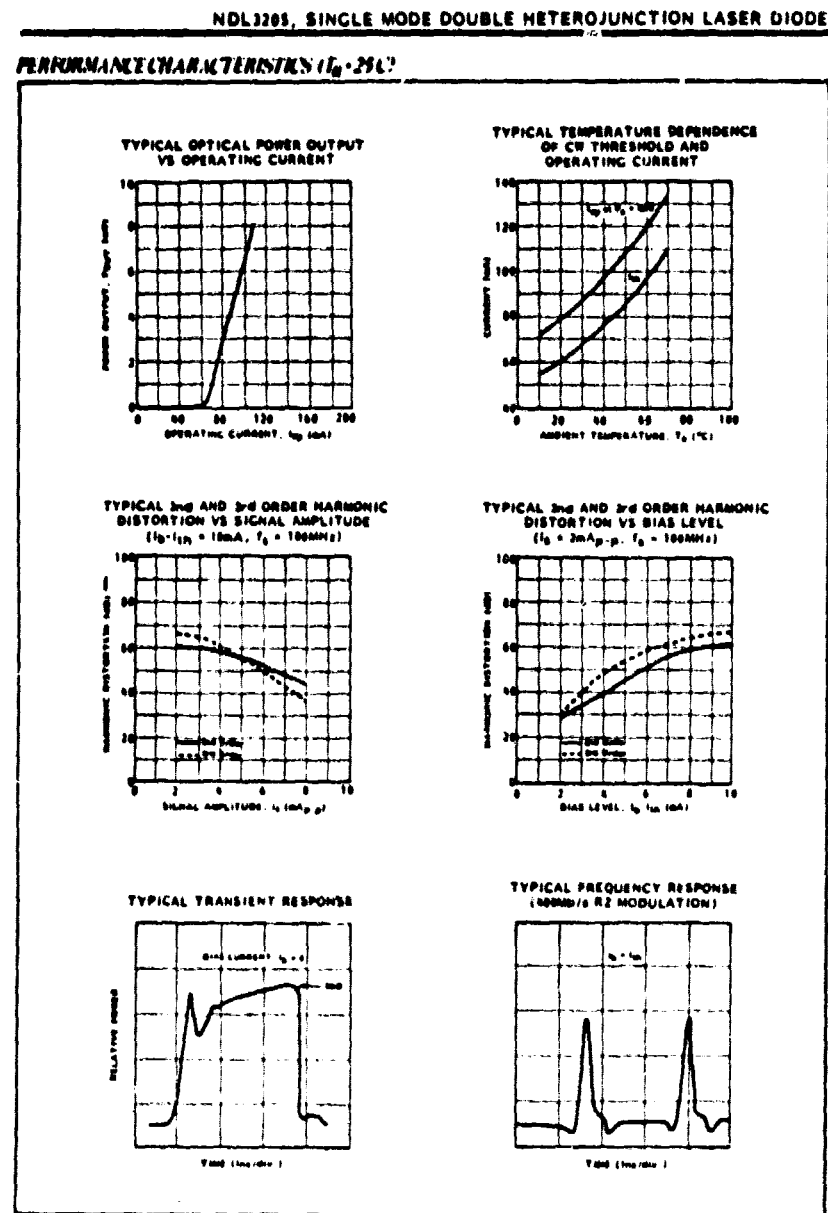


FIGURE 2.4 INJECTION LASER DIODE PERFORMANCE DATA

Among photoconductive junction devices, photodiodes are most commonly used due to their inherently fast response (~ 1 nanosecond). Below 100 KHz, phototransistors such as photo FET's offer the greatest potential sensitivity. When properly designed, optical receivers using photo FET's are very stable with temperature and power supply variations.

Photodiodes are usually either made of a gainless PIN structure, or of a structure wherein avalanche multiplication takes place. PIN photodiodes are very simple to use, requiring low voltage power supplies and no temperature or bias stabilization. Avalanche photodiodes are the fastest and are extremely sensitive because signal gain is generated before the noise sources of the receiver preamplifier. Bias and temperature stabilization is necessary for optimum usage, and bias voltages may be as great as 300 volts. PIN photodiodes are often suitable for short links where sensitivity is not of prime concern.

Present technology of fibers and emitters (and detectors) dictates that the wavelength of operation be in the range of 0.8 to 0.9  $\mu$ . Silicon detectors operate with high efficiency in this region (typically 75%) and thus find the most usage.<sup>(12)</sup> As the technology shifts towards the 1.3  $\mu$  region of wavelength, where silica fibers reach attenuation and dispersion minima, detectors will probably be made with InGaAsP.<sup>(13)</sup> It is expected that the technology at 1.3  $\mu$  will become available in the early 1980's.

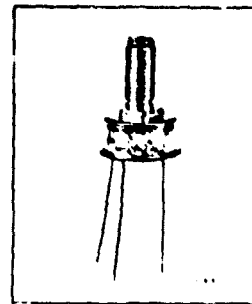
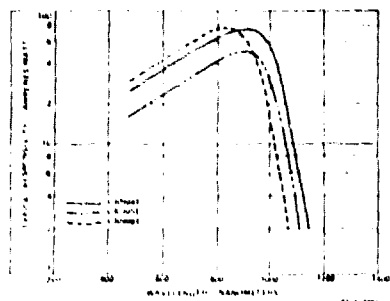
The devices most appropriate for the current SPS phase distribution link are silicon avalanche photodiodes (APD) due to their superior speed of response, low noise performance and high responsivity. Typical gain-bandwidth products are in the range of 80 GHz to 100 GHz, and a speed of response (bandwidth) and gain (responsivity) may be traded for APD's. A high field region is required for the gain mechanisms to occur, and generally the longer the region, the greater the responsivity. For fast speed, short drift times are required which imply shorter regions. Most commercial

APD's appear to have thicknesses near  $30 \mu$  which causes a frequency response rolloff somewhat below 1 GHz. It is expected that detector phase may be sensitive in the rolloff region, and therefore it is desirable that a diode with a thinner junction be selected for the SPS application.

RCA was chosen as the supplier for the avalanche photodiodes. They were willing to hand-select units with junction thicknesses in the neighborhood of 15 to  $20 \mu$  which would guarantee a flat response past 1 GHz. Diode responsivity at 800 nm to 900 nm would be only slightly reduced. RCA offers a special package for APD's which contain an integral light pipe. The package eliminates the need for fiber pigtailing and, with the aid of an RCA-available adapter bushing, a fiber optic connector may mate directly to the device. The part number is C30908F, and specification information is given in Figure 2.5.

### Optical Characteristics

Numerical Aperture of Light Pipe      0.60  
Refractive Index (n) of Core      1.61



Typical Spectral Responsivity Characteristics

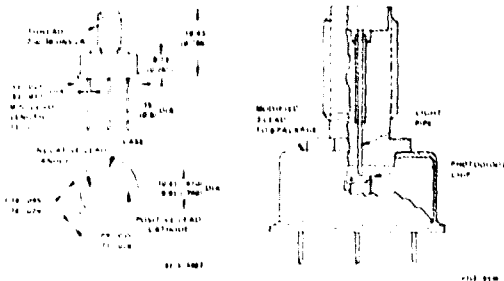
### Electrical Characteristic\*

Electrical Characteristic*	At an ambient temperature ( $T_A$ ) of 22°C and the DC reverse operating voltage ( $V_R$ ) value supplied with each device b									Units	
	C30904E			C30905E			C30908E				
	Min.	Typ.	Max.	Min.	Typ.	Max.	Min.	Typ.	Max.		
Breakdown Voltage, $V_BR$	300	375	475	375	390	490	185	225	265	V	
Temperature Coefficient of $V_R$ for Constant Gain	-	2.2	-	-	2.2	-	-	0.6	-	mA/°C	
Gain	-	120	-	-	80	-	-	160	-		
Responsivity											
At 830 nm	60	88	-	40	48	-	20	27	-	A/W	
At 900 nm	65	75	-	43	50	-	55	65	-	A/W	
At 1060 nm	15	18	-	10	12	-	-	-	-	A/W	
Quantum Efficiency											
At 830 nm	-	85	-	-	85	-	-	75	-	%	
At 900 nm	-	85	-	-	85	-	-	60	-	%	
At 1060 nm	-	18	-	-	18	-	-	-	-	%	
Total Dark Current, $I_D$	-	50	200	-	100	400	-	15	30	nA	
Dark Current, $I_D$											
$f = 10 \text{ kHz}, T = 23^\circ\text{C}$	-	1	2	-	1	2	-	0.23	0.50	DAINH <sup>1/2</sup>	
Capacitance, $C_D$	-	2	4	-	3.5	5.0	-	1.6	2.0	pF	
Series Resistance											
Rise Time, $t_r$	-	15	-	-	15	-	-	15	32		
$R_L = 50 \Omega, \lambda = 800 \text{ nm}$	-	-	-	-	-	-	-	-	-		
10% to 90% points	-	2	3	-	3	4	-	0.50	0.75	ns	
Fall Time											
$R_L = 50 \Omega, \lambda = 800 \text{ nm}$	-	-	-	-	-	-	-	0.50	0.75	ns	
90% to 10% points	-	2	3	-	3	4	-	-	-		

- \* Performance characteristics are referred to the input surface of the light pipe
- b A specific value of  $V_R$  is supplied with each device. When the photodiode is operated at this voltage, the device will meet the electrical characteristic limits shown above. The voltage values will be within the ranges specified below.

Type      Range of  $V_R$  (Recommended operating voltage)

C30904E      275 - 425 V  
C30905E      275 - 475 V  
C30908E      180 - 250 V



### 3.0 60 MHZ THERMAL PHASE SENSITIVITY TESTS

The objective of the 60 MHz tests was to determine the relative phase sensitivity versus temperature for the four fibers selected through the fiber investigation discussed previously. The 60 MHz frequency was used for the tests because of the existence of transmitters and receivers in the Boeing Fiber Optic Test Laboratory.

The test setup is shown in Figures 3.1 and 3.2. Each fiber was wrapped on a separate mandrel and inserted individually into an environmental test chamber for testing. A fiber optics transmitter modulated at 60 MHz was used to couple the signal into the fiber, and a suitable receiver was used at the far end.

As the temperature was varied (in 25°C increments), the relative phase change was monitored by the vector voltmeter. The phase of the 60 MHz signal at the transmitter was used as the reference signal and any phase change in the electronics was monitored by replacing the test fiber with a short (three meter) length fiber held at room temperature. The phase change within the electronics in all cases was found to be negligible, typically within one degree during a test cycle.

The test plan for the 60 MHz tests is attached in Appendix I. The pertinent specifications for the four selected fibers are given in Figures 2.3 and 3.3 below.

<u>Fiber</u>	<u>Manufacturer</u>	<u>Length</u>	<u>Refractive Index</u>	<u>Attenuation</u>	<u>Bandwidth</u>	<u>N.A.</u>
1.	Corning (IVPO)	303m	1.47	3.9 db/Km	870 MHz-Km	0.218
2.	Corning (OVPO)	1060m	1.47	4.0 db/Km	1400 MHz-Km	0.204
3.	Times Wire and Cable	202m	1.46	6.0 db/Km	291 MHz-Km	0.170
4.	Nippon Glass "Selloc"	324m	Data not supplied	7.0 db/Km	Data not supplied	Data not supplied

Figure 3.3 Specifications of Test Fibers

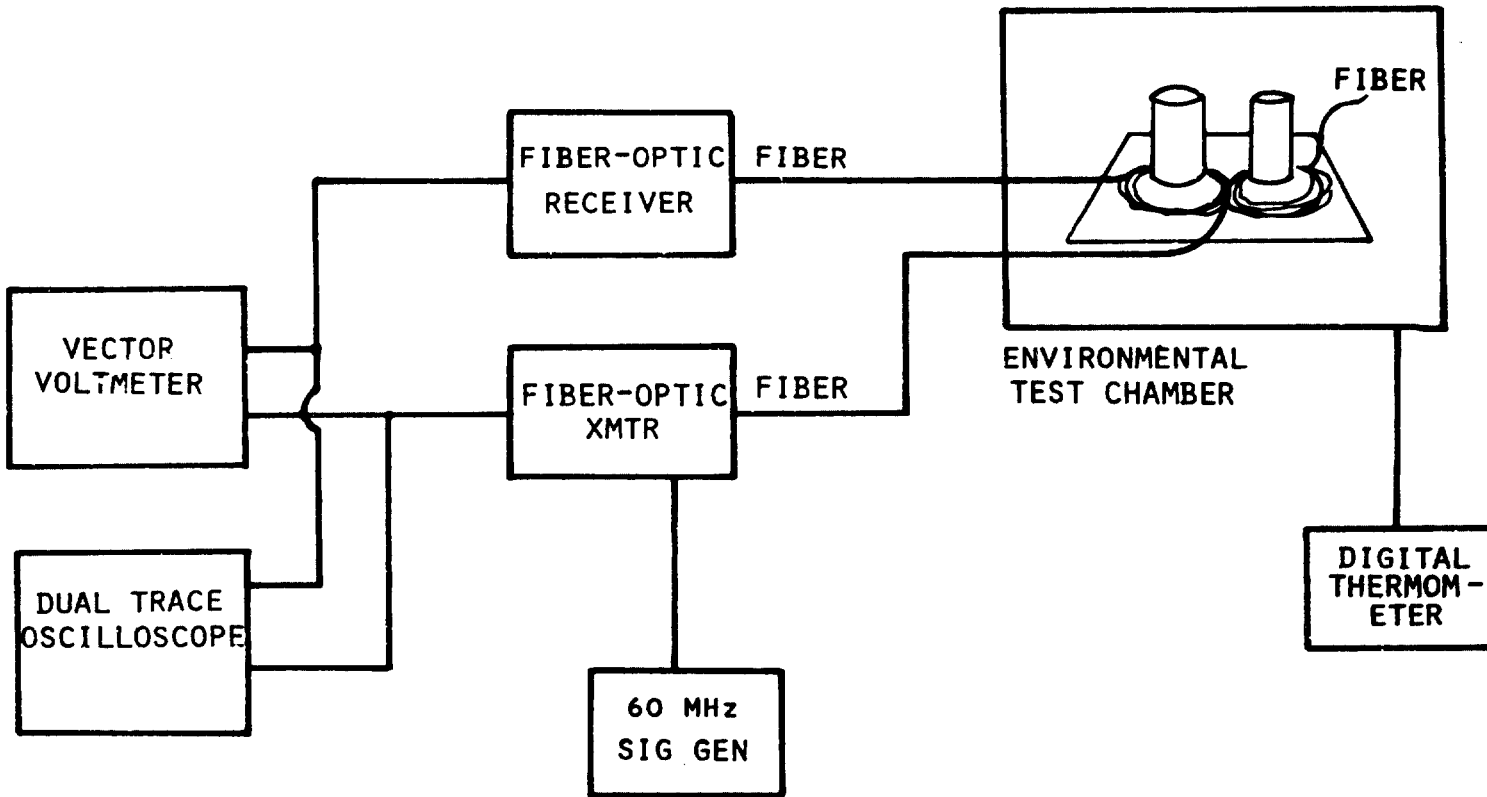


FIGURE 3.1. 60 MHz PHASE TEST - BLOCK DIAGRAM

D180-25888-1

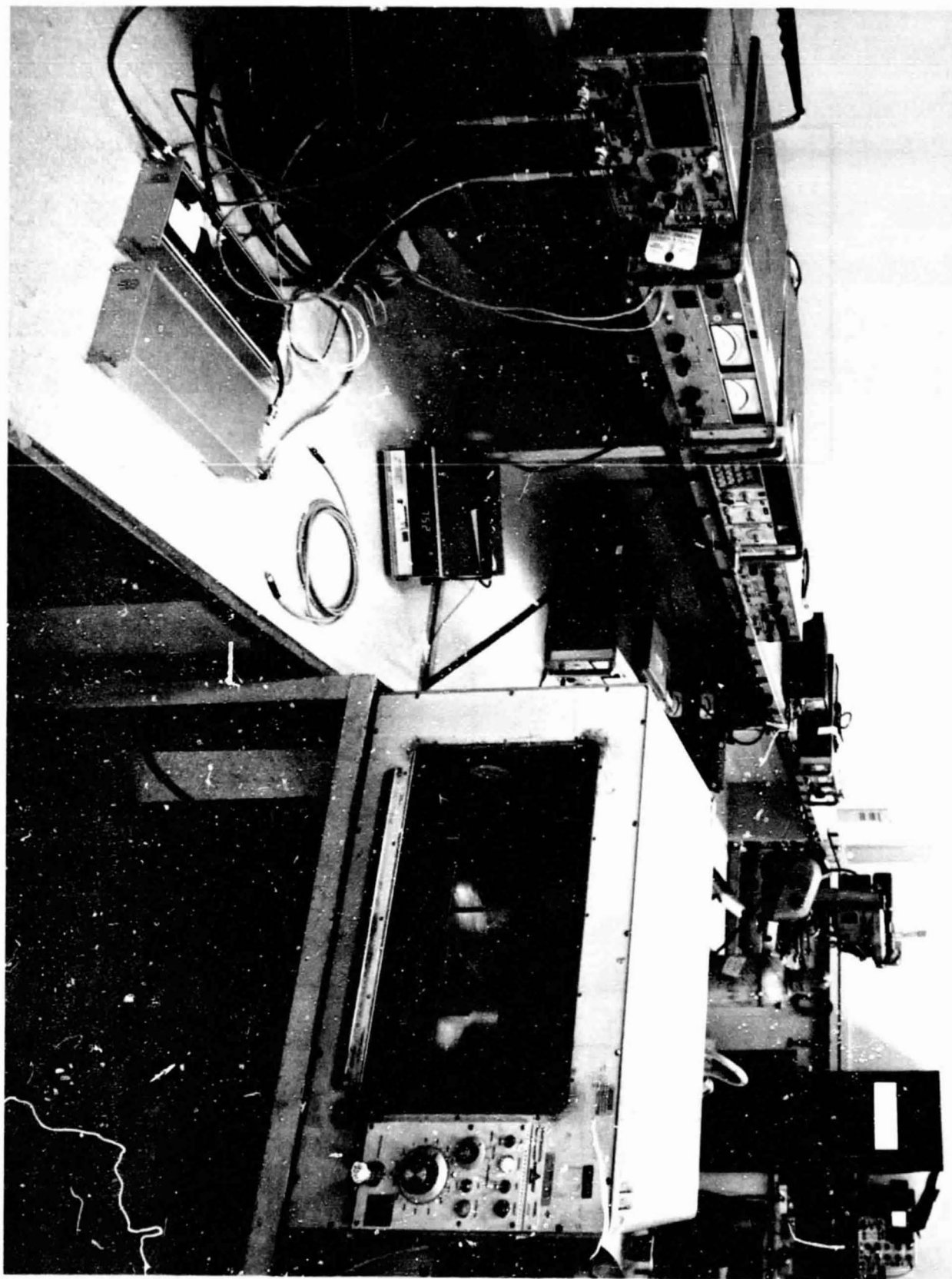


FIGURE 3.2.: PHOTOGRAPH OF 60 MHZ PHASE TEST

The specifications for the remainder of the test setup are given below:

**Transmitter**

Emitter - RCA C30130 Injection Laser Diode, AlGaAs

Wavelength - 820 nm

Optical Power - 620 microwatts average

Modulation Source - HP 8660 Frequency Synthesizer, 60 MHz

**Receiver**

Detector - Texas Instruments TIXL 56 APD with Pigtail

Sensitivity - < 10 nw for 20 dB SNR

**Environmental Test Chamber** - Delta Design, Model #5708

**3.1 TEST RESULTS**

The measured relative phase change for the four fibers is shown in Figure 3.4. The ordinate is scaled on a per Hz and per meter basis such that the absolute value of phase change may be determined for any length fiber at any frequency of use.

The results for the two Corning fibers are nearly identical and approach the results expected for pure fused silica. Figure 3.5 shows the data for the two Corning fibers plotted on an expanded scale.

It was anticipated the "Selloc" would be the most sensitive to temperature due to its multi-component structure. However, the majority of the differences are best explained by the thermal effects of the various buffer coatings used. The Corning fibers use a very thin acetate lacquer layer for a buffer, but both the "Selloc" fiber and the sample from Times Wire and Cable

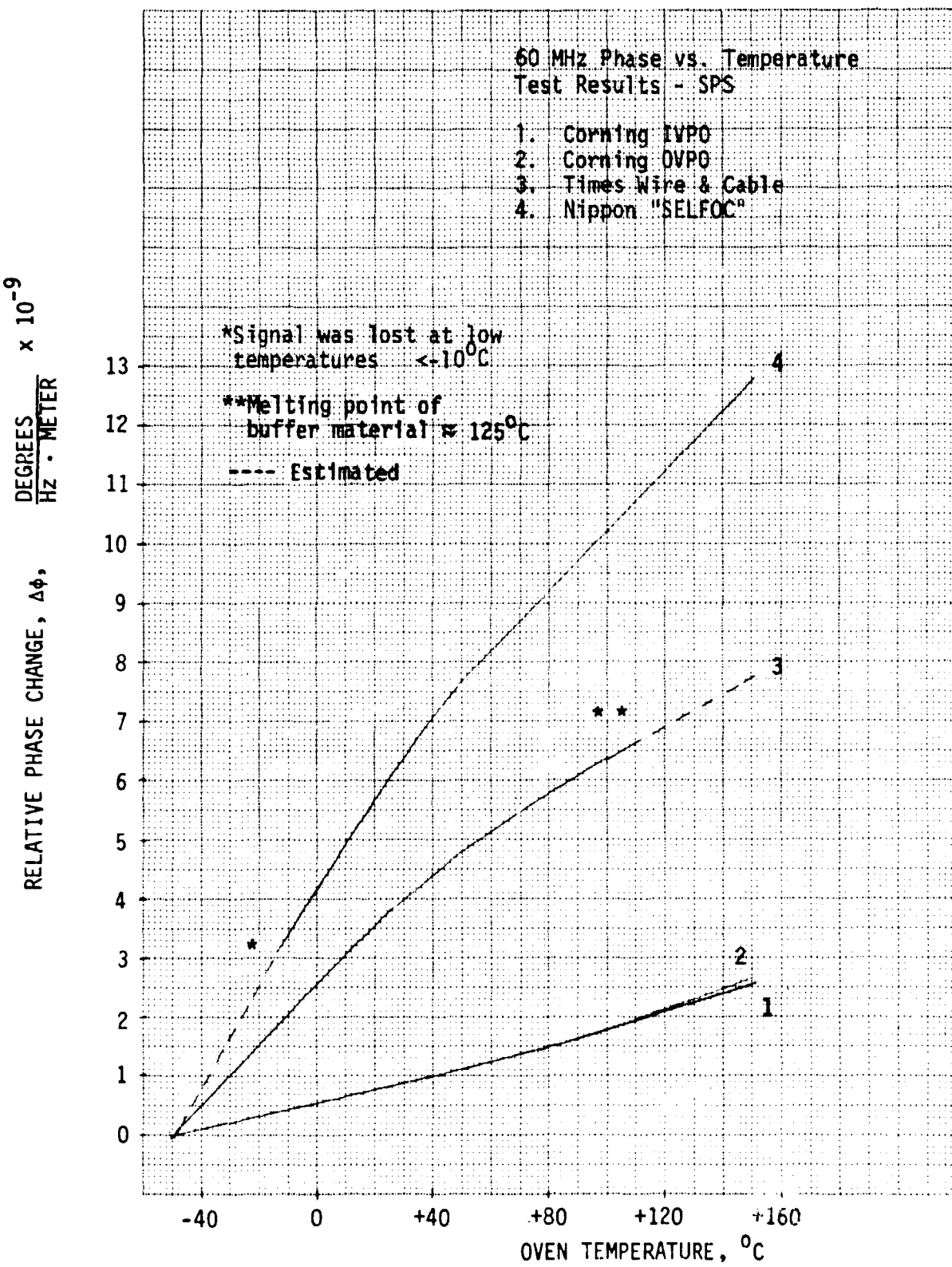


FIGURE 3.4. 60 MHZ PHASE VS TEMPERATURE TESTS

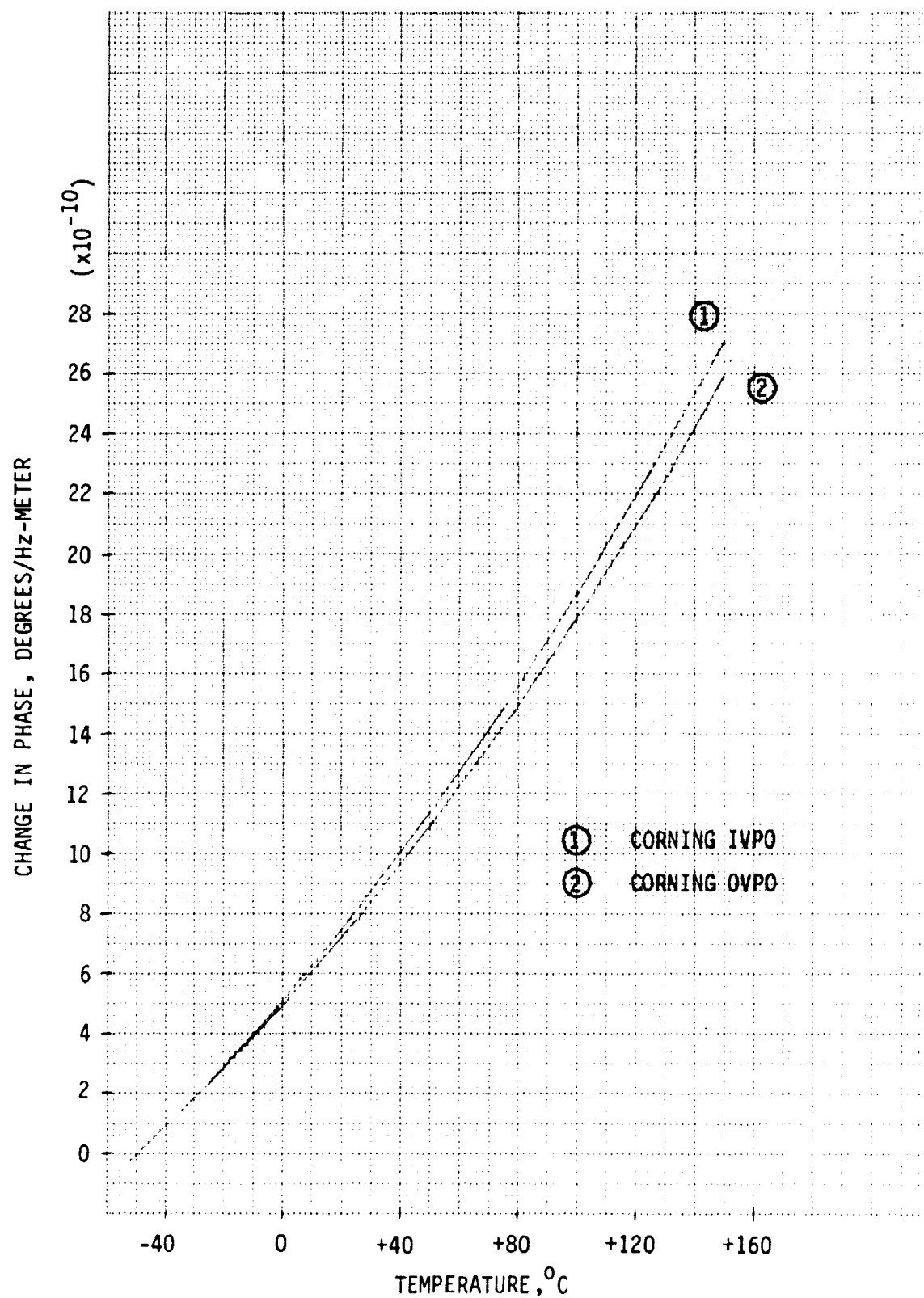


FIGURE 3.5 PHASE VS TEMPERATURE FOR CORNING FIBERS

use a thicker silicone buffer coated with a layer of a thermo-plastic which expands or contracts greatly with temperature changes. This fact becomes obvious if we consider that the fiber from Times is highly similar to the Corning fibers in both composition and manufacturing process. The additional plastic buffer coatings act to "stretch" or "compress" the fiber, causing a larger phase variation.<sup>(9)</sup>

It is also interesting to note that the signal throughput was lost at low temperatures for the Selfoc fiber. This effect is probably caused by severe microbending due to the contraction of the buffer coatings. Microbending causes the propagation modes to be coupled to radiation modes and to be lost from the fiber core. The Times Wire and Cable fiber was not tested above 115°C (as suggested by the manufacturer) to ensure that the Hytrel buffer would not melt. The dashed lines in Figure 3.4 are predictions of results at the temperature extremes so that the four fibers may be better compared.

It is clear that a proper choice of buffer coating is important for the SPS application. A buffer coating is necessary to protect the fiber proper from chemical contaminants and to prevent the introduction of nicks or scratches to the glass. The heavier, plastic buffers are perhaps better for fiber protection, but obviously impose serious effects on the phase properties. Similarly, cabling processes which extrude a tight plastic jacket onto the glass should be avoided. The Siecor Co. uses fibers manufactured by Corning and uses a "loose tube" approach in which the actual fiber forms a very sloppy, loose fit within the jacket. This scheme allows some independence between the jacket and the fiber, thereby creating less of a potential phase change problem. One significant conclusion of this study is the fact that the entire buffer/cabling question is significant with respect to the SPS phase control application and deserves as much attention as the choice of the fiber itself.

The Corning IVPO fiber is the least sensitive to temperature. The equation for phase change, as given earlier, is:

$$\Delta\phi^\circ = \frac{360 f_{\text{mod}}}{c} n_1 \left( \frac{dn}{dT} + \frac{d\ell}{dT} \right) \Delta T$$

The terms inside the brackets represent the fractional change of refractive index with temperature, and the fractional change of length with temperature, respectively. Over the temperature range involved, the test showed that:

$$\left( \frac{dn}{dT} + \frac{d\ell}{dT} \right)_{\text{exp.}} = 7.494 \times 10^{-6} \text{ per } ^\circ\text{C.}$$

Previously run tests at Corning on IVPO fibers to determine the temperature coefficient of linear expansion indicate that:  $\frac{d\ell}{dT} = 1.75 \times 10^{-6}$  per  $^\circ\text{C}$ . The refractive index of fused silica (14) is expected to vary as:

$\frac{dn}{dT} = 5.6 \times 10^{-6}$  per  $^\circ\text{C}$  over the temperature range of interest. Adding the above two terms gives a predicted value  $\left( \frac{dn}{dT} + \frac{d\ell}{dT} \right) = 7.35 \times 10^{-6}$  per  $^\circ\text{C}$ . which checks closely the experimentally measured figure of  $7.494 \times 10^{-6}$  per  $^\circ\text{C}$ . The results for Corning's OVPO fiber are similar. The more complex analyses for plastic-buffered fibers are dealt with in Reference 8.

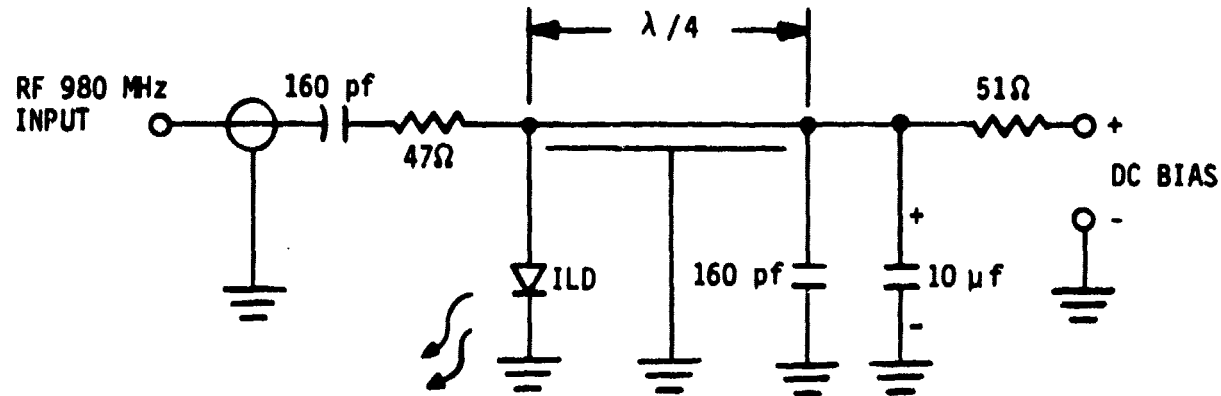
#### 4.0 980 MHz LINK DESIGN

To facilitate evaluation of the fiber optic links at NASA-JSC, an attempt was made in the design to phase match the two links operating in the opposing direction. The effort in this section was to design such a dual link which would consist of the source and detector modules used together with laboratory equipment such that this condition could be met. Another design goal for the 980 MHz link was to develop simple, yet effective signal coupling schemes for the emitters and detectors which are described in this section.

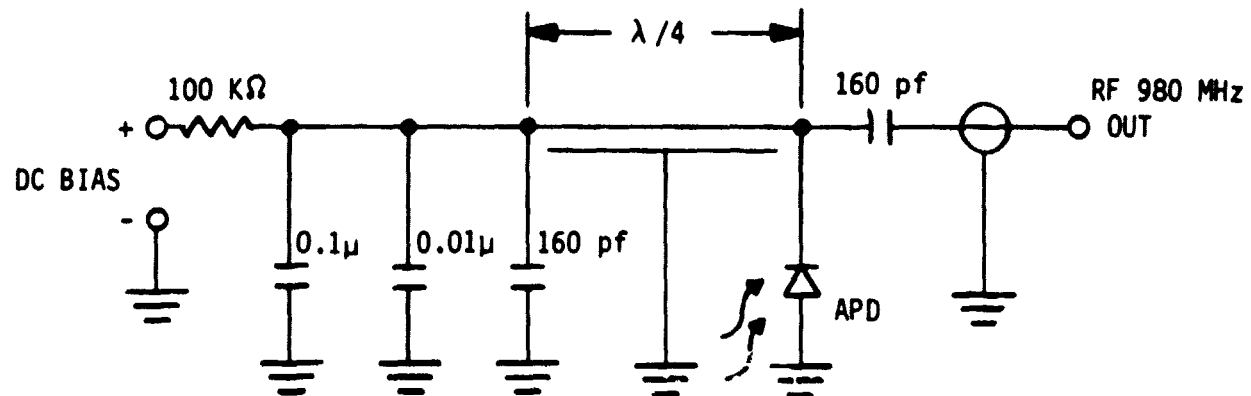
#### 4.1 EMITTER MODULE DESIGN

The approach chosen for the emitter module is illustrated in Figure 4.1. According to manufacturers, the input impedance of an injection laser diode is approximately 2 to 3 ohms of resistance in series with a few ohms of reactance, with both values dependent on drive and bias levels. Thus, the use of an impedance matching scheme, such as a transformer, a cavity resonator, or stripline network, is questionable because (1), the impedance seen by the 50 ohm driving source would not be constant and (2), the drive current into the laser diode would not be linear with drive levels. This situation would create a non-linear optical waveform due to the direct relationship between optical power and instantaneous drive current.

The method shown in Figure 4.1 uses the 47 ohm resistor (specifically chosen for high frequency use) to swamp out the effects of the varying diode impedance. It causes approximately 50 ohms to be seen by the driver at all times, and it also aids in converting the driver output to a current source as required by the diode for linearity. The 47 ohm resistor reduces efficiency, but for this study, the loss of efficiency when weighed against the simplicity and effectiveness of this technique, was determined to be insignificant.



(a) 980MHz Emitter Module Schematic



(b) 980MHz Detector Module Schematic

FIGURE 4.1 980 MHz MODULE SCHEMATIC DIAGRAMS

The DC bias is coupled to the laser diode through a quarter-wave microstrip which is AC shorted to ground at the far end from the diode. Ideally, the impedance seen on any transmission line at a point one quarter of a wavelength from a short will approach infinity, which would, therefore, not impose any loading on the 980 MHz signal paths.

The propagation delay of a microstrip line may be calculated by<sup>(15)</sup>:

$$t_{\lambda d} = 1.017 \sqrt{0.475 e_r + 0.67} \text{ ns/ft.}$$

The propagation delay for the line is dependent only on the dielectric constant of the circuit board and not on the line width or board thickness. For the fiberglass epoxy boards used,  $e_r \approx 5$  and the propagation delay of the microstrip line is found to be 1.11 ns/ft. The time required for one quarter-wave of a 980 MHz signal is:

$$t_{\lambda/4} = \frac{1}{4 \times 980 \times 10^6} = 2.551 \times 10^{-10} \text{ seconds. Therefore, the length of the microstrip line becomes: } l = \frac{2.551 \times 10^{-10}}{1.77 \times 10^{-9}} = 0.1441 \text{ ft.} = 1.73 \text{ inches.}$$

High frequency "chip" capacitors were used for the AC line shorting and also for coupling the AC signal from the driver to the diode.

It is important that the injection laser diode be stabilized against temperature variations. A laser diode's threshold current knee is a strong function of temperature (typically 1 ma per °C), and if the temperature is allowed to vary, the optical output will vary excessively, possibly leading to diode destruction. Thermal stability is also required to keep the emitting wavelength (.25nm per °C) within set limits in order not to exceed phase errors due to refractive index changes in the fiber with wavelength changes.

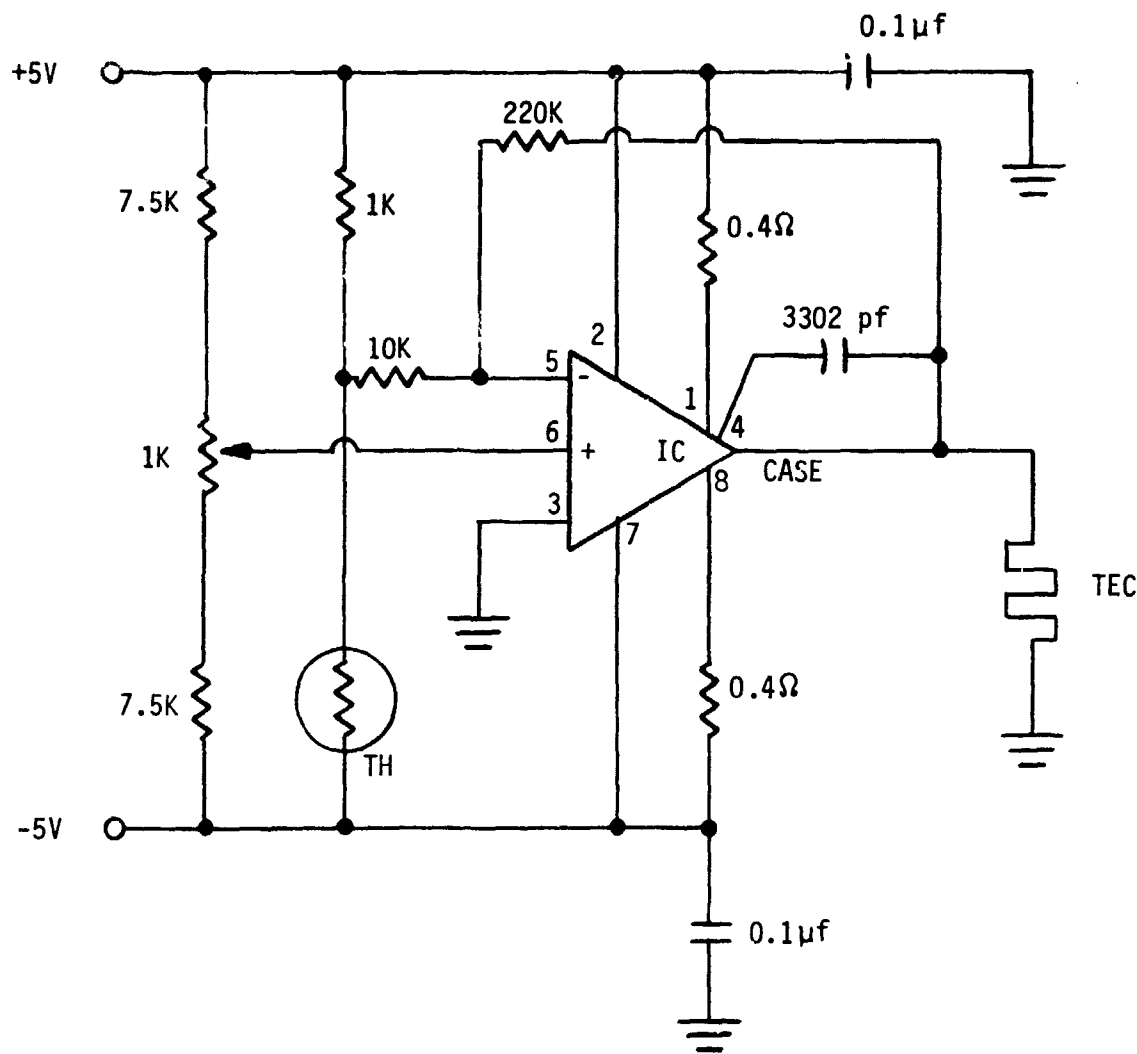
Between 800 nm and 1,000 nm, the refractive index for fused silica varies approximately  $-1.5 \times 10^{-3}$  per nm. By mathematically combining the effects, for every degree of temperature change of the laser diode,  $\Delta\theta = 4.5^\circ$  per Km of fiber per degree C.

Temperature stability for the diode was achieved by mounting it together with a thermoelectric cooler unit in a thermal feedback loop and attaching the entire assembly to a heat sink. A schematic of the cooler circuitry is shown by Figure 4.2. The heat sink also serves as the front panel for the emitter modules and all of the interfaces are mounted through it. Details of the packaged emitter module, with the bias inputs at the top, the fiber optic connection (lower left) and the RF input connection (lower right) are shown in Figure 4.3, with the internal view given in Figure 4.4. The thermoelectric cooler PC board is mounted on the right side, while the ILD driver PC board is on the left side. The cooler unit is mounted behind the laser. The laser pigtail was terminated with a fiber optic connector, looped around, and fed into a bulkhead feedthrough connector mounted in the heat sink. Package drawings are contained in Appendix II.

#### 4.2 DETECTOR MODULE DESIGN

The approach chosen for the detector signal coupling scheme is illustrated schematically by Figure 4.1. Avalanche photodiodes are best modeled as high impedance current sources in parallel with a few picofarads of capacitance. As such, true impedance matching techniques would be difficult to implement and would most likely be more lossy than beneficial.

In the approach used, the signal photocurrent is coupled through a DC blocking capacitor directly into the (50 ohm) input impedance of the preamp. The current x impedance product is a voltage which is then amplified. This scheme has been the most successful at lower frequencies, is actually the least noisy, and should provide the best performance at 980 MHz, particularly in a single frequency application. This eliminates any difficulties created by a frequency dependent input impedance.



TEC, MARLOW INDUSTRIES MI-1022

TH, #31A2 THERMISTOR,  $1\text{ k}\Omega @ 25^\circ\text{C}$ 

IC, NATIONAL LH0021 CK

FIGURE 4.2 INJECTION LASER DIODE THERMOELECTRIC COOLER SCHEMATIC

D180-25888-1

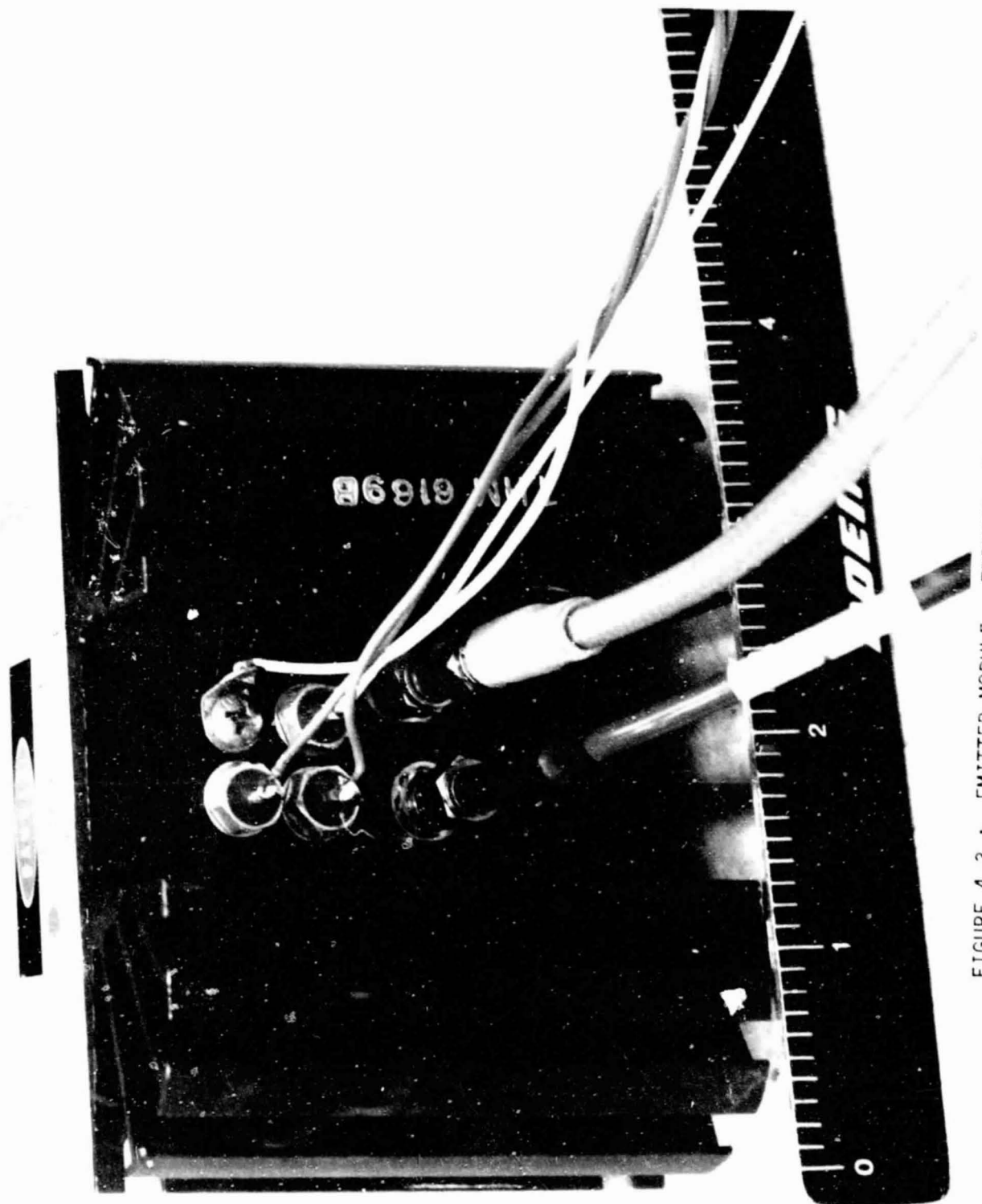
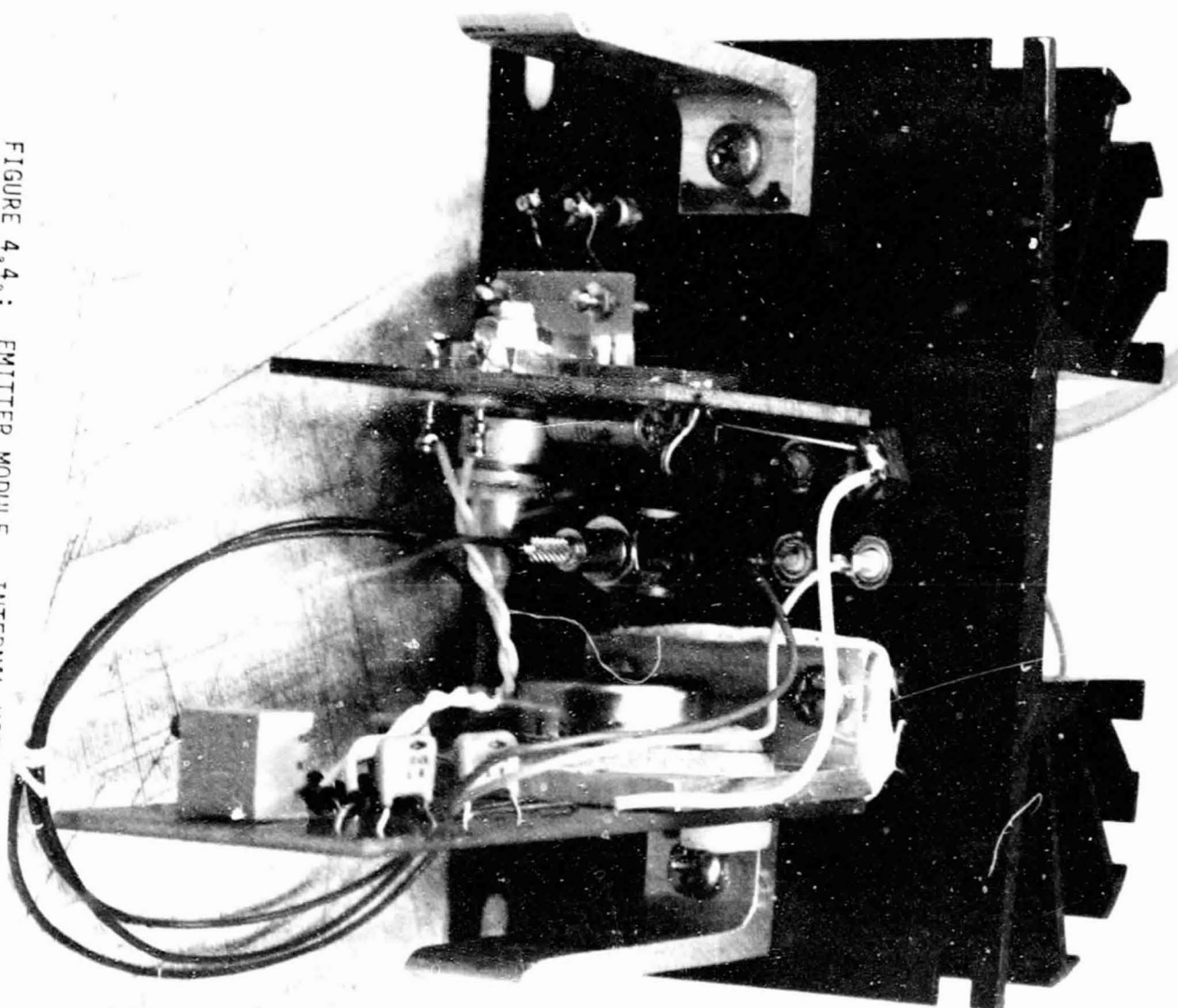


FIGURE 4.3.: Emitter Module - FRONTAL VIEW

ORIGINAL PAGE IS  
OF POOR QUALITY

D180-25888-1

FIGURE 4.4.: Emitter Module - INTERNAL VIEW



The DC bias for the detector was coupled through a quarter-wave microstrip in a fashion identical to that used for the emitter module. A 100 k ohm resistor was used in series with the bias supply to limit the photocurrent and, hence, the detector power dissipation. The continuous power rating for the APD's is 100 milliwatts and if, for example, the APD was biased at 180 volts and had a responsivity near 100 amps per watt, an optical power level as small as 5 microwatts could cause burnout from excessive dissipation. With the same 180 volt bias source and the 100 k ohm resistor in place, the maximum possible detector dissipation is 90 milliwatts, regardless of optical power. The DC photocurrent produced in the APD by the incident light will flow through the resistor which will create a voltage drop and thereby reduce the bias (and the gain) of the diode.

RCA 30908E's were used in the detector module largely because of the convenience of the integral light pipes which allowed simplified coupling to the fiber optic cables. Figure 4.5 is a perspective view showing the fiber optic connector at the right side, the RF output exiting the left end of the module, and the high voltage bias wires trailing from the far end. Figure 4.6 shows an open-box view with the APD mounted through the box at the top of the picture. The RF output port is at the left end and the bias inputs at the right end of the box. A large 0.1  $\mu$ f capacitor dominates the photograph.

#### 4.3 FIBER OPTIC CABLE AND CONNECTOR SELECTION

Based on the results of the thermal tests, the Corning fibers are an obvious choice for the 980 MHz tests. Siecor Cables use Corning fibers in their product line, and although the IVPO fiber was slightly less sensitive to phase change than the OVPO fiber, OVPO fiber was purchased because of substantial lead-time and cost savings. Siecor offers a strengthened two-fiber cable using the loose-tube approach discussed in Section 3.3, and the cable construction is shown in Figure 4.7. The cable (#222) uses fibers specified with attenuation of less than 6 db/Km and a bandwidth greater than 400 MHz-Km. For a link length of 200 meters, the signal response will be down less than 1 db at 980 MHz.

D180-25888-1

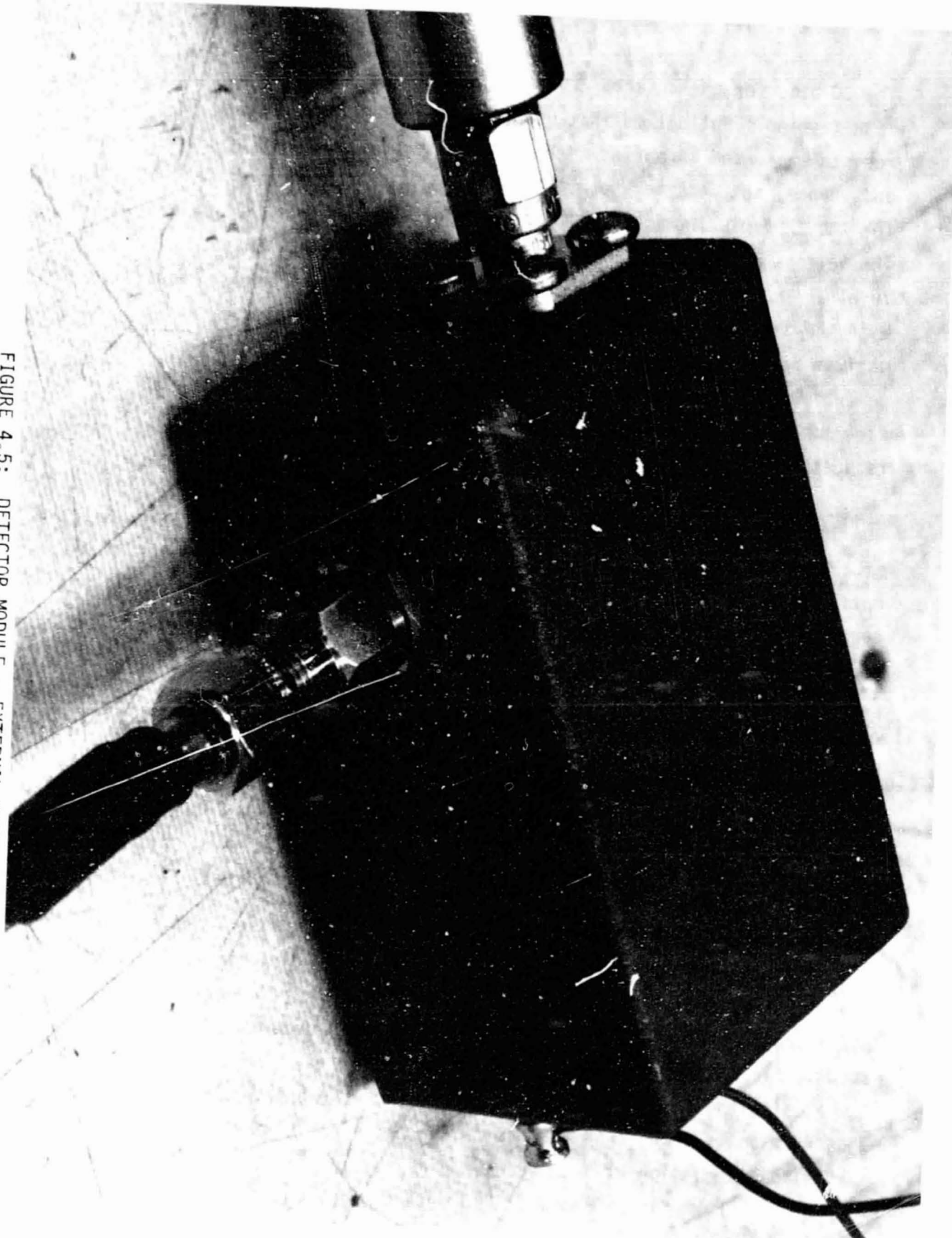
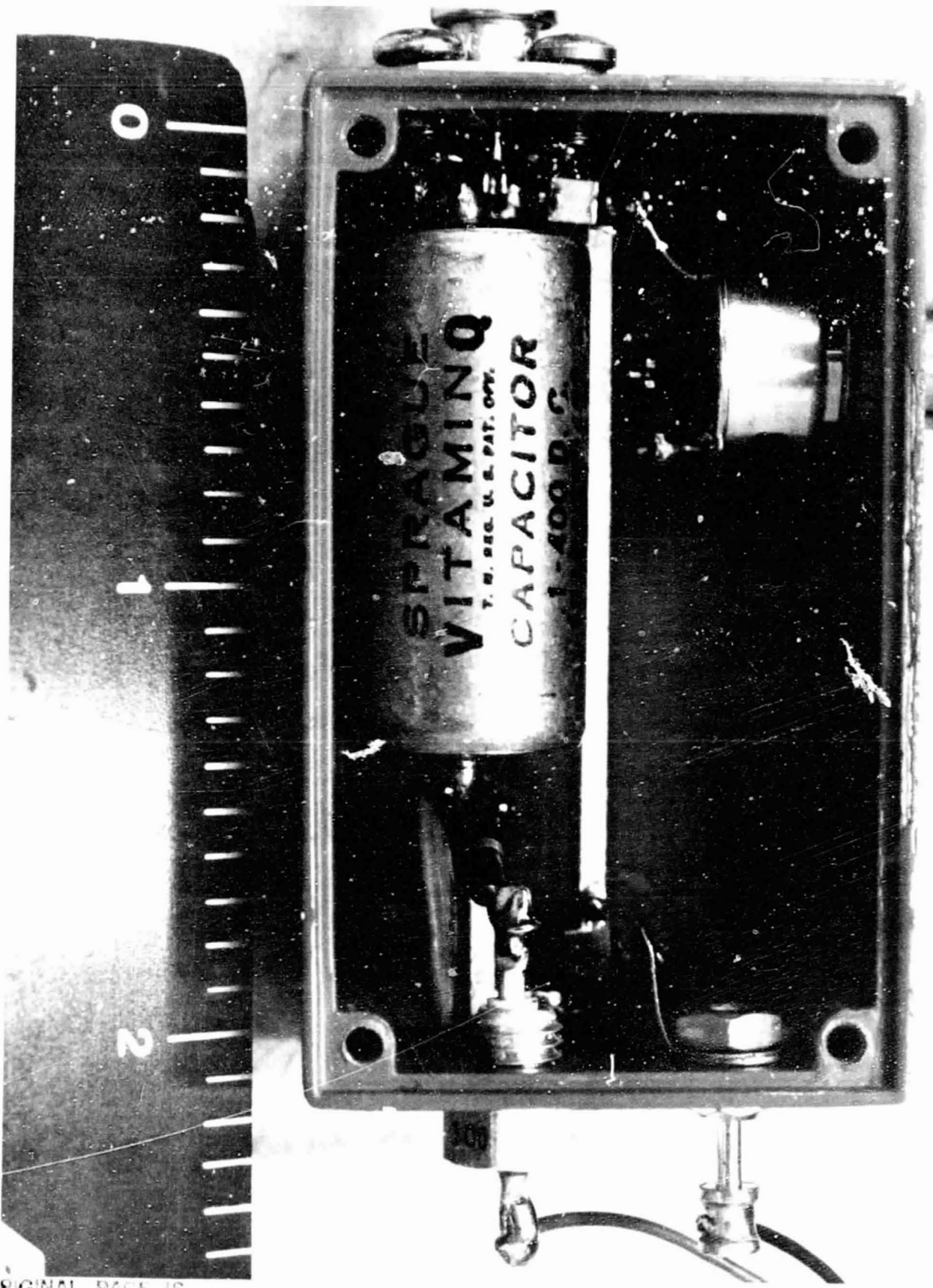


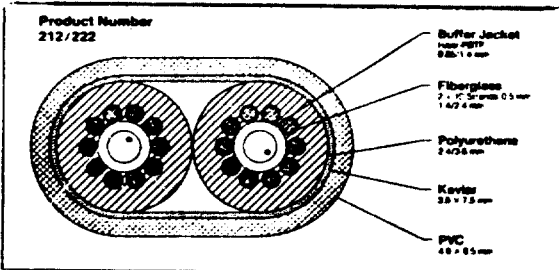
FIGURE 4.5: DETECTOR MODULE - EXTERNAL VIEW

D180-25888-1



ORIGINAL PAGE IS  
OF POOR QUALITY

FIGURE 4.6.: DETECTOR MODULE - INTERNAL VIEW

**Cable design**

Reliability of fiber optic cables is best achieved by maintaining the fibers in a stress-free condition. To achieve high reliability, the cables use a "loose buffer" design pioneered by SIECOR. Each optical fiber is mechanically isolated by spiraling it loosely inside an oversized buffer jacket. This permits considerable expansion and contraction of the cable from temperature change or mechanical loads before any stress is applied to the fibers, minimizing chances of increased attenuation or failure from stress fatigue. Also, when local stress is applied, the fiber accommodates it by sliding within the buffer jacket to reach the lowest possible stress level. Because of their design, SIECOR cables are rugged and perform well over a wide temperature range.

**Cable Construction and materials**

Each fiber is surrounded by a tough, double-layer buffer jacket that protects the fiber against impact and crushing forces. The buffer jacket is flexible, resists buckling, and can easily be removed mechanically for splicing and terminating. Stranded around each buffer jacket are ten 0.5 mm yarns of fiberglass embedded in a polyurethane inner sheath. The fiberglass gives added protection from crushing forces and contributes to cable strength. A layer of aramid yarn gives additional cushioning and provides most of the cable's longitudinal tensile strength. The outer sheath of polyvinylchloride (PVC) is fire retardant, pliable, scuff-resistant, and easily removed.

**CABLE PROPERTIES****SIECOR product number****Transmission specifications****Number of fibers**

Maximum attenuation @ 820 nm.

dB/km

Minimum bandwidth (-3 dB) @ 800 nm. MHz-km

**Installation characteristics**

Storage temperature range, on shipping reel

Operating temperature range, installed

Maximum tensile load for installation

Maximum tensile load, long-term operation

Minimum bend radius for installation, at 400 N

Minimum bend radius, unloaded (free sample)

**Mechanical properties**

Cable outside diameter, nominal

Cable weight, nominal

Crush resistance (between parallel plates, minimum value for negligible attenuation increase after force is removed)

Impact resistance (minimum value for fiber breakage, 13 mm hammer radius)

Flexing (50 mm radius,  $\pm 180^\circ$ , 1.0 N)**Structural cable strength****Fiber data****Fiber:**

Core diameter  
Outer diameter  
Coated outside diameter (lacquer coating, acetone stripable)  
Numerical aperture (100%, short length)

112	122	212	222
1		2	
10	6	10	6
200	400	200	400
-30 to +60°C			
-20 to +50°C			
400 N* (90 lb)			
50 N (11 lb)			
150 mm			
30 mm			
4.8 mm	4.9 x 8.5 mm		
24 kg/km	44 kg/km		
400 N/cm			
30 times at 1.5 Nm			
6000 times			
2000 N	4000 N		
63 $\mu$ m			
125 $\mu$ m			
136 $\mu$ m			
.21			

\*One Newton (N) is approximately equal to 0.225 pound force (lb.) or 0.102 kilogram force (kg.).

FIGURE 4.7. SIECOR 2 - FIBER CABLE SPECIFICATIONS

Amphenol connectors were chosen for the SPS link because of familiarity and generally good results in previous applications. Connections are normally less than 2 db of loss and very rugged and repeatable (with proper cleaning precautions). The part number is #906-110-5005.

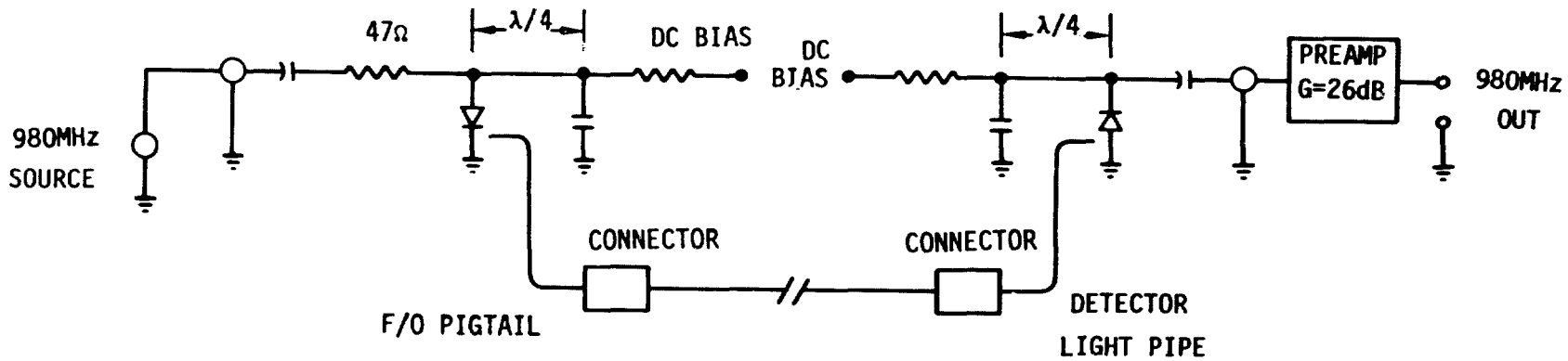
## 5.0 980 MHz ONE-WAY LINK TESTS

The 980 MHz tests were intended to evaluate fiber optic emitters and detectors at room temperature for signal throughput, modulation depth and sensitivity, and to investigate various effects in an optical fiber due to temperature variations. The effects included propagation delay (phase sensitivity), attenuation, and bandwidth changes. The tests employed one each of the emitter and detector modules constructed for the 980 MHz two-way link and the fiber selected was Corning IVPO fiber used in the 60 MHz thermal tests. The detailed test plans are attached in Appendix I. The emitter module was driven through a short length of high-frequency coaxial cable by a frequency synthesizer set to 980 MHz. The test fiber was placed in an environmental chamber and coupled to the detector module which was in turn connected to a small 50 ohm preamplifier. Current meters were used to monitor the emitter and detector bias currents. The 980 MHz source and the environmental chamber were the same units that were employed in the 60 MHz tests.

## 5.1 TEST RESULTS

Measurements of phase delay and attenuation were conducted at a fixed room temperature (Section 7) and at a variable temperature. The output voltage waveforms were monitored using a sampling oscilloscope and the trace was stable and clean throughout the entire test procedure. The basic test setup is depicted in Figure 5.1 which also indicates the optical and electrical signal levels used for the test.

The 980 MHz phase versus temperature test was run according to the test plan and the results are plotted in Figure 5.2 on a per Hz and per meter basis. Also plotted are the data points for the same fiber measured at 60 MHz, which lie on an identical curve. Clearly frequency scaling within the specified bandwidth product ( $\sim 1 \text{ GHz-Km}$ ) is valid.

EMITTER

- o NEC INJECTION LASER DIODE
- o BIAS COUPLED THROUGH QUARTER-WAVE MICROSTRIP
- o  $I_{BIAS} = 88\text{mA DC}$
- o OPTICAL POWER =  $437 \mu\text{watt}$  @ Emitter Digitail
- o  $V_{980\text{MHz}} = 0.7 \text{ VOLTS RMS}$

FIBER

- o CORNING IVPO, GRADED INDEX
- o LENGTH = 303 METERS
- o ATTEN. =  $3.9\text{dB/km}$
- o BW =  $870\text{MHz-km}$
- o N.A. = 0.213

DETECTOR

- o RCA AVALANCHE PHOTODIODE
- o BIAS COUPLED THROUGH QUARTER-WAVE MICROSTRIP
- o  $V_{BIAS} = 180 \text{ VOLTS DC}$
- o OPTICAL POWER =  $228 \mu\text{watt}$  @ DETECTOR LIGHT PIPE
- o  $V_{980\text{MHz}} = 135 \text{ mv RMS OUT OF PREAMP}$

FIGURE 5.1 INITIAL SPS 980MHz FIBER OPTIC LINK TEST

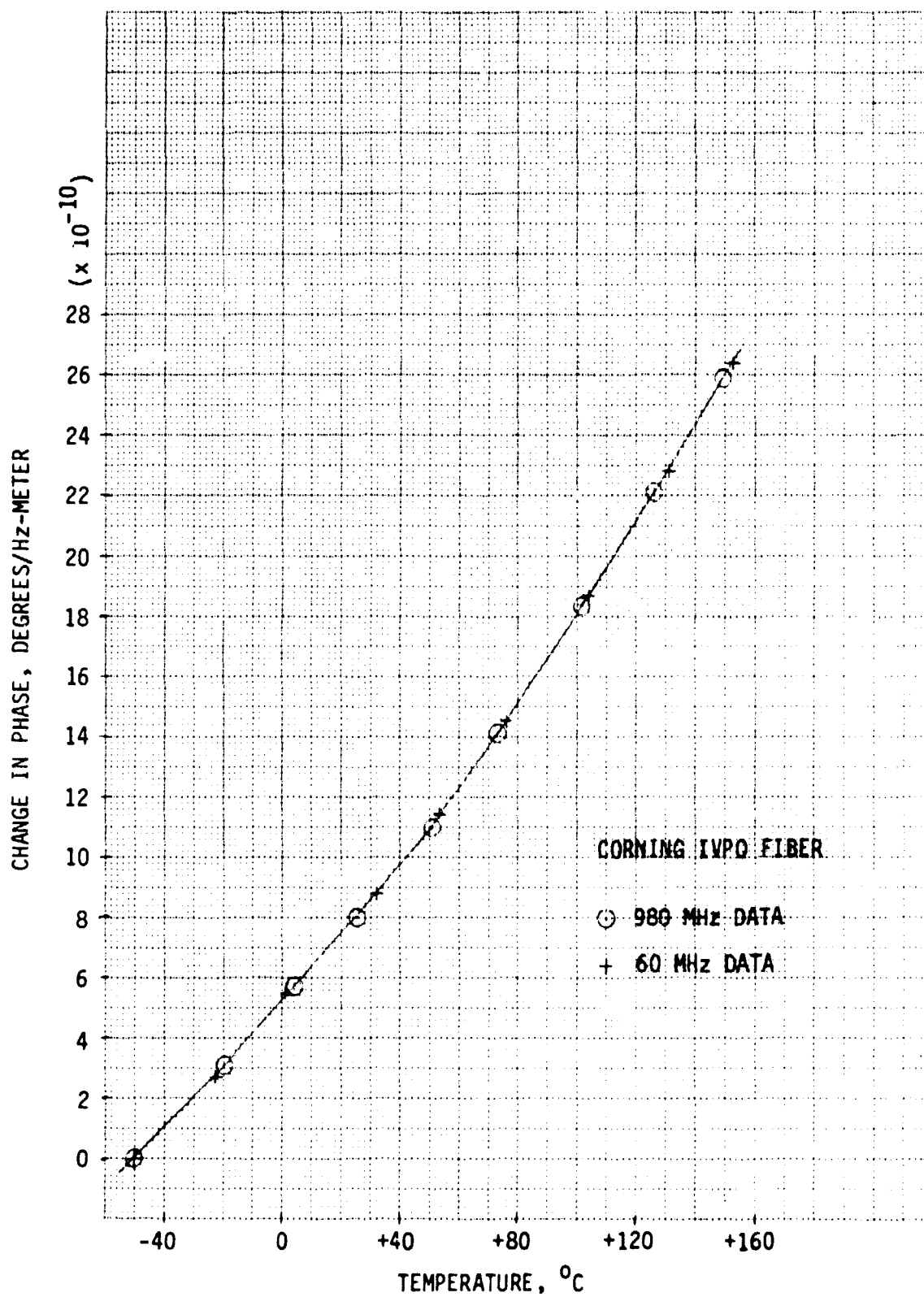


FIGURE 5.2. 980 MHz PHASE VS TEMPERATURE TEST

The identical results at the two frequencies stem from the fact that linear thermal expansion and index of refraction variation are bulk properties of the fiber, affecting all propagation modes equally. Each effect serves to introduce a change in the time for the light to travel through the fiber, causing the phase to change according to:

$$\Delta\theta^\circ = \frac{360}{f_{\text{mod}}} \Delta t$$

Where:

$\Delta\theta^\circ$  = phase change, in degrees

$\Delta t$  = change in fiber propagation time due to a temperature change

$f$  = modulation frequency (980 MHz, etc.)

The fiber will transmit different wavelengths of light at different velocities due to variations of refractive index with wavelength, but any effects due to sideband generation are insignificant because the modulation frequencies are so far below that of the optical frequency ( $f_0 = c/\lambda_0 = 3.49 \times 10^{14}$  Hz). In both cases, negligible hysteresis between increasing and decreasing temperature cycles was observed, so long as adequate time to obtain thermal equilibrium was allowed.

The 980 MHz attenuation versus temperature tests were run according to the test plan except that the electrical output out of the detector and the optical incident power level were recorded simultaneously, thereby allowing a more valid comparison. Optical power could be measured directly by removing the fiber end from the detector module and inserting it into the photometer head (and vice versa), but connector repeatability may introduce inaccuracies. An alternate solution, and the one utilized, was to monitor the DC current from the detector module high voltage supply. The DC current was used directly as a measure of small changes in optical power ( $\pm 10\%$ ), since it is actually the average photocurrent produced by the average optical power. The relationship between the DC current and the incident optical power was determined at room temperature, and all other optical powers were calculated proportionally.

The test results are plotted in Figure 5.3.

The lower curve shows a negligible variation of the transmitted optical power with temperature. The power was measured to be continually between 227 and 229 microwatts, which is less than 1% total change and is within test equipment accuracy. It can thus be concluded that the fiber optical attenuation is constant over the temperature range of the tests.

The upper curve shows the response of the link at 980 MHz. The ordinate shows the rms voltage at 980 MHz measured out of the preamp with the vector voltmeter. The difference between the lower curve and the upper curve gives an indication of the effects of temperature on the bandwidth. A slight rolloff can be seen between 0°C and -50°C. The bandwidth is not affected between 0°C and +50°C, but above 50°C a drop in response is again observed, with the curve flattening out again towards +150°C.

The full explanation of the effects is not yet clear; a possible explanation may arise in that as the refractive index varies with temperature, the precisely controlled index grading may be disturbed which, in turn, may reduce the bandwidth. Further study is recommended.

The exact relationship between the fiber length and its frequency response is a complex subject.<sup>(12)</sup> Frequently it is assumed that the fiber length times its 3 db frequency response roll-off point is a constant. This constant for the test fiber (measured by Corning) at room temperature is 870 MHz-Km which implies that the response at 980 MHz for 1 Km will be 3.56 db below the response at low frequencies. This value must be added to the normal optical attenuation figure ( 3.9 db/Km) to obtain the actual 980 MHz component attenuation value of 7.16 db/Km. An additional loss (Fig. 5.3) is observed at higher temperatures, approximately equal to 0.45 db, which for a constant length-bandwidth product translates to 1.48 db/Km.

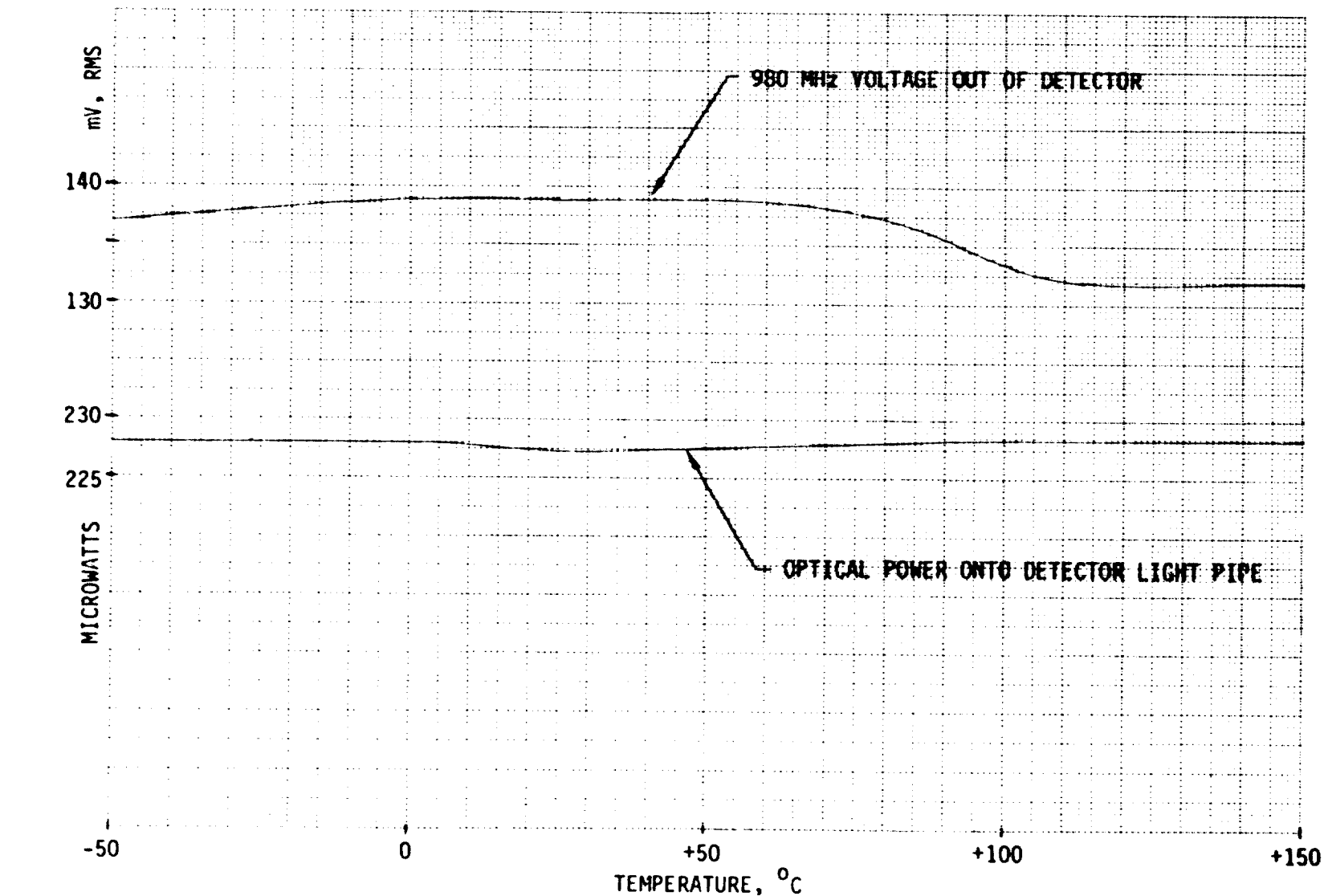


FIGURE 5.3. 980 MHZ ATTENUATION VS TEMPERATURE TESTS

D180-25888-1

## 6.0 980 MHz TWO-WAY LINK DEVELOPMENT

The two-way link development involved three tasks:

- (1) Determination of the optimum operating conditions for each emitter module, including bias and drive levels.
- (2) Determination of the optimum operating conditions for each detector module, including bias and optical input power levels.
- (3) Phase-matching of the two links by adjusting the fiber lengths to within  $\pm 90^\circ$  at 980 MHz; however, the links were successfully matched to  $\pm 10^\circ$ .

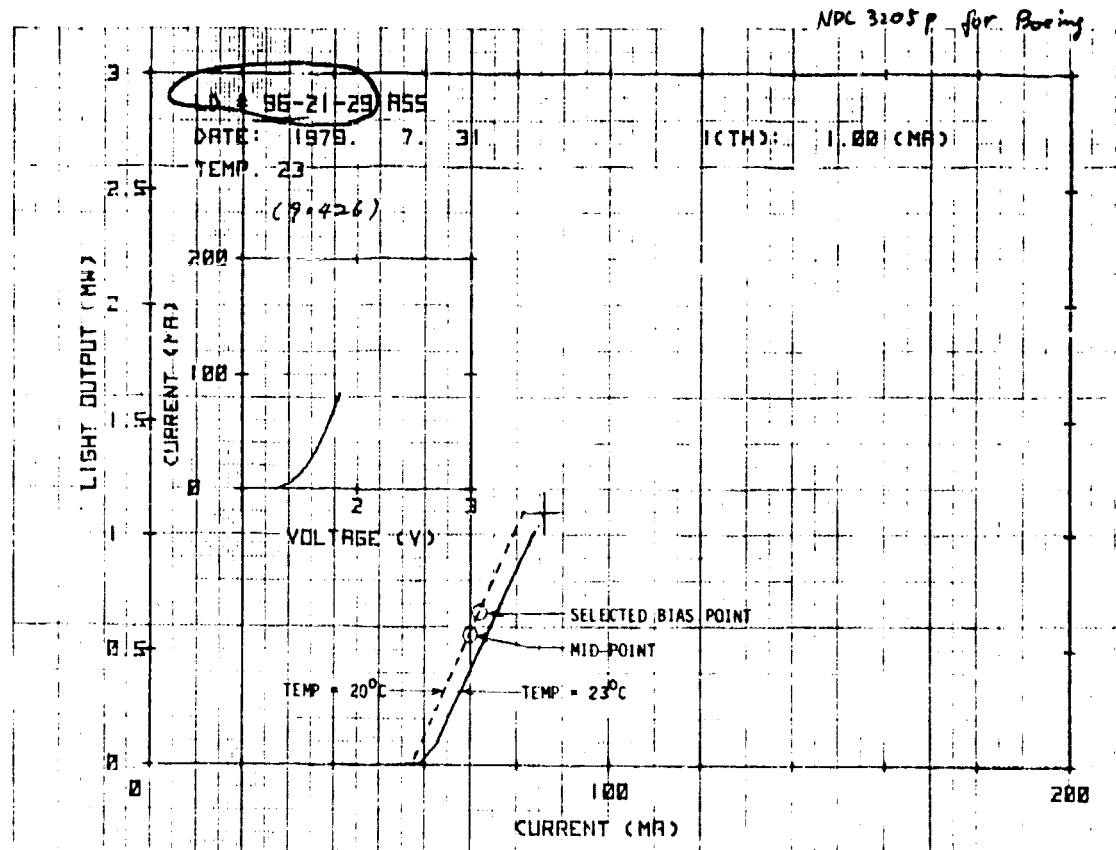
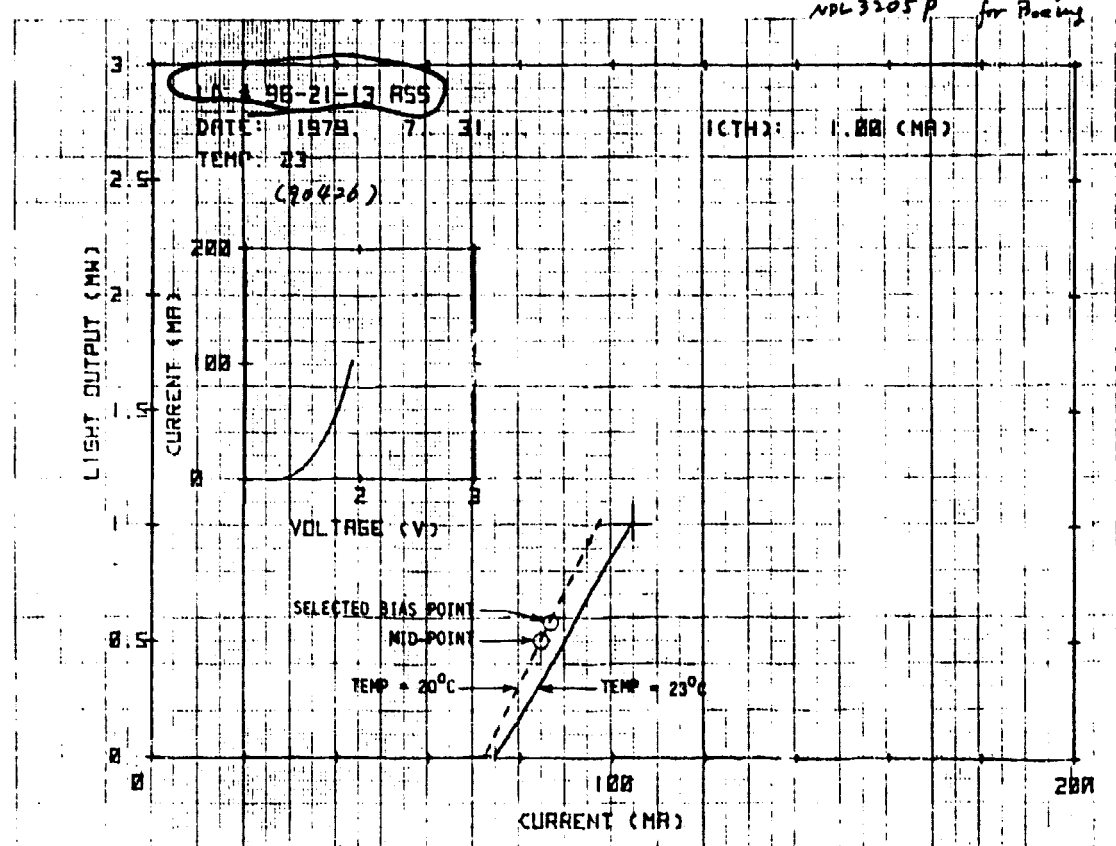
### 6.1 EMITTER OPERATING CONDITIONS

To accomplish thermal stabilization of the emitter module, a thermistor is used as a sensor in an active feedback loop and the potentiometer gives the ability to set the diode standard temperature to a desired value. The temperature value used is not critical, but does have an effect on the bias requirements and wavelength of operation. Since neither has much system significance, the temperatures were arbitrarily set to  $20^\circ\text{C}$ .

The NEC supplied data of optical power versus bias current at  $23^\circ\text{C}$  for each of the laser diodes was replotted in Figure 6.1 at the reduced temperature of  $20^\circ\text{C}$ . For a fixed value of bias current, a small change in temperature can have a large effect on the optical output power validating the need for thermal stabilization.

The linear portion of the curves above the threshold knee represents the range in which the devices are operated. The mid-points for each of the curves is indicated and correspond to the current levels for the DC bias for normal sinusoidal modulation. It was determined, however, that a slight

D180-25888-1



ORIGINAL PAGE IS  
OF POOR QUALITY

FIGURE 6.1. INJECTION LASER DIODE BIAS CURVES

bias current increase served to extend the lasers' frequency response such that the resonance peaks were pushed farther away from 980 MHz. Phase transmission was found to be more stable, and the selected current values are also indicated on the curves. The crosses at the upper ends of the curves represent the peak power output points as recommended by NEC for long device lifetimes.

For each device, the maximum modulation signal was determined by varying the signal swing magnitude and concurrently monitoring the optical output power. Maximum modulation was attained when a sudden increase was observed in the average optical power reading, implying that the laser was being driven into cut-off on the negative AC current peaks. For emitter module # 96-21-29 the rms voltage applied should be less than 0.7 volts; whereas, the maximum applied voltage for emitter # 96-21-13 is 0.8 volts rms.

The above empirical values may be compared to values obtained by graphical analyses. For both ILD's, the peak current swing from the bias point to the cut-off point is 14 ma which becomes 0.70 volts peak required at the 50 ohm input terminals to the modules, or 0.5 volts rms. The discrepancy is not presently understood, but clearly some overdrive is allowed, implying that the AC slope is more horizontal than the plotted DC bias curve slope. Further investigation is suggested. The DC bias current and, to a lesser extent, 980 MHz drive levels, both affect the phase lag through the emitter modules. Measured data are discussed in Section 7.2.

## 6.2 DETECTOR OPERATING CONDITIONS

Pertinent test data which were supplied by RCA for each avalanche photodetectors are given in Figure 6.2. A value for breakdown voltage is listed for each device, above which excess shot noise is observed. For Diode # 0223, the selected bias value was 175 volts, and for Diode # 0225 it was 180 volts. The actual bias voltages applied to the detector will

TYPE: C30908ESERIAL NO: 0227• TEST DATA AT 22°C

OPERATING VOLTAGE 173 VOLTS  
 BREAKDOWN VOLTAGE 178 VOLTS  
 DARK CURRENT 16 NANO AMPS  
 RESPONSIVITY .77 AMPS/WATT AT 930 nm  
 NOISE CURRENT  $2 \times 10^{-13}$  AMPS/HZ $\frac{1}{2}$   
 RISETIME <.5 NANoseconds

• FOR TYPES C30903E THROUGH C30908E THE  
 OPTICAL MEASUREMENTS ARE REFERRED TO  
 RADIATION FALLING ON THE INPUT OF THE  
 LIGHT PIPE.

*B. S. Giffen*  
Feb 220 79

TYPE: C30908ESERIAL NO: 0225• TEST DATA AT 22°C

OPERATING VOLTAGE 179 VOLTS  
 BREAKDOWN VOLTAGE 184 VOLTS  
 DARK CURRENT 16 NANO AMPS  
 RESPONSIVITY .77 AMPS/WATT AT 930 nm  
 NOISE CURRENT  $2 \times 10^{-13}$  AMPS/HZ $\frac{1}{2}$   
 RISETIME <.5 NANoseconds

• FOR TYPES C30903E THROUGH C30908E THE  
 OPTICAL MEASUREMENTS ARE REFERRED TO  
 RADIATION FALLING ON THE INPUT OF THE  
 LIGHT PIPE.

*B. S. Giffen*  
Feb 220 79

FIGURE 6.2. AVALANCHE PHOTODIODE BIAS DATA

always be less than the supply voltages due to the action of the 100 K ohm resistors and will vary as the incident light level varies. The bias will affect the width of the internal depletion region which will, therefore, alter the diodes' drift rates and the system frequency response. A roll-off in frequency response will have a detrimental effect on phase lag, and therefore, should be beyond 980 MHz. A high value of bias is required for extended frequency response, and the selected approach was to limit the incident optical power by inserting small spacers inside the connectors of the emitter modules.

Tests were run to determine the effect of varying the incident optical power on the phase delay. The test setup was configured as in Figure 6.3 and the critical data points are recorded in Figure 6.4. As a compromise between operating in the flatter regions of the curves and good signal-to-noise ratios, the decision was made to adjust the optical powers close to the indicated peak response points. With optical powers greater than these values, the rms output voltages began to decrease in amplitude due to the reduced frequency response effects discussed above, even though the input signal was actually stronger. The phase sensitivity above the peak response points is also obvious.

The emitter-detector pairing was as shown in Figure 6.5. After the spacers were inserted into the respective emitter module fiber optic connectors, the actual values of incident optical powers and DC photocurrents were:

<u>Detector</u>	<u>DC Current</u>	<u>Incident Optical Power</u>
#0223	0.39 ma	82 microwatts
#0225	0.39 ma	73 microwatts

If the 980 MHz signal source was removed from the emitter modules, only noise should remain at the detector outputs. However, in both cases, the noise power was insufficient to be measured directly with the RF power meter. Using detector module #0223 as an example, a mathematical noise analysis can be performed.

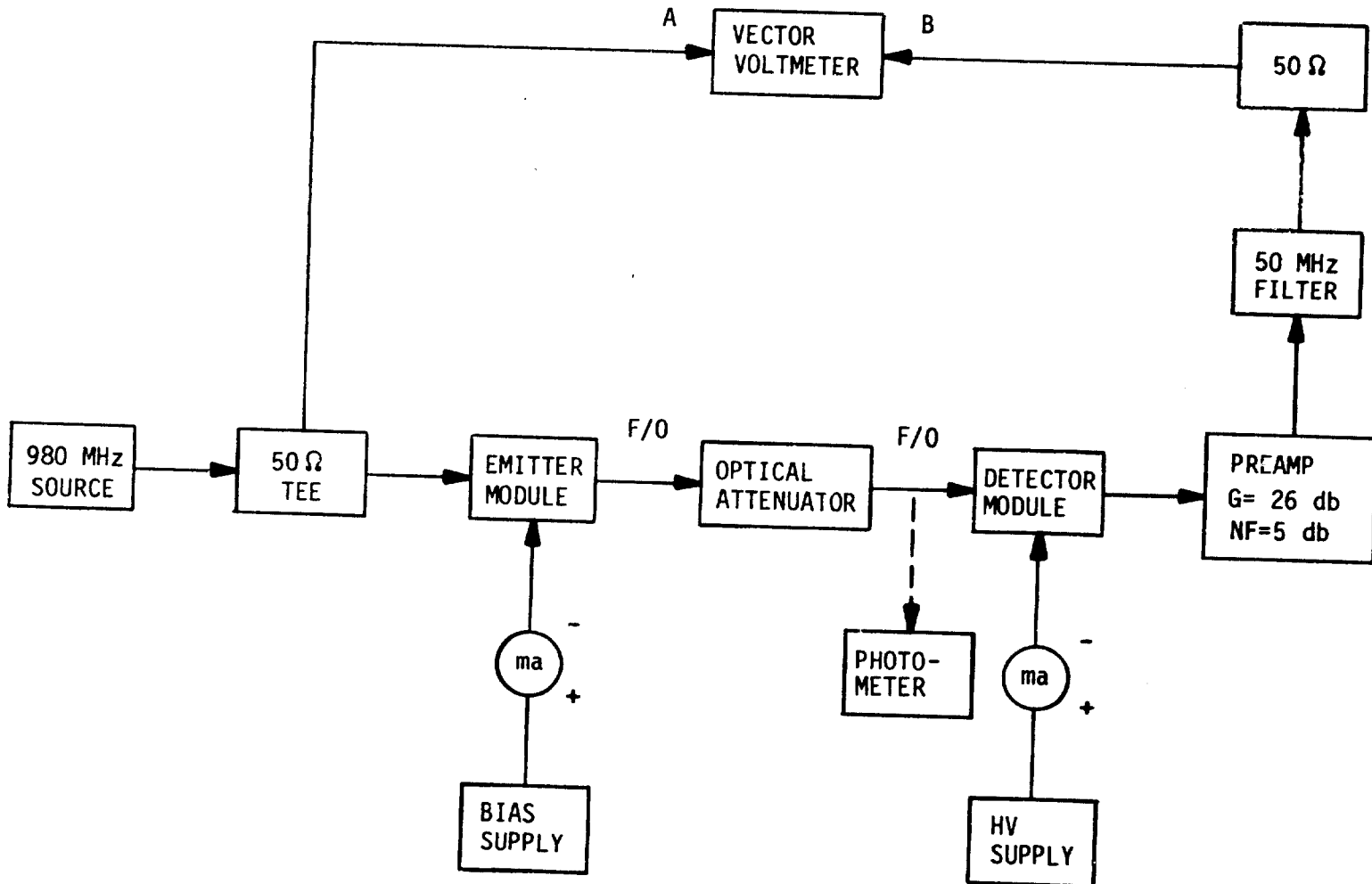


FIGURE 6.3 DETECTOR MODULE PHASE TEST

D180-25888-1

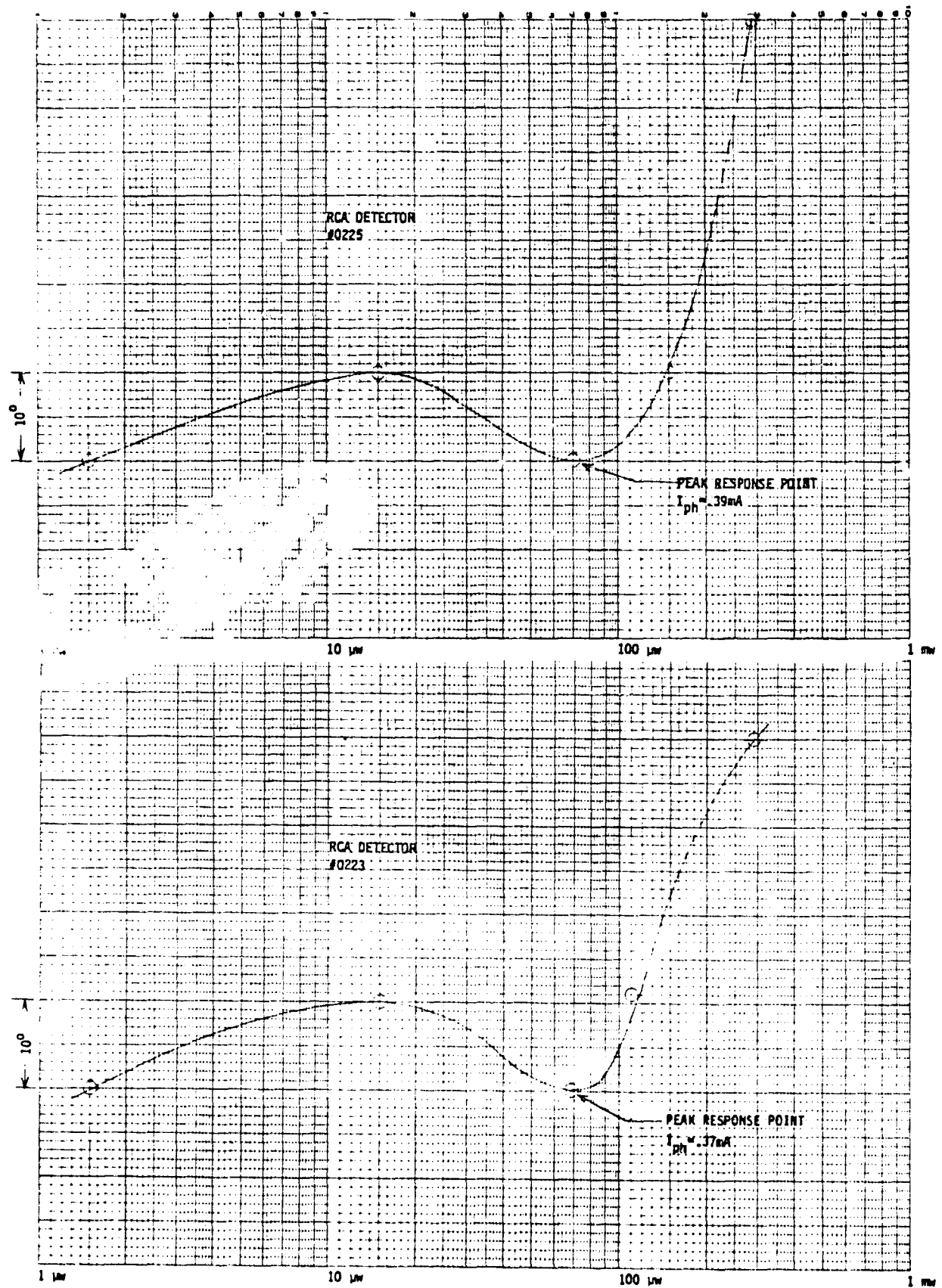


FIGURE 6.4 DETECTOR MODULE PHASE SENSITIVITY **ORIGINAL PAGE IS OF POOR QUALITY**

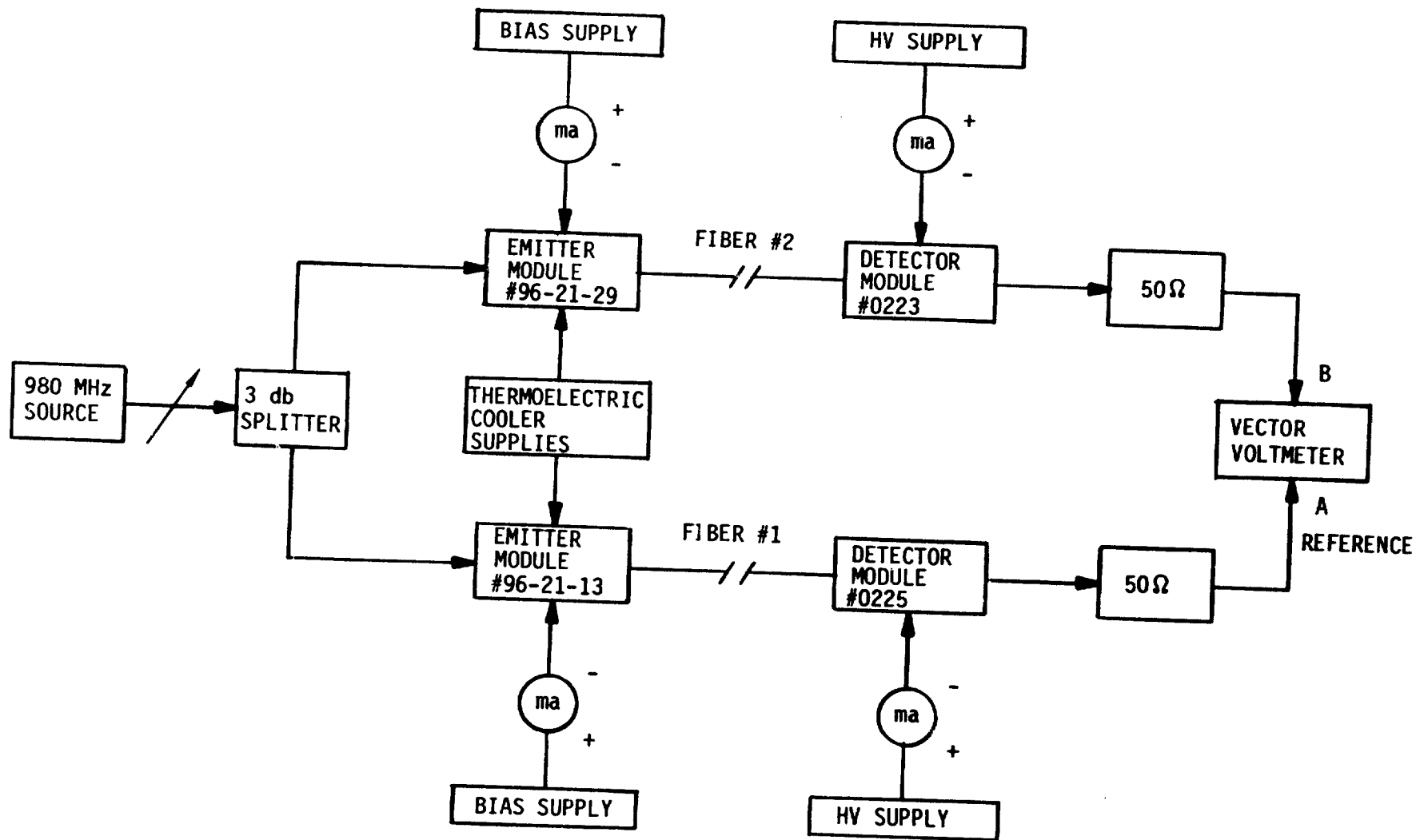


FIGURE 6.5 PHASE MATCHING OF 980 MHZ TWO-WAY LINK

Assume that the APD quantum efficiency is 75% and that the coupling efficiency of the fiber to the detector surface through the light pipe is 50%. The DC responsivity is given as:

$$R = \frac{n_c n_q G q \lambda}{hc} \text{ amps per watt}$$

Where  $R$  = APD responsivity

$n_c$  = coupling efficiency

$n_q$  = quantum efficiency

$G$  = internal avalanche gain

$q$  = the electronic charge ( $1.6 \times 10^{-19}$  coul)

$\lambda$  = optical wavelength (860 nm)

$h$  = Planck's constant ( $6.625 \times 10^{-34}$ )

$c$  = speed of light in a vacuum ( $3 \times 10^8$  meters/sec)

By insertion of the given values,  $R = 0.26 G$  amps per watt. The measured value for  $R$  is given by taking the quotient of the DC photocurrent and the incident optical power:  $R = \frac{0.39 \times 10^{-3}}{82 \times 10^{-6}} = 4.76$  amps per watt, and, therefore, the avalanche gain,  $G = 18.3$ .

The post-detection amplifier used in the tests had a gain of 26 db, and a noise figure of 5 db at 50 ohms. A filter followed the preamp which had a noise bandwidth of approximately 50 MHz, centered at 980 MHz.

If a preamp is said to have a noise figure of 5 db at 50 ohms, it is implied that its output noise power, if referred back to the input, is 3.16 times the noise power of a 50 ohm resistor when that 50 ohm resistor is connected as its source. If we assume that the preamplifier's noise is independent of source impedance, then, since noise powers add, the amplifier's output noise, if referred to the input when the resistor is removed, becomes 2.15 times the noise power of a 50 ohm resistor. At room temperature, 290°K, the mean square noise current for a 50 ohm resistor (Johnson noise) is given as:

$$\langle i_{50}^2 \rangle = \frac{4 k T \Delta f}{50} \text{ amps}^2 = 1.601 \times 10^{-14} \text{ amps}^2$$

where  $\langle i_{50}^2 \rangle$  = mean square 50 ohm noise current,  $\text{amps}^2$   
 $k$  = Boltzmann's constant =  $1.38 \times 10^{-23}$   
 $T$  =  $290^\circ$  Kelvin  
 $\Delta f$  = noise equivalent bandwidth (50 MHz)

and, therefore, the preamplifier noise current becomes:

$$\langle i_a^2 \rangle = 2.16 \langle i_{50}^2 \rangle = 3.458 \times 10^{-14} \text{ amps}^2$$

When a DC current flows through a semiconductor junction, such as an ADP, a shot noise is created; also due to some randomness in the avalanche gain mechanisms, excess noise is also generated. Empirically,<sup>(16)</sup> it has been determined that this noise contribution can accurately be modeled as:

$$\langle i_{ph}^2 \rangle = 2q I_{ph} G^{1.5} \Delta f \text{ amps}^2$$

where:  $\langle i_{ph}^2 \rangle$  = mean square photocurrent noise  
 $I_{ph}$  = DC photocurrent = 0.39 ma

and inserting values yields:  $\langle i_{ph}^2 \rangle = 4.885 \times 10^{-13} \text{ amps}^2$ .

The noise term due to dark current is included in the effects of the measured DC photocurrent. Summing the mean square noise terms gives the total noise referred to the amplifier input as  $\langle i_T^2 \rangle = \langle i_{ph}^2 \rangle + \langle i_a^2 \rangle = 5.231 \times 10^{-13} \text{ amps}^2$ .

The noise power into 50 ohms after an amplification of 26 db becomes:

$P_N = \langle i_T^2 \rangle \cdot 50 \cdot 26 \text{db} = 1.041 \times 10^{-8} \text{ watts}$ . The noise value of the 980 MHz signal component at the same point, measured with an RF power meter, was  $6.370 \times 10^{-4}$  watts. Therefore, the signal-to-noise ratio is calculated as:  
 $\text{SNR} = \frac{6.370 \times 10^{-4}}{1.041 \times 10^{-8}} = 6.118 \times 10^4 = 47.9 \text{ db}$  (Detector #0223).

A similar analysis for detector #0225 yields:  $\text{SNR} = \frac{6.970 \times 10^{-4}}{1.226 \times 10^{-8}} = 5.686 \times 10^4 = 47.55 \text{ db.}$

It is possible to calculate the AC efficiency product for each emitter-detector pair. If the AC efficiency product was unity, then the peak AC current value out of the detector would be equal to the DC photocurrent, provided the dark current was negligible. If the measured output powers are referred back to the detector module output by the preamplifier gain (26 db) and converted to AC current values into 50 ohms, it is found that:

$$i_{\text{AC}} (\text{rms}) = 1.780 \times 10^{-4} \text{ amps (Detector #0223)}$$

$$i_{\text{AC}} (\text{rms}) = 1.871 \times 10^{-4} \text{ amps (Detector #0225)}$$

Multiplying each value by  $\sqrt{2}$  gives the sinusoidal peak value for each:

$$i_{\text{AC}} (\text{peak}) = 2.530 \times 10^{-4} \text{ amps (Detector #0223)}$$

$$i_{\text{AC}} (\text{peak}) = 2.646 \times 10^{-4} \text{ amps (Detector #0225)}$$

and, thus, the emitter-detector efficiency products are seen to be:

$$\frac{0.253 \text{ ma}}{0.390 \text{ ma}} = 64.9\% \text{ (Detector #0223)}$$

$$\text{and } \frac{0.2646 \text{ ma}}{0.390 \text{ ma}} = 67.8\% \text{ (Detector #0225)}$$

which are felt to be excellent figures at 980 MHz. It is possible to increase the efficiencies even more (at the expense of a small amount of harmonic distortion) if the emitter RF drives are increased. The effects of fiber bandwidth also play a role in the efficiency term. At this time, the tools for distinguishing the various effects are not available. The effect of bias on detector phase change is discussed in Section 7.

### 6.3 980 MHz DUAL LINK PHASE MATCHING

Experimental measurements of total link phase delay indicated a significant phase mismatch between the two links. By using a common fiber and detector, it was found that Emitter Module #96-21-13 lagged Emitter Module #96-21-29 by approximately 50° at 980 MHz. This was higher than expected, but the difference was stable. It was also determined that one of the fibers in the two-fiber cable was optically shorter, even though their physical lengths appeared to be identical. As a consequence, the optically shorter fiber (designated as Fiber #1) was used with Emitter #96-21-13 in the link to provide some compensation for effects. The phase difference between the detector modules was measured to be only about 10°.

The dual links were configured into the test setup shown by Figure 6.5. By decreasing the RF frequency, it was found that the phase difference traveled through zero degrees at approximately 300 MHz intervals. This implied a path length difference of  $\frac{980}{300} = 3.27$  wavelengths at 980 MHz.

Phase matching of the two links was accomplished by physically trimming the lengths of the two fibers. The calculated physical wavelength for one 980 MHz cycle (360°) is 8.2 inches along a fiber. Three wavelengths ( $\approx 24$  inches) were cut from the optically longer fiber, thereby causing the phase difference to monotonically approach zero degrees with decreasing frequency. At this point, the final length cut was determined by the formula:  $L = \frac{1}{360} \cdot \frac{C}{n \text{ 980 MHz}}$  (meters), where  $\theta$  = the measured phase

difference in degrees. After two attempts, the technique proved successful, and the fibers were terminated. The final apparent length difference was 26.5 inches, and the phase difference between the two links was, to within test equipment tolerances, less than  $\pm 10^\circ$  at 980 MHz. Fiber #2 appears physically shorter.

The total length of the Siecor cable is approximately 250 meters, and thus the percent difference in length is 0.27%. The difference could be explained by imbalances in the cabling process, such as a difference in fiber tension as the fibers were reeled off their spools. The cable uses a loose-tube construction and it is conceivable that one of the fibers was pulled fairly straight, whereas the other was laid in a helical fashion causing it to appear shorter. It is also possible that a difference in refractive index exists between the two fibers. Nominally, the core index value is equal to 1.470, and if, for example, the dopant process was upset, an index in the second fiber of 1.474 could cause the required length difference. According to Corning, such a difference is not likely, but is possible. Realistically, the difference is probably best explained by a combination of the two factors.

The phase discrepancy between the two emitter modules is not clearly understood at this time. However, a suggested explanation stems from the observation that the resonance frequency points for the two ILD's were different. The resonance frequency for Emitter Module #96-21-13 was appreciably lower than that of Emitter Module #96-21-29 and not much greater than 980 MHz ( $\approx 1$  GHz). Phase sensitivity is expected to be high in this region. In addition, a slight physical length mismatch may exist between the two ILD fiber pigtauls.

## 7.0 980 MHz TWO-WAY LINK CHARACTERISTICS

This section describes all of the bias and drive level requirements, input and output optical power levels and input and output RF power measurements. In addition, data are plotted for phase variation versus emitter bias, emitter RF drive, and detector bias. The link characterization test setup is shown in Figure 7.1 which shows the link, the vector voltmeter, the RF source, and the necessary power supplies and parameter measurement instruments.

### 7.1 INPUT AND OUTPUT LEVEL SPECIFICATIONS

The 980 MHz two-way link test setup is described in Figure 6.5. All of the pertinent operating characteristics are shown in Figure 7.2. It is suggested that the emitter bias currents, detector bias voltages, and emitter RF power inputs be as close to the chart figures as is possible in order to maintain the phase match and close balance between detector RF power outputs.

The thermoelectric coolers may alternate between cooling (positive supply current) and heating (negative supply current) for a short period after turn-on or if the injection laser diodes are not biased on and there is no heat load. Immediately upon turn-on there will be a large cooling current surge which will last for a few seconds and then subside to normal conditions. It is recommended that the lasers never be operated while the coolers are not functioning.

### 7.2 PHASE MISMATCH VERSUS INPUT PARAMETERS

In order to determine the link-to-link phase mismatch variations which can be tolerated in the SPS path length compensation scheme, the phase delay through the link as a function of input bias and drive parameters was measured. In each case, all other parameters were held at their nominal values as given in Figure 7.2. Emitter bias was by far the most sensitive parameter (Figure 7.3), and therefore, extra efforts should be taken to assure that the bias currents match the suggested values.

D180-25888-1

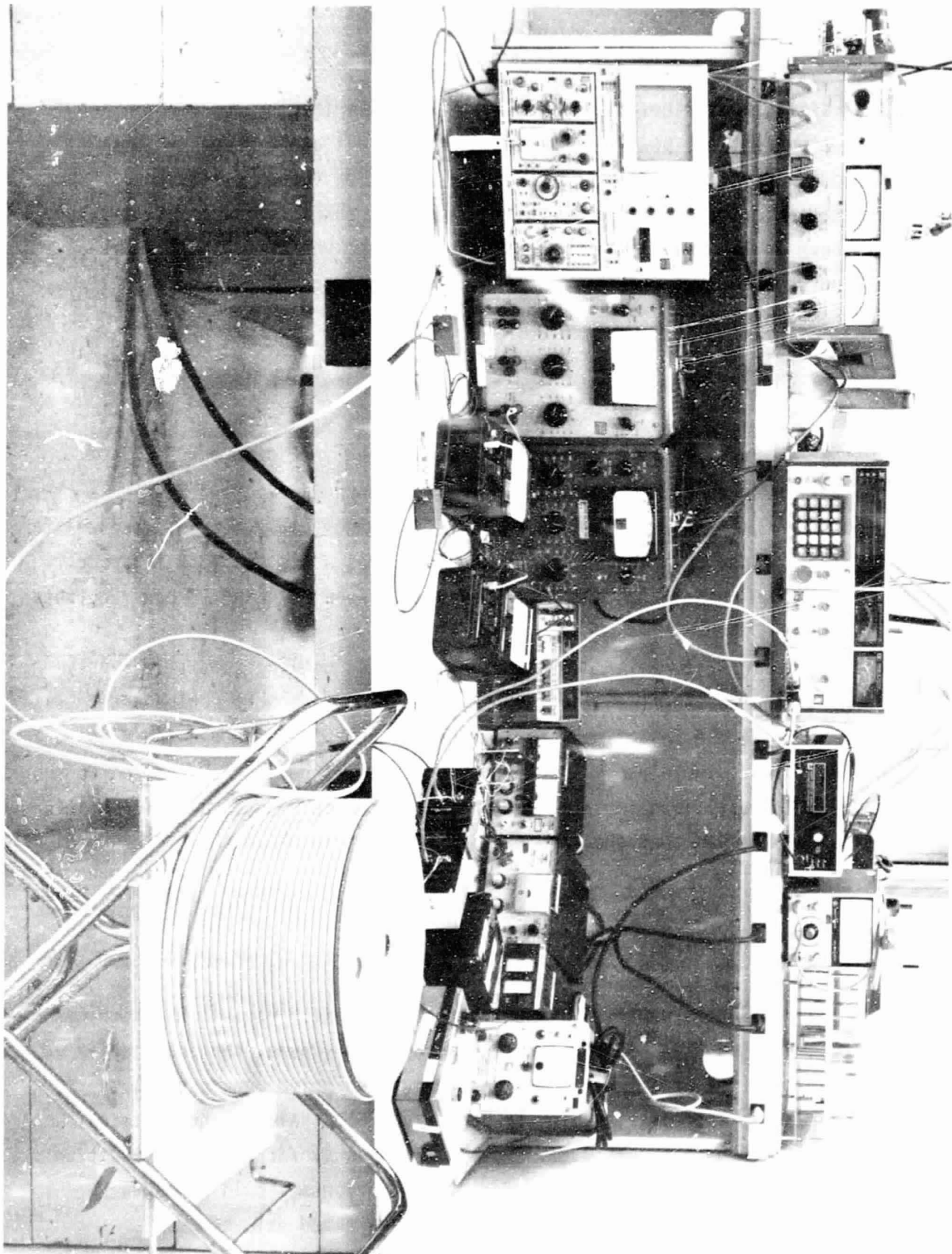


FIGURE 7.1.: DUAL LINK CHARACTERIZATION TEST SETUP

EMITTER MODULE CHARACTERISTICS

<u>Emitter Module</u>	<u>DC Bias Current</u>	<u>DC Bias Voltage</u>	<u>RF Power Input @ 50Ω</u>	<u>Optical Power Out</u>
#96-21-29	72 ma	+5.7 volts	6.4 mw	650 microwatts
#96-21-13	87 ma	+6.5 volts	6.9 mw	580 microwatts

DETECTOR MODULE CHARACTERISTICS

<u>Detector Module</u>	<u>DC Bias Voltage</u>	<u>Optical Power In</u>	<u>DC Photocurrent</u>	<u>RF Power Output @ 50Ω</u>
#0223	+175 volts	82 microwatts	0.39 ma	1.6 milliwatts
#0225	+180 volts	73 microwatts	0.39 ma	1.75 milliwatts

THERMOELECTRIC COOLER REQUIREMENTS  
(WITH Emitter Modules)

<u>DC Bias Voltage</u>	<u>DC Bias Current @ 72°F</u>
+5 volts	0.2 amps each at steady state
-5 volts	<100 ma each at steady state

FIGURE 7.2 980 MHz TWO-WAY LINK OPERATING CHARACTERISTICS

Detector bias, when varied as in Figure 7.4, showed little effect until it dropped below 160 volts in both cases. Operation much above the suggested values is discouraged because of the possibility of destruction of the APD's. Emitter RF drive (980 MHz), as plotted in Figure 7.5, had little effect on phase, but it is recommended that high drive levels be maintained to ensure good receiver signal-to-noise ratios.

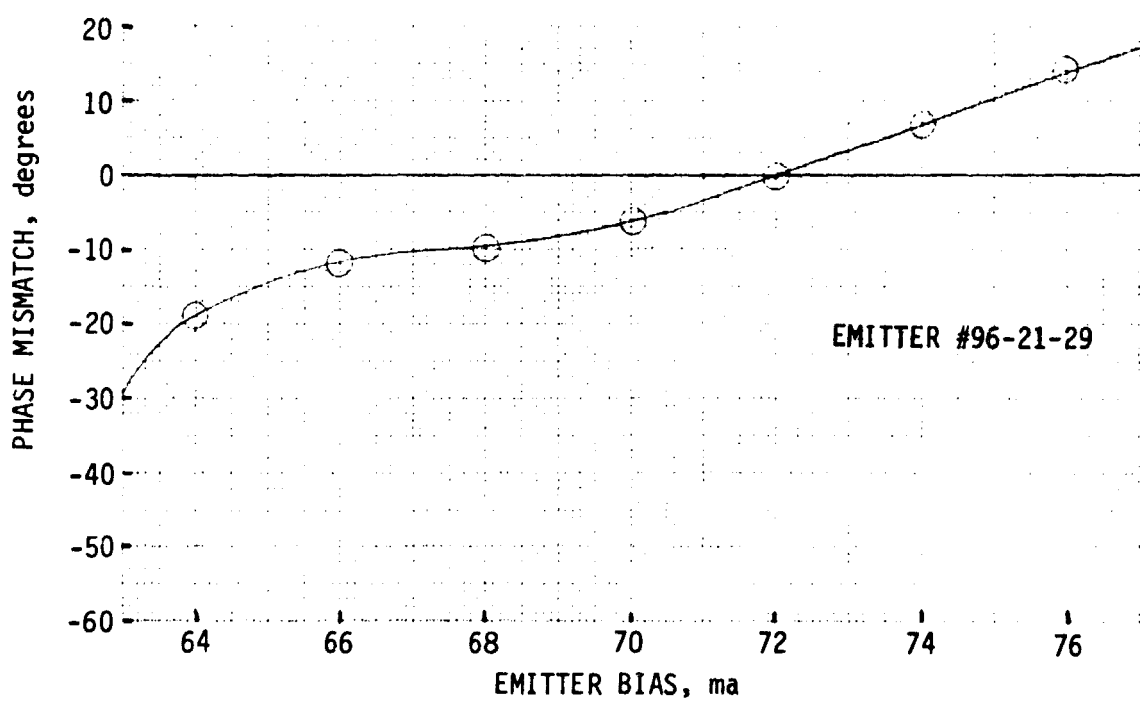
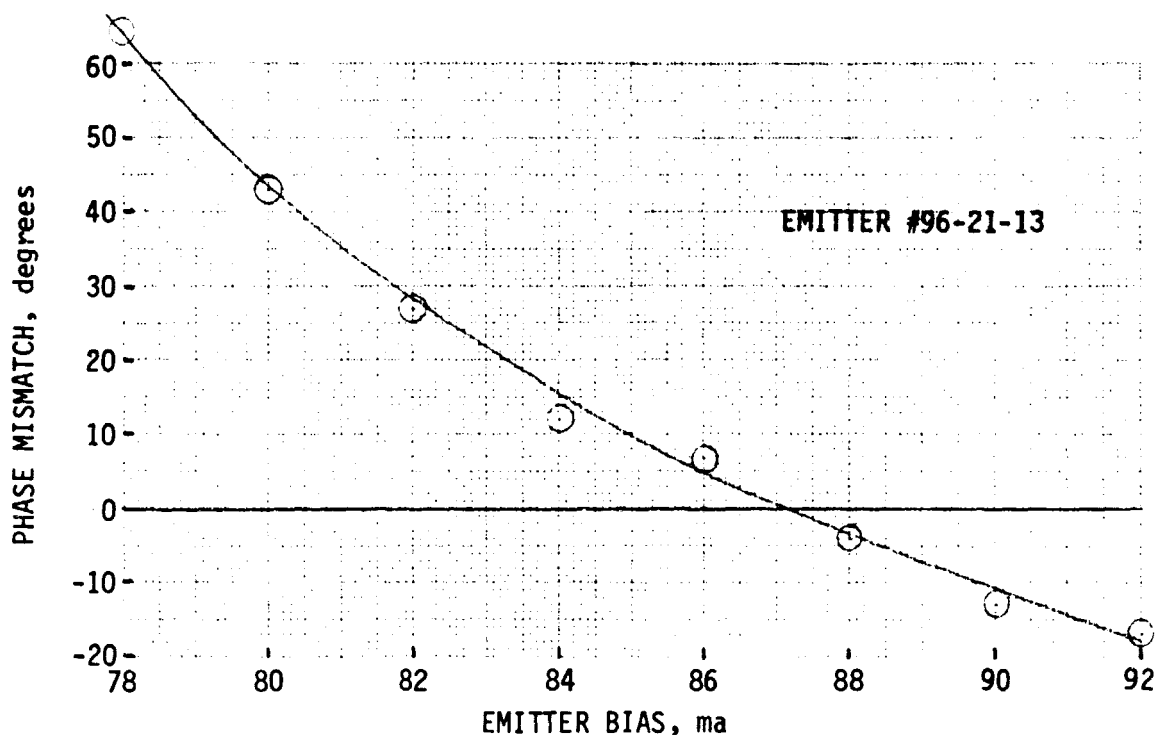


FIGURE 7.3. PHASE MISMATCH VS. EMITTER BIAS

ORIGINAL PAGE IS  
OF POOR QUALITY

D180-25888-1

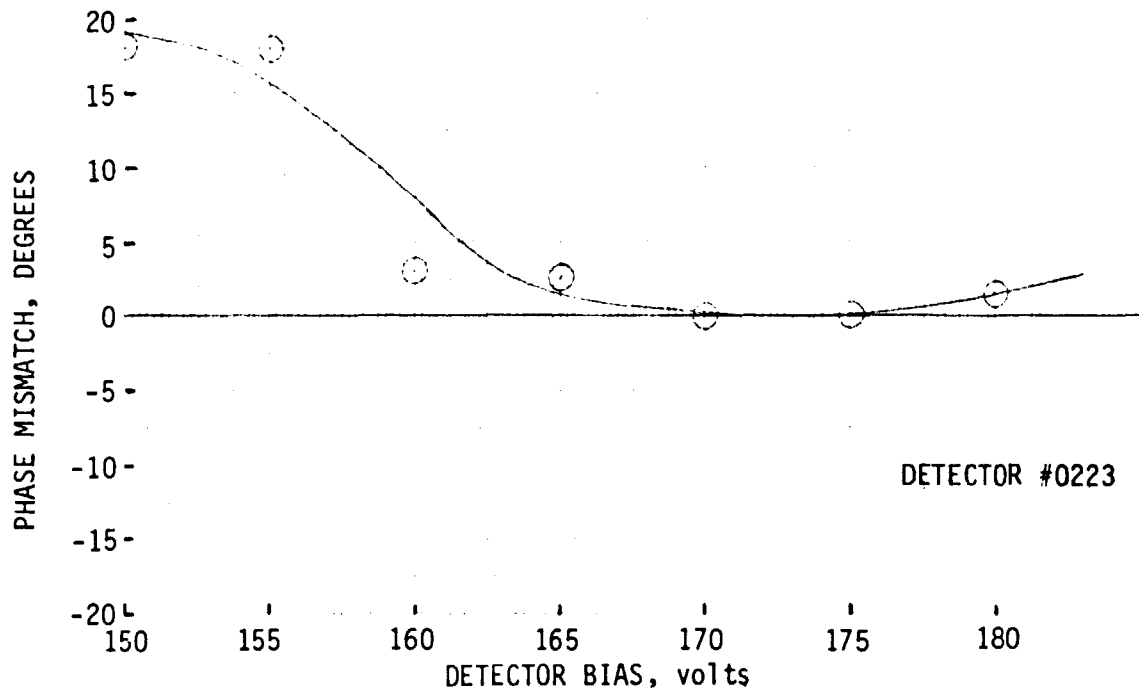
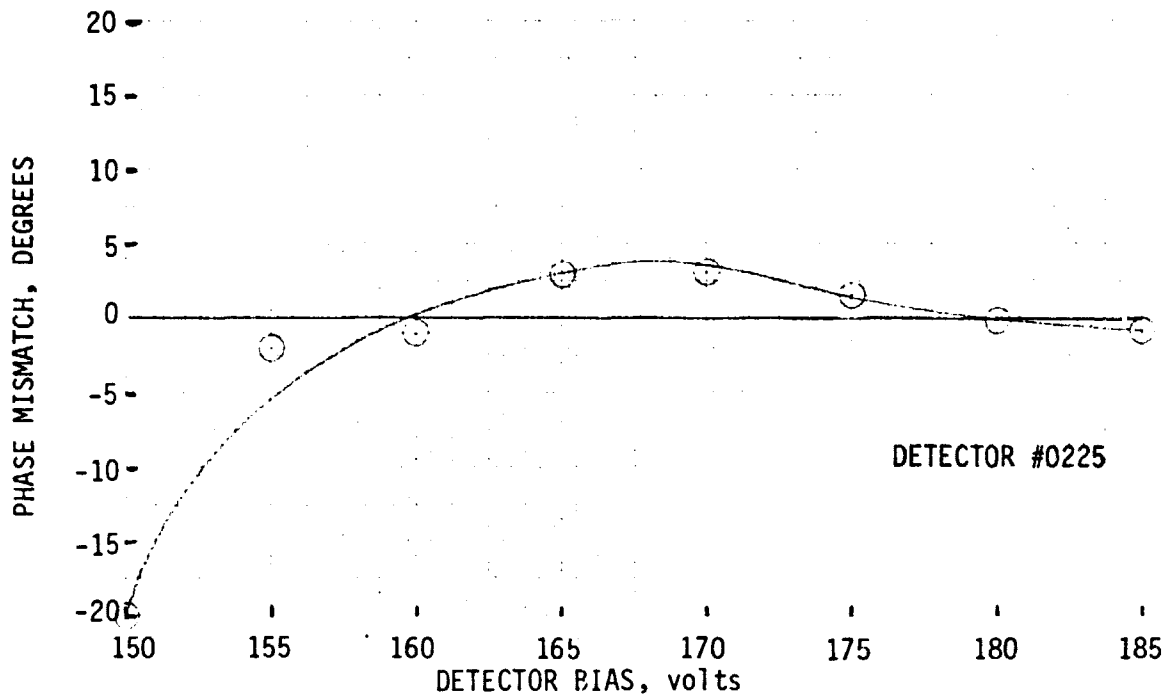


FIGURE 7.4. PHASE MISMATCH VS DETECTOR BIAS

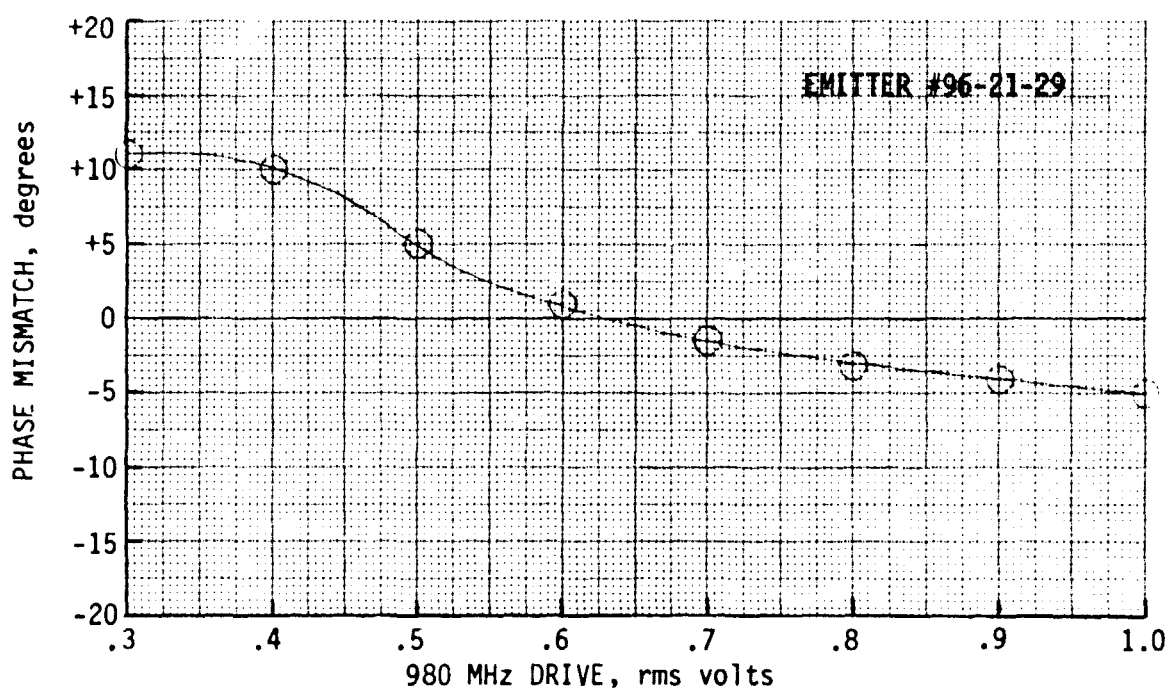
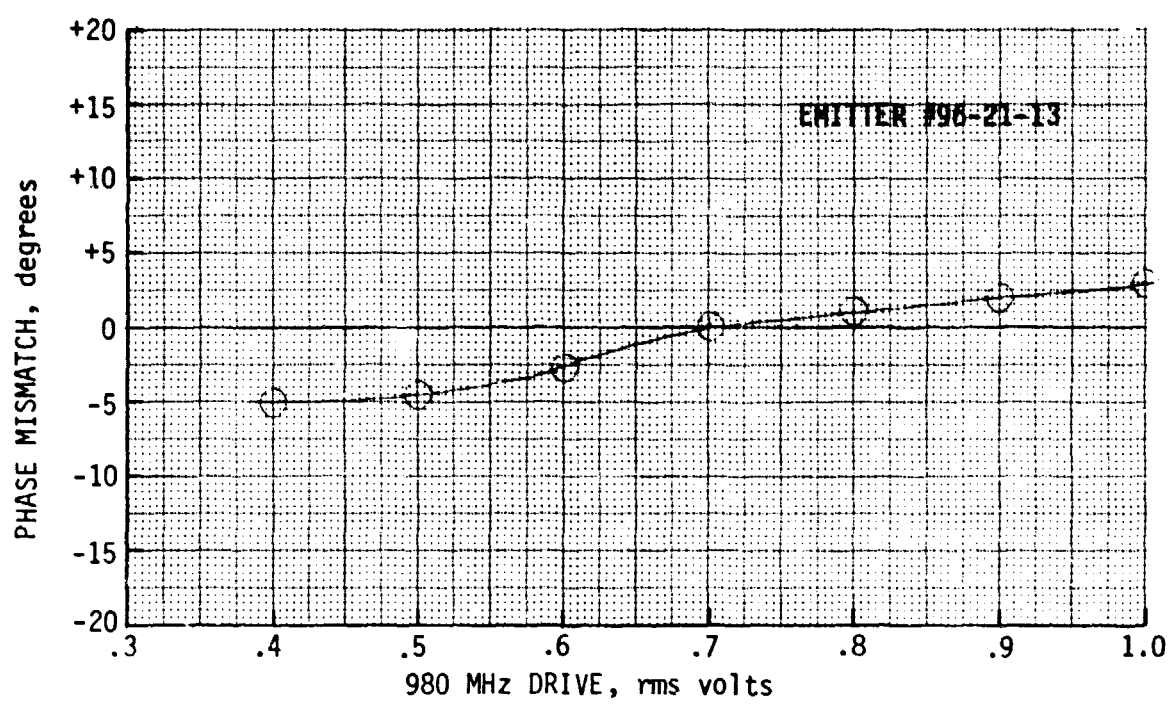


FIGURE 7.5. PHASE MISMATCH VS EMITTER RF DRIVE

## 8.0 CONCLUSIONS AND RECOMMENDATIONS

The feasibility of transmitting a 980 MHz phase signal along a fiber optic link has been successfully demonstrated. The transmitted phase signal was stable and exceptionally strong and clear and no difficulty should arise in its use as a control signal. Also, a nearly identical return link was built with an equal optical path length so that the received information of the first link may be returned to the source VCO for any required phase correction.

During the study, however, several questions arose which need investigation before a fiber optic design approach can be confidently adopted for the SPS phase distribution application.

### (1) Fiber Optic Cable Considerations

To phase-match the dual link developed within this study, an apparent physical length difference of 0.3% was required between the two fibers. Since the concept of the dual link requires that the path lengths be matched to some degree for proper compensation, the question arises as to fiber-to-fiber phase match requirements for proper path length compensation. Ideally, the two fibers should be identical not only in optical but in physical length so that the fibers will see the same environment along any incremental length and thus, provide accurate tracking.

The ramifications of the dissimilar fiber problem for the SPS application are not clear at this time, and further study is required. If the problem is found to be serious, special coordinated efforts are needed with a fiber cabling company to assure that matching requirements are met. It may be necessary to form the two-fiber cables with two fibers cut from the same draw for the best match of characteristics. Special efforts would also be required to pull the two fibers with identical tension.

It may also be possible to develop a temperature-hardened, phase-stable cable that could tolerate the wide SPS thermal environment with only minor effects. Coaxial companies have been working on the problem for years, and some of the technology should be applicable to fiber optics.

(2) Emitter and Detector Considerations

Little is known about the causes and mechanisms of phase delay through injection laser diodes and avalanche photodiodes. All external parameters were found to have interrelated effects on phase delay, but more work is required to obtain a firm understanding of the mechanisms to determine the impact to the SPS application, and to prevent potential problems from occurring.

A change in temperature appears to have effects on phase delay as well. If the phase on only one emitter (or detector) varied for any reason, the subsequent phase change would cause a phase error to be transmitted. Since the total phase error is limited to less than  $10^\circ$  rms, it may be necessary to house all of the emitter and detector modules in controlled environments.

One remedy may be a closed-loop system for the emitters in which the rear facet of the laser diode is monitored by a PIN photodiode, the demodulated output compared with the modulation input, and corrected for drift. The concept is felt to be worthy of laboratory testing if controlled environments are not possible.

It is also suggested that further investigation be undertaken to determine the full impact of detector and emitter (and fiber) frequency response on phase transmission. Efforts were made in the present study to ensure that frequency response was of little consideration but should other IF frequencies be suggested (above 1 GHz) these effects need to be investigated.

It was found that the present link operated slightly above 1 GHz.

**(3) System Level Recommendations**

Upon resolution of the above questions, it is recommended that a sample leg of the four-level SPS phase distribution network be built and tested. The network should include the proposed phase-locked loops, splitters, and drivers, and should be a good working model of the entire distribution network. This would demonstrate the phase control concept and the ability of fiber optics technology to challenge the stringent requirements of space-borne applications. Subsequent to this, a working model of a four-level "tips" system could be built, providing quantitative data on the total phase error budget of the SPS phase control at the module level.

LIST OF REFERENCES

1. Rodriguez, G., "Microwaves", Vol. 8, No. 2, Feb. 1969, p. 42.
2. Memo to E. J. Nalos, April 1979, Subject: Testing of an Optical Fiber for Variations in Propagation Delay Over a Temperature Range.
3. Garmine, E., "Optical Spectra", Vol. 13, No. 4, April 1979, p. 50.
4. L. Prod'homme, "Physics and Chemistry of Glasses", Vol. 1, No. 4, Aug. 1960, p. 119.
5. Baak, T., "Journal of the Optical Society of America", Vol. 59, No. 7, July 1966, p. 851.
6. Malitson, I. H., "Journal of the Optical Society of America", Vol. 55, No. 10, Oct. 1965, p. 1205.
7. Reprint from the Galileo Electro-Optics Corporation, "The Communications Revolution 1976- ( )".
8. Hartog, A. H., et al., "Optical and Quantum Electronics", No. 11, 1979, p. 262.
9. Cohen, L. G. and Fleming, J. W., "Bell System Technical Journal", Vol. 58, No. 4, April 1979, p. 945.
10. Takahashi, S. and Shibata, S., "Journal of Non-Crystalline Solids", No. 30, 1979, p. 359.
11. Giallorenzo, T. G., Proceedings of the IEEE, Vol. 66, No. 7, July 1978, p. 744.
12. Barnoski, M. K., Fundamentals of Optical Fiber Communications, Academic Press, New York, 1976.
13. Cunningham, R. C., "Electro-Optical Systems Design", May 1979, p. 31.
14. Morey, G. W., The Properties of Glass, Reinhold Publishing Co., New York, 2nd Edition, pp. 436-439.
15. Blood, W. R. Jr., MECL Design Handbook, 2nd Edition, December, 1972, p. 39. (Motorola)
16. Hubbard, W. M., "Bell System Technical Journal", Vol. 52, No. 5, May-June, 1973, p. 731.

**APPENDIX I**

**SPS FIBER OPTIC LINK ASSESSMENT TEST PLANS**

**60MHz AND 980MHz**

SPS F/O LINK ASSESSMENT - TEST PLAN  
60 MHZ OPTICAL FIBER PHASE VS. TEMPERATURE TESTS

1. Purpose - The purpose of this test plan is to define the test procedures necessary to do comparative testing of the phase variation of a signal transmitted through fiber optics as environmental temperature is varied.
2. Procedures
  - 2.1 Fibers to be tested - The following fibers have been procured for the test and shall be tested.
    - a) Corning Glass Works, graded-index, IVPO process
    - b) Corning Glass Works, graded-index, OVPO process
    - c) Times Wire & Cable, graded-index, OVPO process
    - d) Nippon Sheet Glass Co., graded-index, "Selfor"
    - e) Corning Glass Works, single-mode fiber
  - 2.2 Fiber Preparation
    - 2.2.1 Construction of Mandrels - Mandrels shall be manufactured onto which the fibers will each be wound in preparation for testing. A construction drawing follows. (Figure 2.2.1.1)
    - 2.2.2 Fiber Winding - Each fiber shall be wound onto its respective mandrel. The radius of the region between the vertical standoffs with respect to the center of the mandrel plate shall be adjusted via best choice of the drilled standoff holes such that this radius is most closely matched to that of the spool obtained from the manufacturer on which the fiber was wound. The "start" end of the fiber shall be secured to the mandrel plate and marked "START". Three (3) feet (approx.) of excess fiber shall be allowed for handling and coupling out of the environmental chamber and into the transmitter.

The main fiber winding procedure shall be to support the manufacturers fiber spool vertically over the respective mandrel and to allow the fiber to gently (and loosely) drop onto the mandrel such that the fiber falls into a circular pattern around, through and between the standoff pairs. As at the start, approximately three (3) feet of excess fiber shall be allowed for coupling out of the chamber and into the receiver. The fiber shall be secured to the mandrel plate as before and marked "END".
    - 2.2.3 Fiber End Preparations - The ends of the fibers must be prepared in a fashion to make them suitable for insertion into a connector. Each fiber end shall be stripped of all buffer and/or other coating, to expose the fiber cladding for a length of approximately 1". The appropriate end preparation procedures for each fiber shall be determined as required. All ends shall be cleaved and cleaned.
    - 2.2.4 Connector Procedures - Amphenol 906 series connectors shall be used to connect the fiber ends to the transmitter and receiver units. In all cases, the fiber ends shall be slipped through their respective connectors such that the fiber ends protrude slightly from the connector ends. The assemblies shall then gently be screwed into their respective receptacles on the transmitter and receiver units. Some connector boring may be necessary to accommodate larger fibers.

D180-25886-1

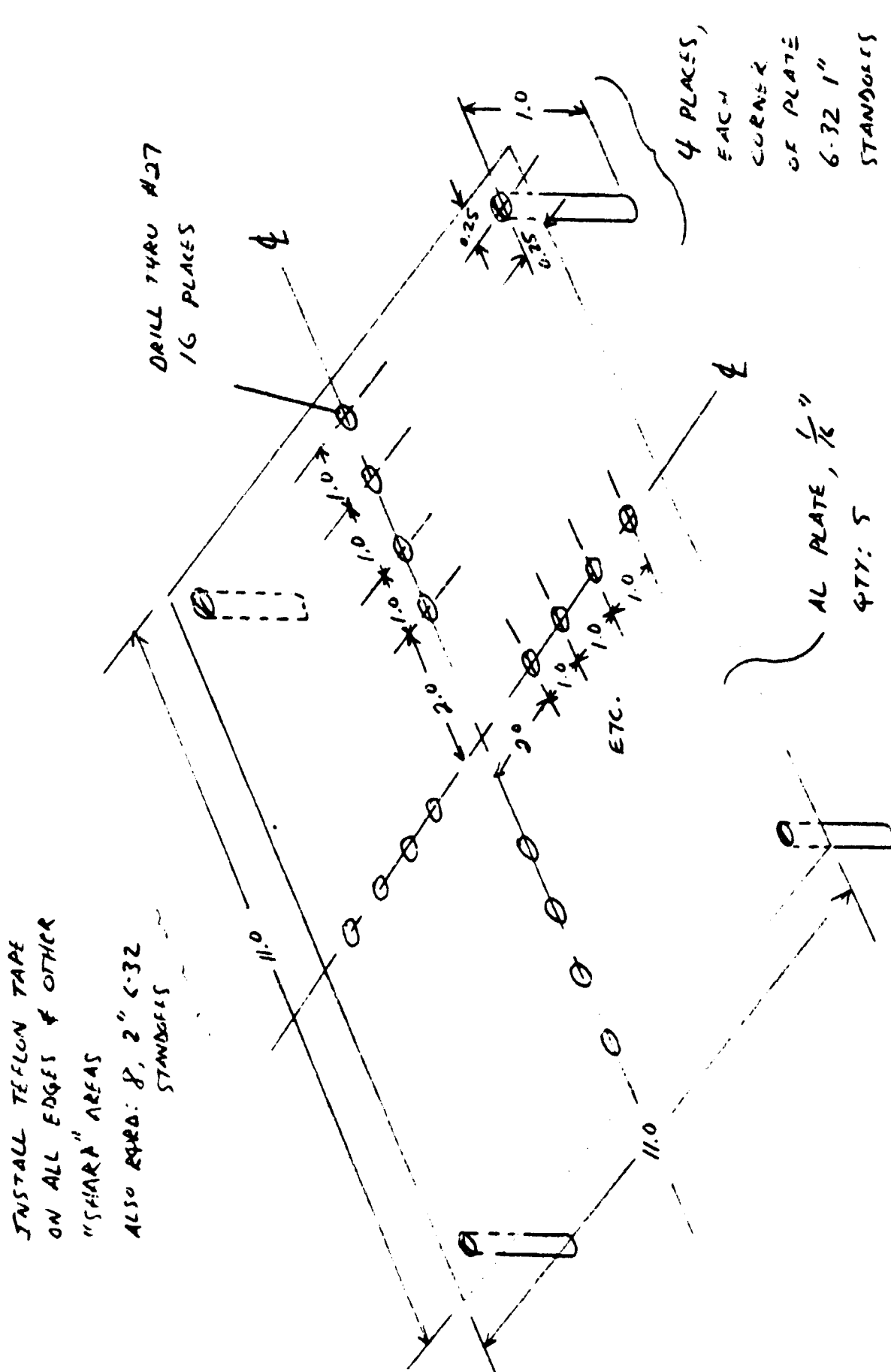


FIG. 2.2.1-1

### 2.3 Test Equipment

**2.3.1 Equipment Required** - The following is a listing of test-equipment required for the job.

- a) CAD/CAM F/O XMTR
- b) CAD/CAM F/O RCVR
- c) Frequency Synthesizer (with capability at 60MHz)
- d) Environmental chamber (with capability -50°C to +150°C and size 12" x 12" x 16" minimum)
- e) Digital thermometer
- f) Oscilloscope (dual trace)
- g) Vector Voltmeter

**2.3.2 Equipment Stabilization** - As a prerequisite to any actual testing, it is mandatory that all equipment be up and running at test conditions for a minimum of 24 hours. Of particular importance, the requirement pertains to the F/O XMTR and RCVR, frequency synthesizer, vector voltmeter, and oscilloscope.

**2.3.3 System Integration** - For assembly of the test system, the equipment shall be interconnected as shown by figure 2.3.3.1. The fiber to be tested shall be inserted into the environmental chamber (aboard its respective mandrel) and the fiber ends shall be brought through the chamber side ports and connected to the F/O XMTR and RCVR units as described in section 2.2.4.

### 2.4 Test Plan

**2.4.1 Information Sought** - The intent of the test, as described by section 1. is to gather only information of the phase of the transmitted signal. The goal is to measure, for each fiber tested, the change in phase of the signal at the receiver end of the fiber with respect to the phase at the transmitter end of the fiber over an environmental temperature change.

**2.4.2 Test Frequency** - The frequency of the transmitted signal shall be 60.000 MHz to the best tolerance of the synthesizer.

**2.4.3 Temperature Range** - The environmental chamber shall be varied from -50°C to +150°C.

**2.4.4 Test Temperature Increments** - The temperature increments between successive test points shall be 25°C + 5°C. The desired mean test points are therefore -50°C, -25°C, 0°C, 25°C, 50°C, 75°C, 100°C, 125°C, 150°C.

**2.4.5 Test Cycles** - The tested fiber shall be cycled through the test one time. That is, the test shall be run fully in the direction of increasing temperature to the maximum temperature of the test, reversed, and run fully in the direction of decreasing temperature to the minimum temperature of the test. It is suggested that the fiber be subjected to one cycle prior to actual testing to effect fiber "break-in".

### 2.4.6 Period of Test Point Readings

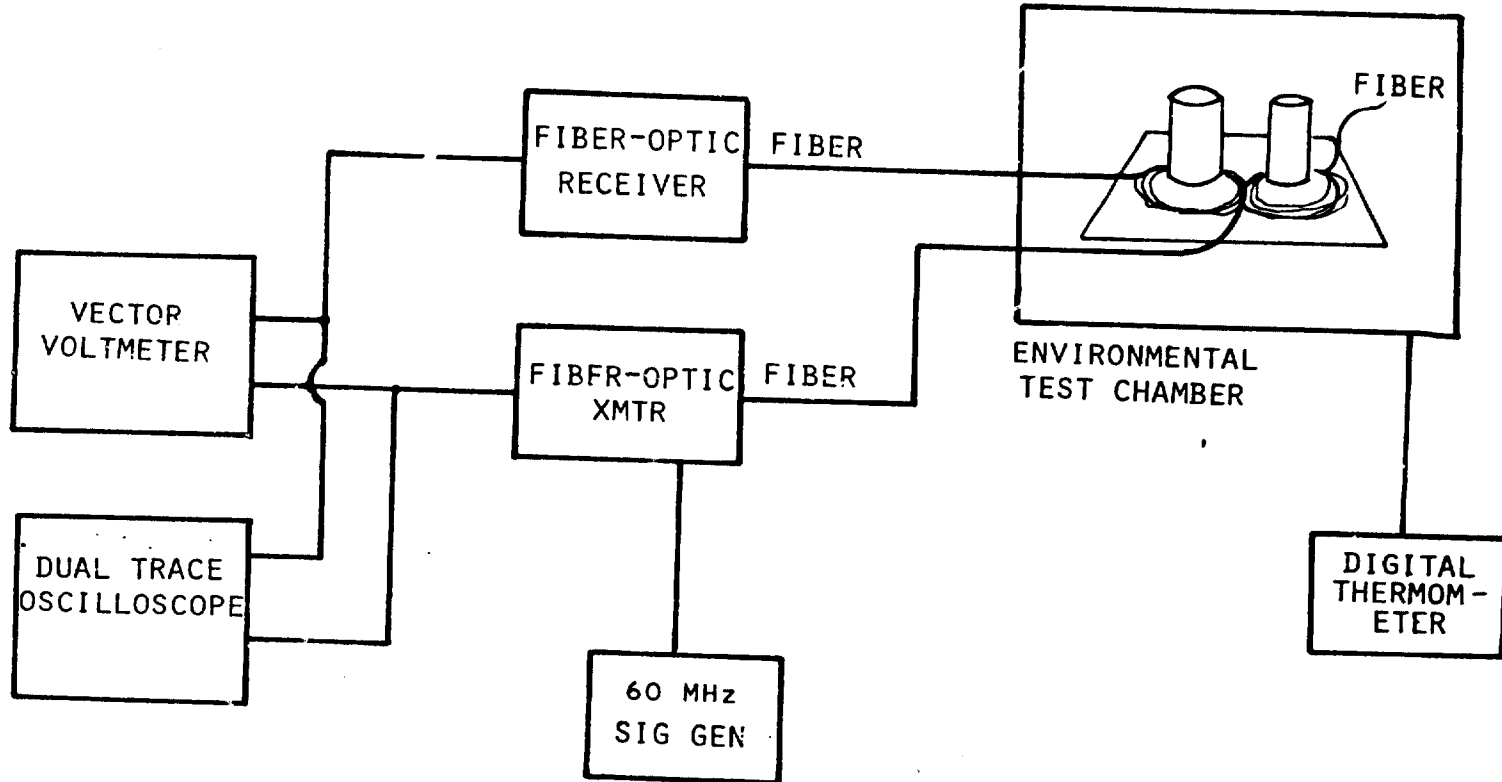


FIGURE: 2.3.3-1

- 2.4.6.1 Temperature range end-points - At the beginning of the temperature range for a test in either direction, the temperature must be allowed to stabilize for 30 minutes,  $\pm$  1 minute.
  - 2.4.6.2 Temperature range mid-points - For any temperature range mid-point readings, the temperature must be allowed to stabilize for 15 minutes,  $\pm$  1 minute.
  - 2.4.7 Test Procedure - After sufficient warm-up (sec. 2.3.2) and system integration (sec. 2.3.3), the test shall begin at  $-50^{\circ}\text{C}$  per sec's 2.4.3, 2.4.4, and 2.4.6.1. A phase vs. temperature reading shall be recorded and the test then incremented per sec.'s 2.4.4 and 2.4.6.2. Readings shall be recorded at each point until the upper temperature point ( $+150^{\circ}\text{C}$ ) is reached. After its reading is recorded, the cycle must be reversed as per sec. 2.4.5 and 2.4.6.1 and readings taken per 2.4.4 and 2.4.6.2 until the minimum temperature is again reached ( $-50^{\circ}\text{C}$ ), and its reading recorded.
3. Presentations of Results
- 3.1 Plotted Data - Data for each fiber tested shall be plotted on linear graph paper showing change in phase versus temperature. Because change of phase is a relative parameter, change of phase shall be set equal to  $0^{\circ}$  at  $-50^{\circ}\text{C}$  temperature. In addition, all test results shall also be plotted together to better illustrate comparative results (on a per meter basis).
  - 3.2 Results Discussion - Results discussion shall include any expected or unexpected findings, test difficulties, suggestions, etc. As a conclusion, a fiber shall be suggested for the 980 MHz F/O system test.

SPS F/O LINK ASSESSMENT-TEST PLAN #2

980 MHz F/O SYSTEM DEMONSTRATION TESTS

1. Purpose - The purpose of this test plan is to define the test procedures necessary for evaluation of a F/O link for use at 980 MHz. The test is intended to evaluate F/O emitters and detectors at 980 MHz at room temperature for signal throughput, modulation depth, sensitivity, etc., and to investigate various effects in an optical fiber due to temperature variation. The effects include propagation delay attenuation, and bandwidth changes.

2. General Test Definition

2.1 Test Link Components

2.1.1 Fiber - The fiber to be tested shall be specified based upon results of Test Plan #1 run at 60 MHz. The fiber will be already wound on a test mandrel.

2.1.2 Emitter System - The emitter shall be an NEC #NDL3025P injection laser diode (ILD) with pigtail and appropriate  $50\Omega$  coupling network. Also included will be the appropriate biasing and drive networks.

2.1.3 Detector System - The detector shall be an RCA #C30902E avalanche photo diode (APD) with pigtail and appropriate coupling network. Also included will be the appropriate biasing and amplifier networks.

2.2 Test Equipment

2.2.1 Equipment Required - The following is a total listing of test equipment required for the jobs.

- a) TWT power/driver amplifier,  $50\Omega$
- b) 980 MHz freq. synthesizer
- c)  $50\Omega$  pre-amplifier
- d) Directional coupler, 10:1
- e) Environmental chamber (with capability  $-50^{\circ}\text{C}$  to  $+150^{\circ}\text{C}$  and size 12" x 12" x 16" minimum)
- f) Oscilloscope
- g) Digital thermometer
- h) Optical power meter
- i) Vector voltmeter
- j) 50 MHz BW filter, centered at 980 MHz
- k)  $50\Omega$  powermeter with sensor

2.2.2 Equipment Stabilization - As a prerequisite to any actual testing, it is mandatory that all equipment be up and running at test condition levels for a minimum of 24 hours.

2.2.3 Connector Procedures - Amphenol 906 series connectors shall be used to connect the fiber's ends to the emitter and detector systems. In all cases, the fiber ends shall be slipped through their respective connectors such that the fiber ends protrude slightly from the connector ends. The assemblies shall then be gently screwed into their respective receptacles on the emitter and detector systems. Full attention shall always be paid to maintaining clean, cleaved fiber ends.

3. Room Temperature Tests

3.1 Test Frequency - The frequency of the transmitted signal shall be 980.000 MHz to the best tolerance of the synthesizer.

3.2 Optical Power Measurements

3.2.1 Information Sought - The intent of these tests is to determine the optical powers (average) found emitting from the source pigtails and also entering the detector pigtails for the case of no modulation and for the case of modulation.

3.2.2 Test Configuration - The test set-up shall be interconnected as per figure 3.2-1.

3.2.3 Power From Emitter Pigtail, Mod. "OFF" - Connect the emitter pigtail directly to the photometer head via a connector, remove all modulation and measure the optical power.

3.2.4 Power From Emitter Pigtail, Mod "ON" - Repeat as per section 3.2.3, but with full modulation.

3.2.5 Power Into Detector Pigtail, Mod "OFF" - Repeat as per section 3.2.3, but measure from the long length of test fiber.

3.2.6 Power Into Detector Pigtail, Mod. "ON" - Repeat as per section 3.2.5, but with full modulation.

3.2.7 Presentation of Data - Data shall be presented and also included shall be any expected or unexpected findings, test difficulties, suggestions, etc.

3.3 Electrical Power Measurements

3.3.1 Information Sought - The intent of these tests is to determine the noise and signal power levels of the 980 MHz receiver system.

3.3.2 Test Configuration - The test set-up shall be interconnected as per figure 3.3-1.

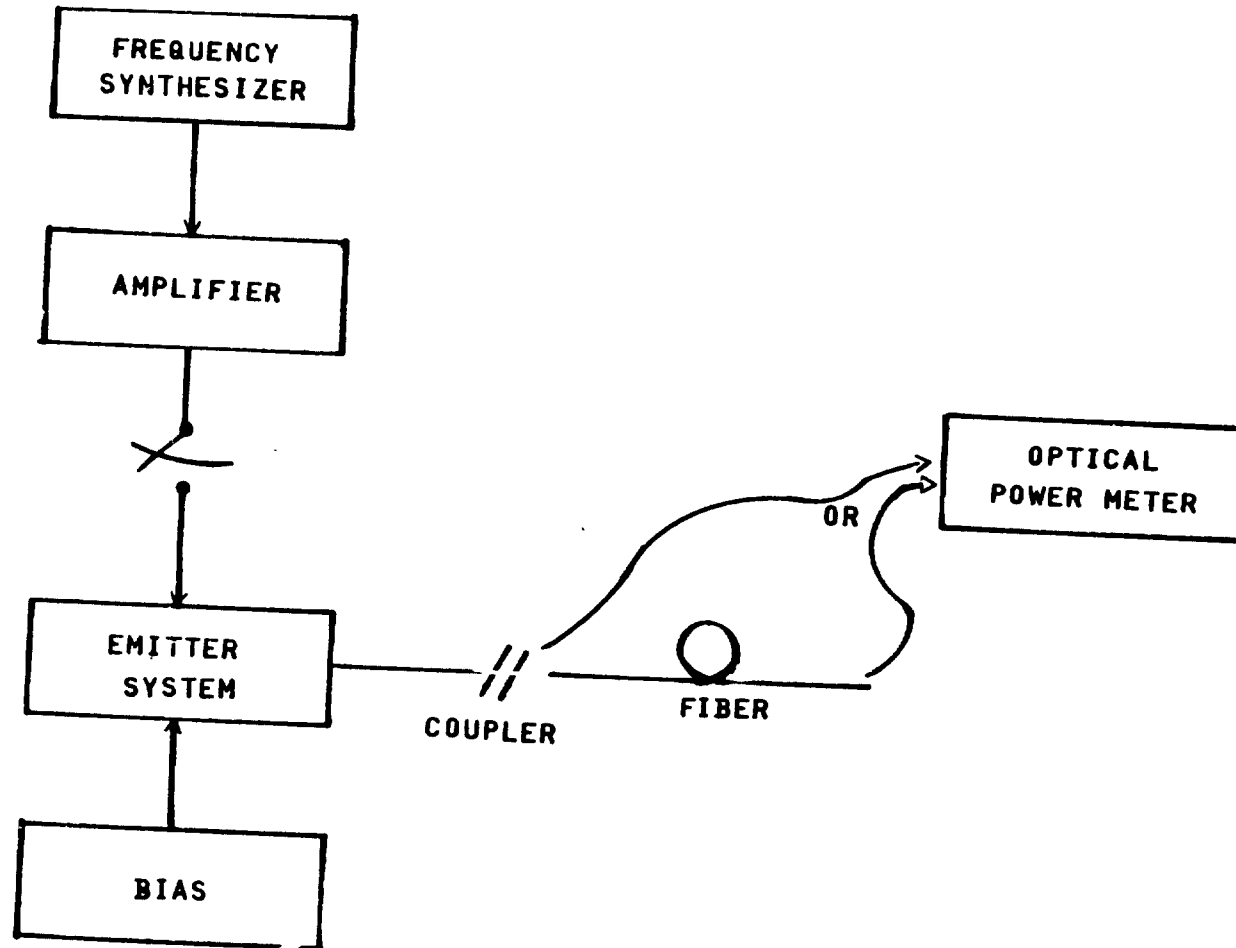


FIG. 3.2-1

1-9  
D180-25888-1

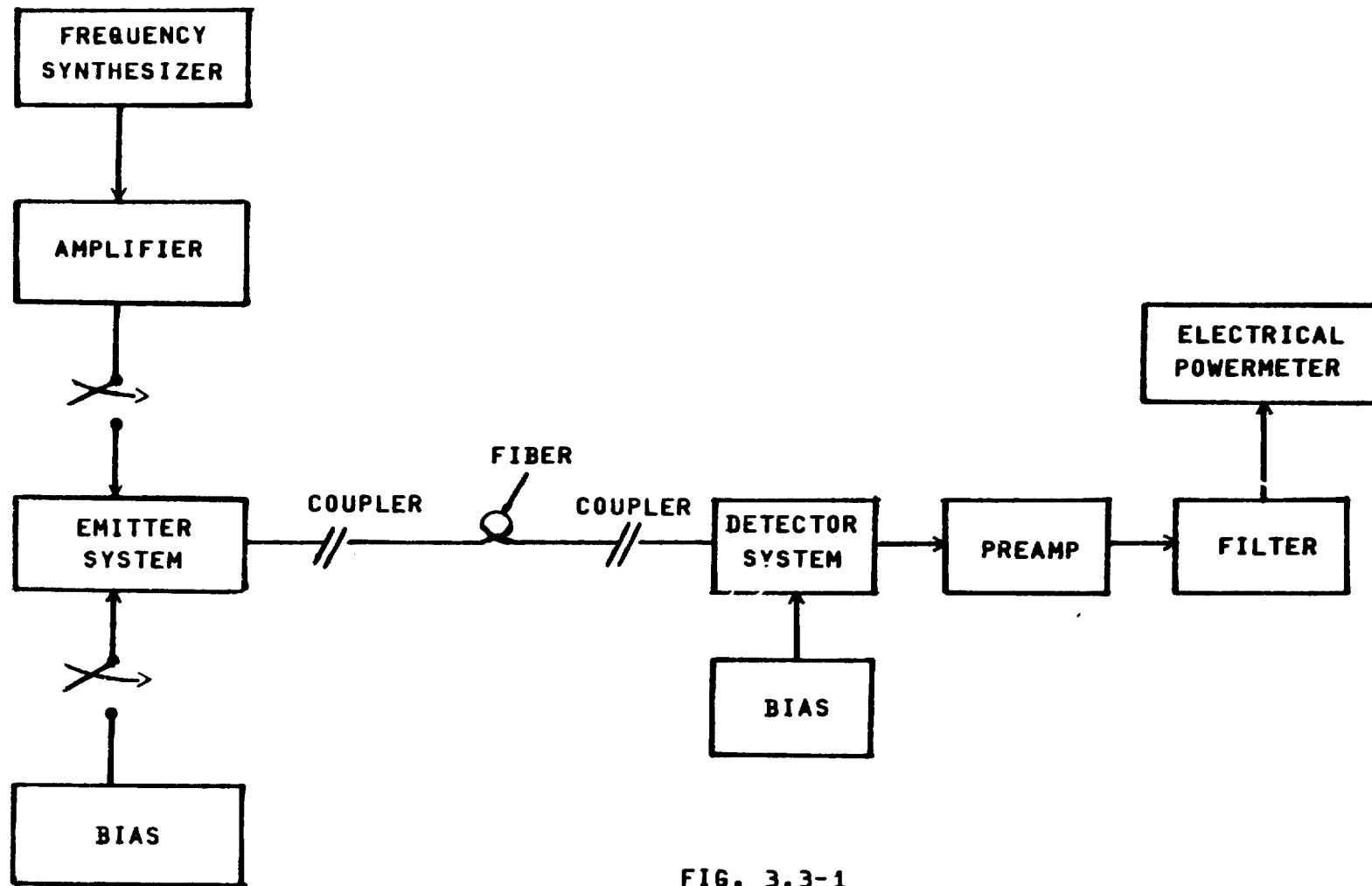


FIG. 3.3-1

- 3.3.3 After Preamp, No Optical Signal - With the optical fiber link disconnected at the detector pigtail, measure the electrical power.
- 3.3.4 After Preamp, Optical Signal, No Modulation - With the fiber reconnected, and with the source power on but with no modulation, measure the electrical power.
- 3.3.5 After Preamp, Optical Signal, Full Modulation - With the link as per section 3.3.4, but with source modulation, measure the electrical power.
- 3.3.6 Presentation of Data - Data shall be presented and also included shall be any expected or unexpected finding, difficulties, suggestions, etc. An attempt will be made to characterize all noise sources as equivalent current sources in parallel with the signal current source to allow for simple analysis and predictable signal to noise ratios.

#### 4. Thermal Tests

- 4.1 Test Frequency - The frequency of the transmitted signal shall be 980.000 MHz to the best tolerance of the synthesizer.
- 4.2 Temperature Range - The environmental chamber shall be varied from -50°C to +150°C.
- 4.3 Test Cycles - The tested fiber shall be cycled through the test one time. That is, the test shall be run fully in the direction of increasing temperature from the minimum temperature to the maximum temperature, reversed, and run fully in the direction of decreasing temperature to the minimum temperature of the test. It is suggested that the fiber be subjected to one cycle prior to actual testing to effect fiber "break-in".

#### 4.4 Period of Test Point Readings

- 4.4.1 End Points - At the end of the temperature range for a test in either direction, the temperature must be allowed to stabilize for 30 minutes,  $\pm$  1 minute.
- 4.4.2 Mid Points - For any temperature range mid-point readings, the temperature must be allowed to stabilize for 15 minutes,  $\pm$  1 minute.

#### 4.5 Phase and Amplitude Tests

- 4.5.1 Information Sought - The intent of this test is to measure the change of phase of the signal at the receiver end of the fiber with respect to the phase at the transmitter end of the fiber over an environmental temperature change. The relative amplitude (in dB) of the signal shall also be monitored over the same temperature range.

- 4.5.2 Test Configuration - The test set-up shall be interconnected as per figure 4.5-1.
- 4.5.3 Temperature Increments - The temperature increments between successive test points shall be  $25^{\circ}\text{C} \pm 5^{\circ}\text{C}$ . The desired mean test points are therefore  $-50^{\circ}\text{C}$ ,  $-25^{\circ}\text{C}$ ,  $0^{\circ}\text{C}$ ,  $25^{\circ}\text{C}$ ,  $50^{\circ}\text{C}$ ,  $75^{\circ}\text{C}$ ,  $100^{\circ}\text{C}$ ,  $125^{\circ}\text{C}$ ,  $150^{\circ}\text{C}$ .
- 4.5.4 Test Procedure - After sufficient warm-up (sec. 2.2.2), the test shall begin at  $-50^{\circ}\text{C}$  (per sec.'s 4.2, 4.4.1). Phase and amplitude readings vs. temperature shall be recorded and the test then incremented (per sec.'s 4.4.2 and 4.5.3). Readings shall be recorded at each point until the upper temperature limit is reached ( $+150^{\circ}\text{C}$ ). After its readings are recorded, the cycle must be reversed (as per sec.'s 4.3, and 4.4.1) and readings taken (per sec.'s 4.5.3 and 4.4.2) until the minimum temperature is again reached ( $-50^{\circ}\text{C}$ ), and its readings recorded.
- 4.5.5 Presentation of Data
- 4.5.5.1 Plotted Data - Data shall be plotted on linear graph paper showing change in phase and amplitude, in dB, versus temperature. Because change of phase and amplitude, in dB, are relative parameters, both parameters shall be set to zero at  $-50^{\circ}\text{C}$  temperature.
- 4.5.5.2 Results Discussion - Results discussion shall include any expected or unexpected findings, difficulties, suggestions, etc.
- 4.6 Attenuation Tests
- 4.6.1 Information Sought - The intent of this test is to determine the effects of temperature on the bulk loss properties of the fiber. By comparing the results of this test with the amplitude results of section 4.5, some feeling for bandwidth effects may also be gathered.
- 4.6.2 Test Configuration - The test set-up shall be interconnected as per figure 4.6-1.
- 4.6.3 Temperature Increments - The temperature increments between successive test points shall be  $50^{\circ}\text{C} \pm 5^{\circ}\text{C}$ . The desired mean test points are therefore  $-50^{\circ}\text{C}$ ,  $0^{\circ}\text{C}$ ,  $+50^{\circ}\text{C}$ ,  $+100^{\circ}\text{C}$ ,  $+150^{\circ}\text{C}$ .
- 4.6.4 Test Procedure - After sufficient warm-up (sec. 2.2.2), the test shall begin at  $-50^{\circ}\text{C}$  (per sec.'s 4.2 and 4.4.1). Optical power vs. temperature shall be recorded and the test then incremented (per sec.'s 4.4.2 and 4.6.3). Readings shall be recorded at each point until the upper temperature limit is reached ( $+150^{\circ}\text{C}$ ). After its readings are recorded, the cycle will be reversed (per sec.'s 4.3 and 4.4.1) and readings taken (per sec.'s 4.4.2 and 4.6.3) until the minimum temperature is again reached ( $-50^{\circ}\text{C}$ ) and its readings recorded. Source modulation shall be "OFF".

I-12

D180-25888-1

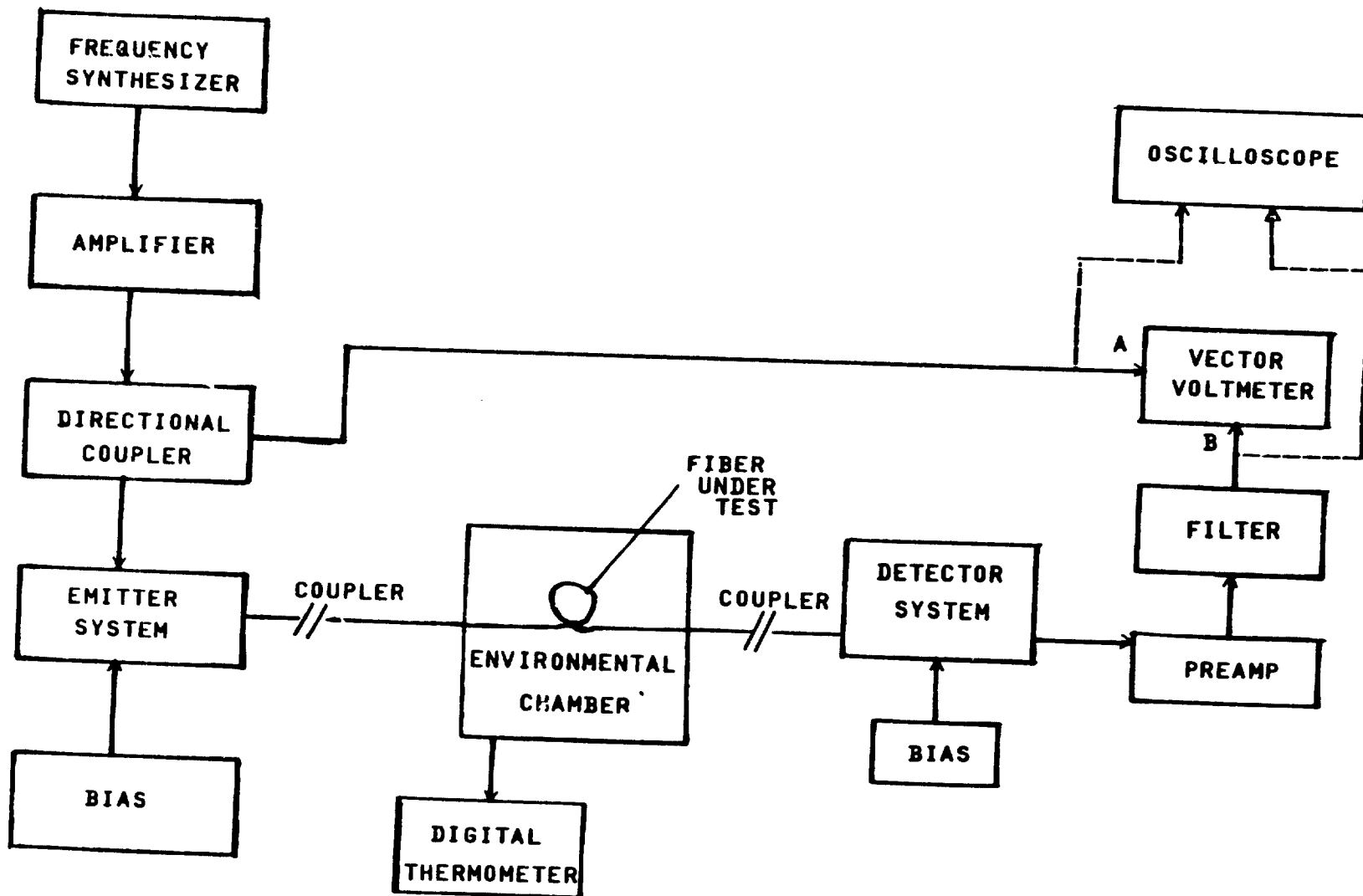
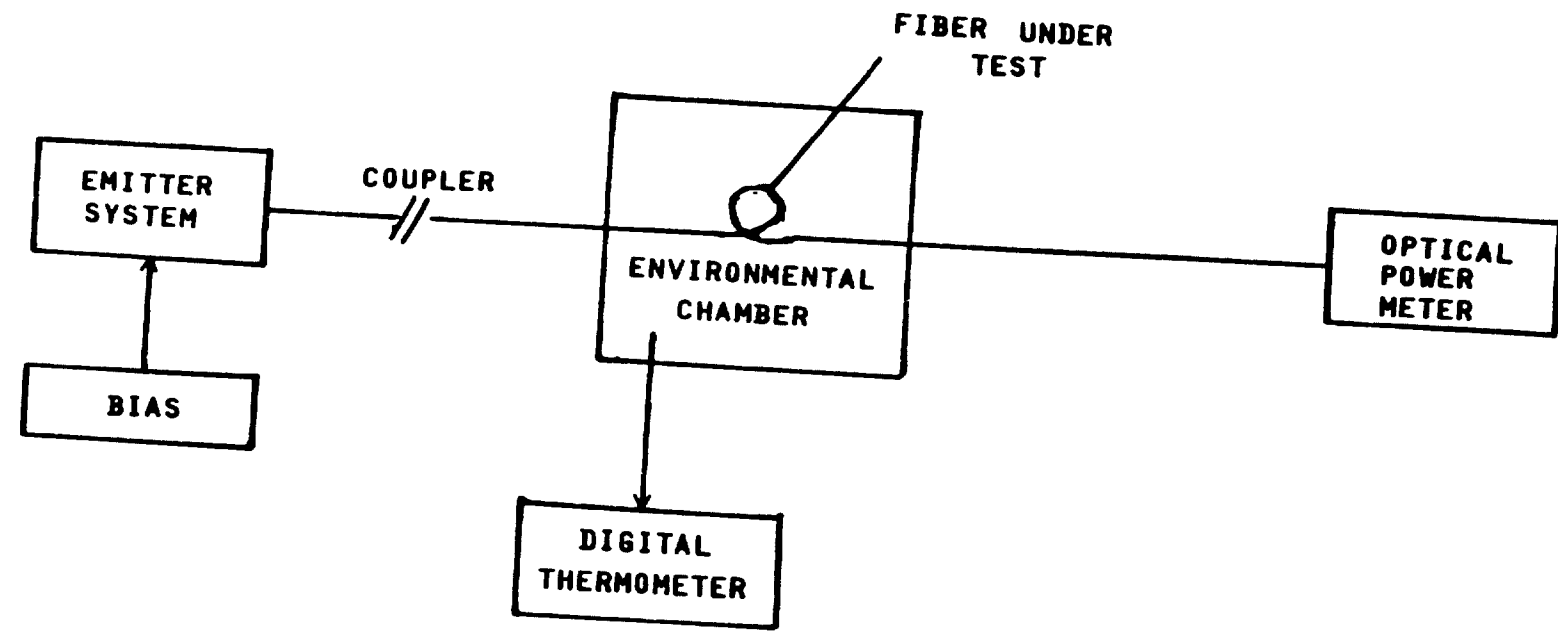


FIG 4.5-1



I-13

D180-25888-1

FIG 4.6-1

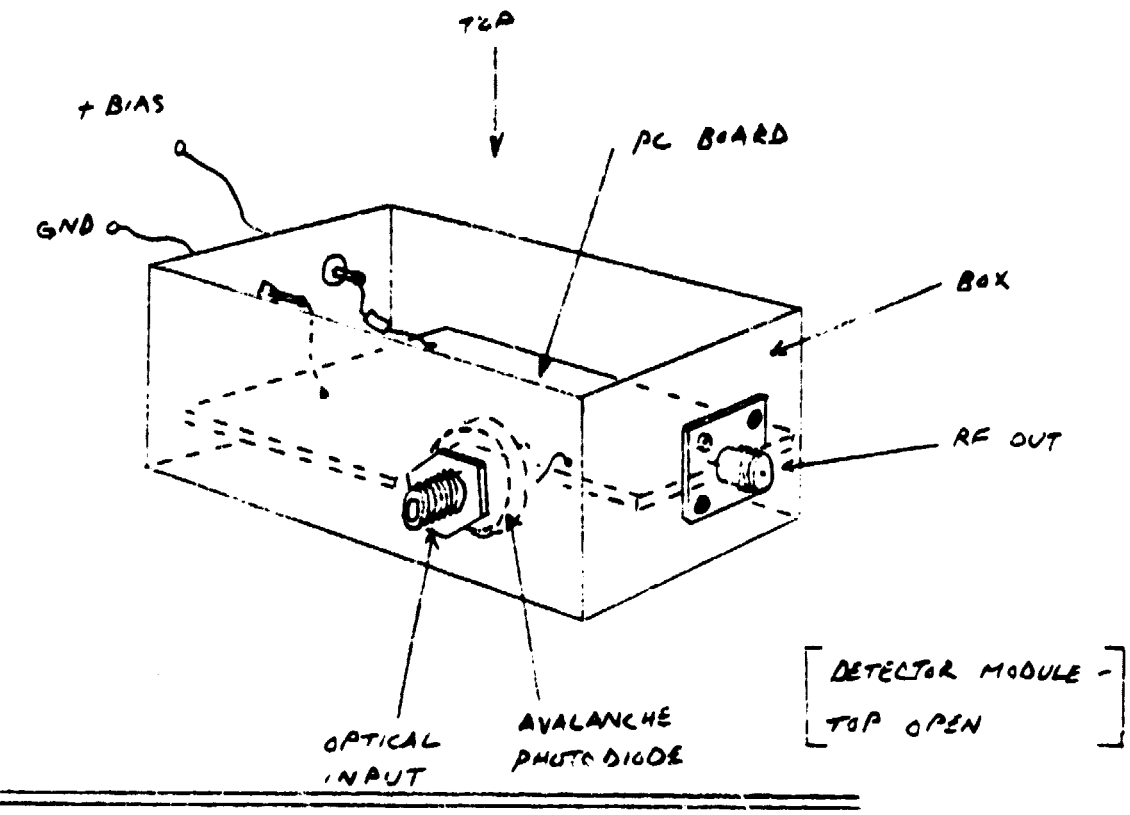
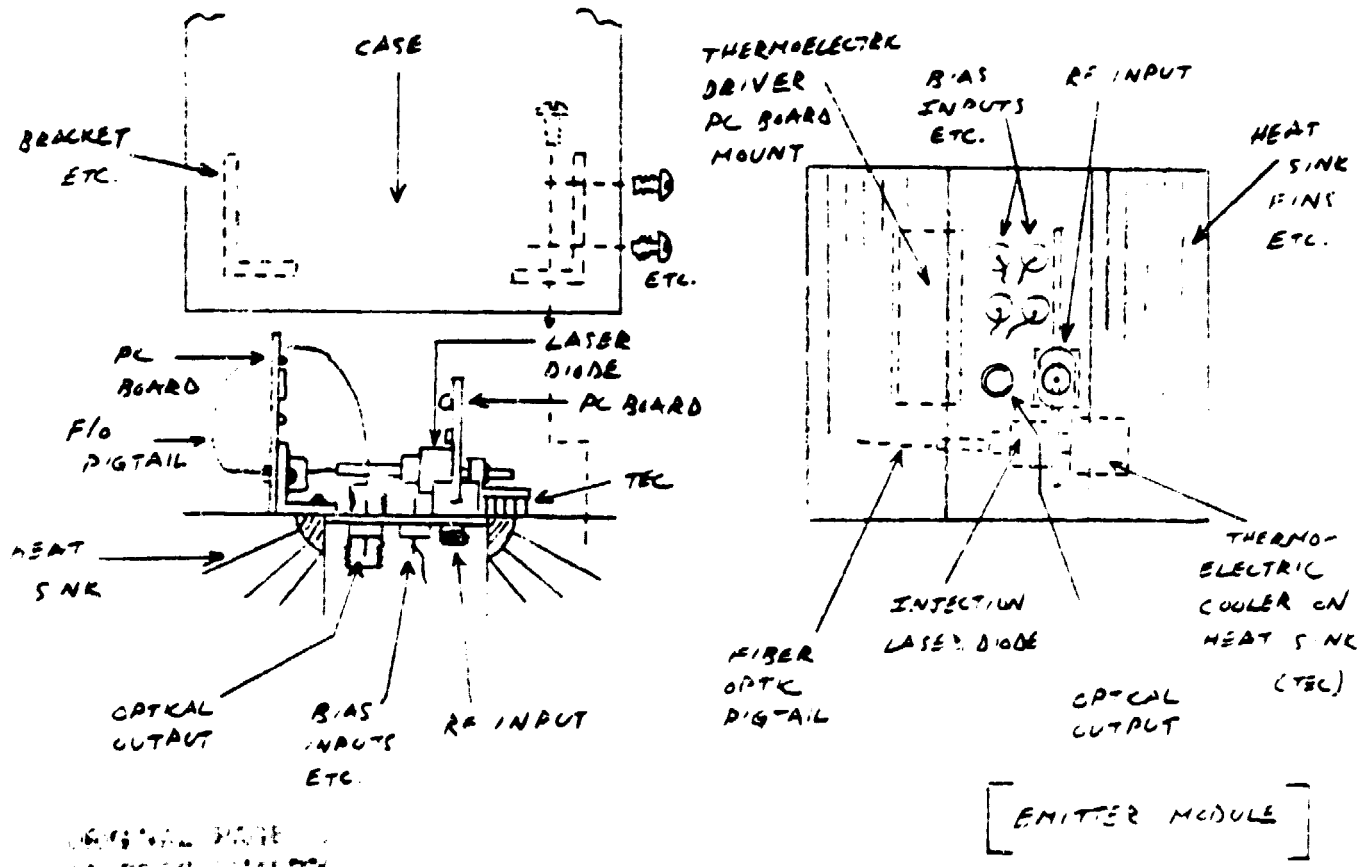
**4.6.5 Presentation of Data**

- 4.6.5.1 Plotted Data - Data shall be plotted on linear graph paper showing relative optical power (in dB) vs. temperature. The parameter shall be set to zero dB at -50°C temperature.**
- 4.6.5.2 Results Discussions - Results discussion shall include any expected or unexpected findings, difficulties, suggestions, etc. Discuss any bandwidth effect observations.**

**D180-25888-1**

**APPENDIX II**

**SPS FIBER OPTIC EMITTER AND DETECTOR MODULE  
PACKAGE DRAWINGS**

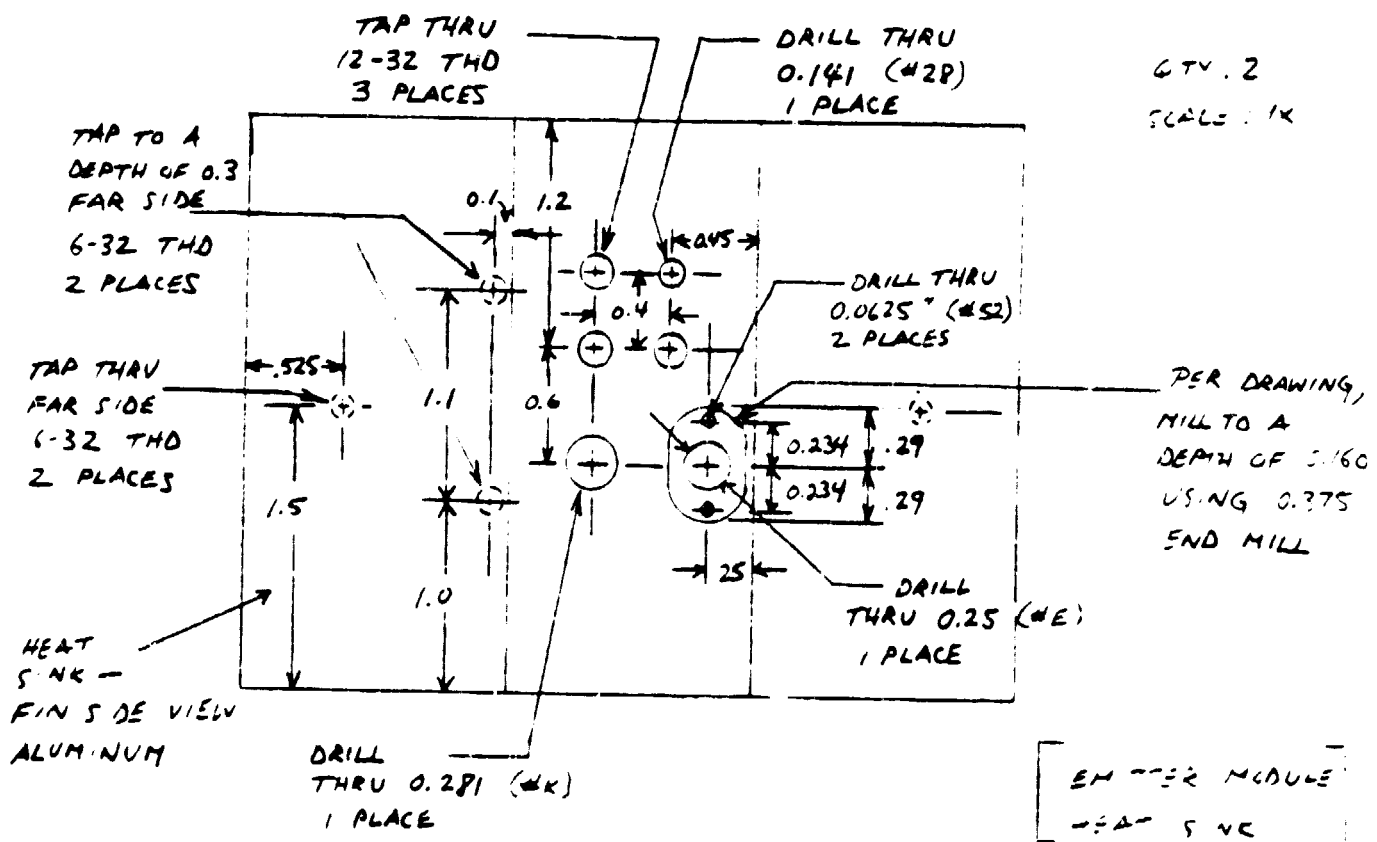
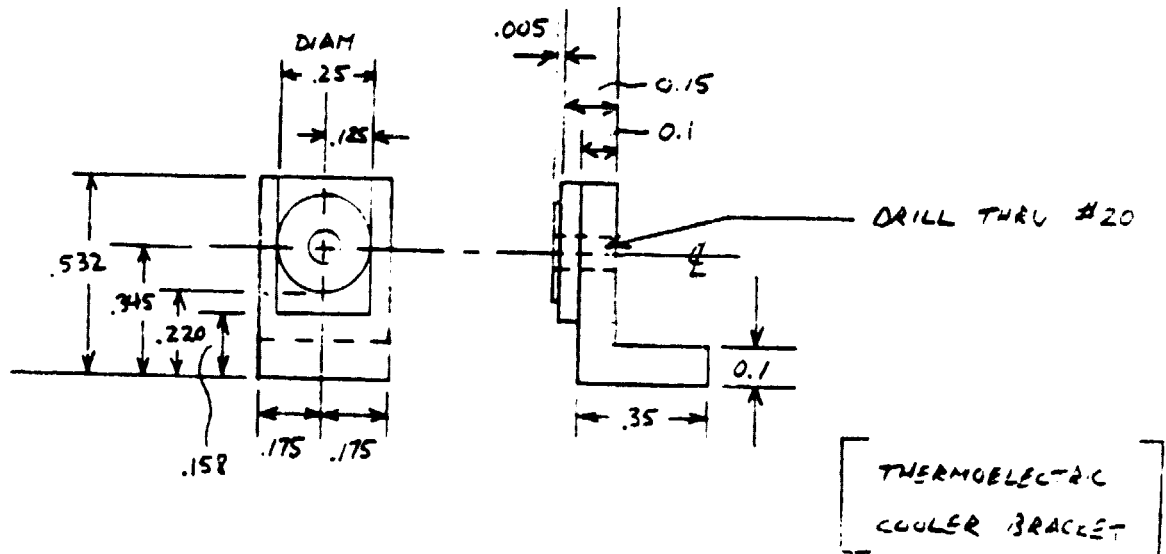
TOP VIEWFRONT VIEW

168-25888-1  
16 DEC 1987

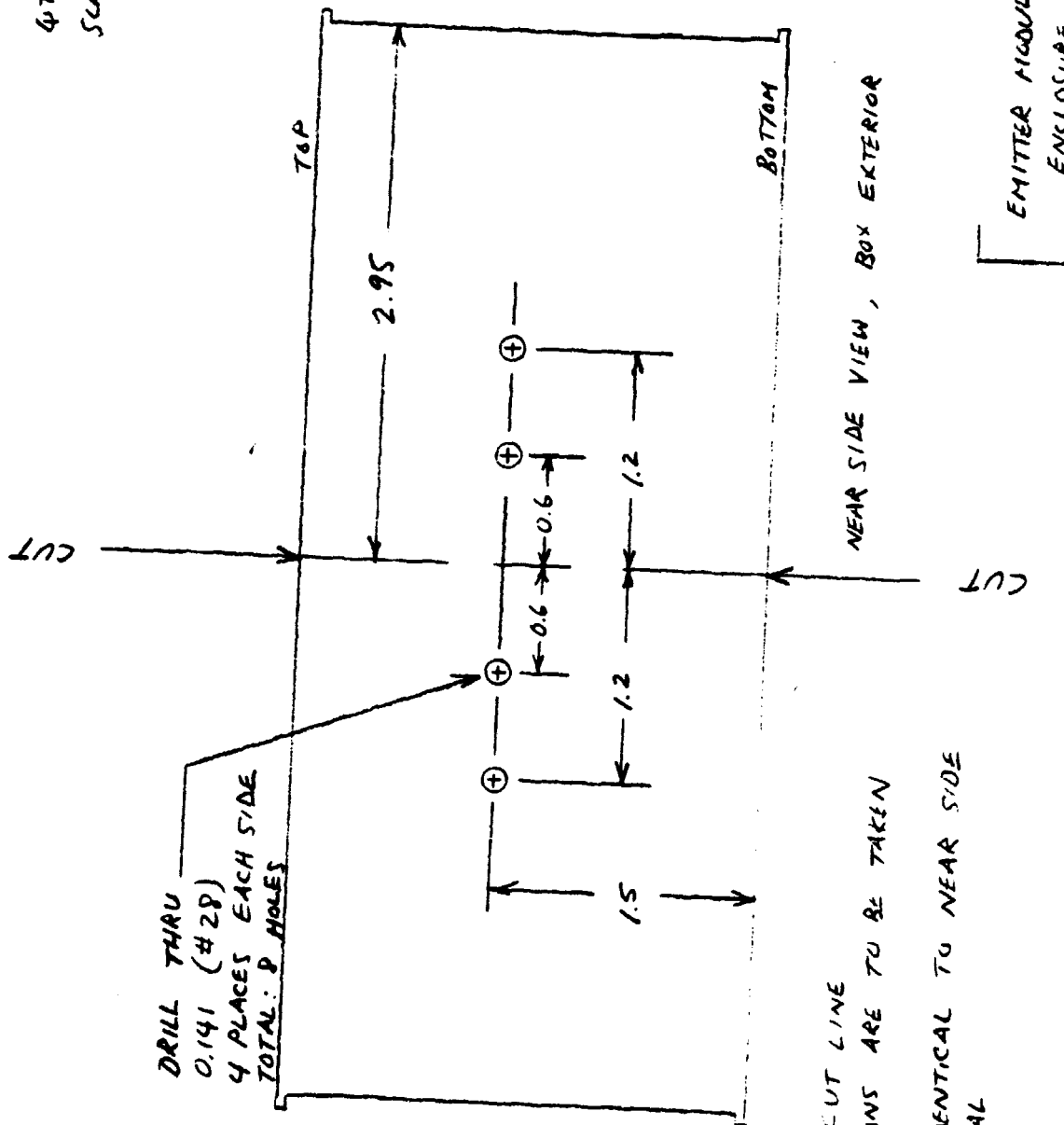
D180-25888-1

MATERIAL:  
ALUM NUM

QTY: 2  
SCALE:  $\times 2$



4TRY: 2  
SCALE: 1x



NEAR SIDE VIEW, BOX EXTERIOR

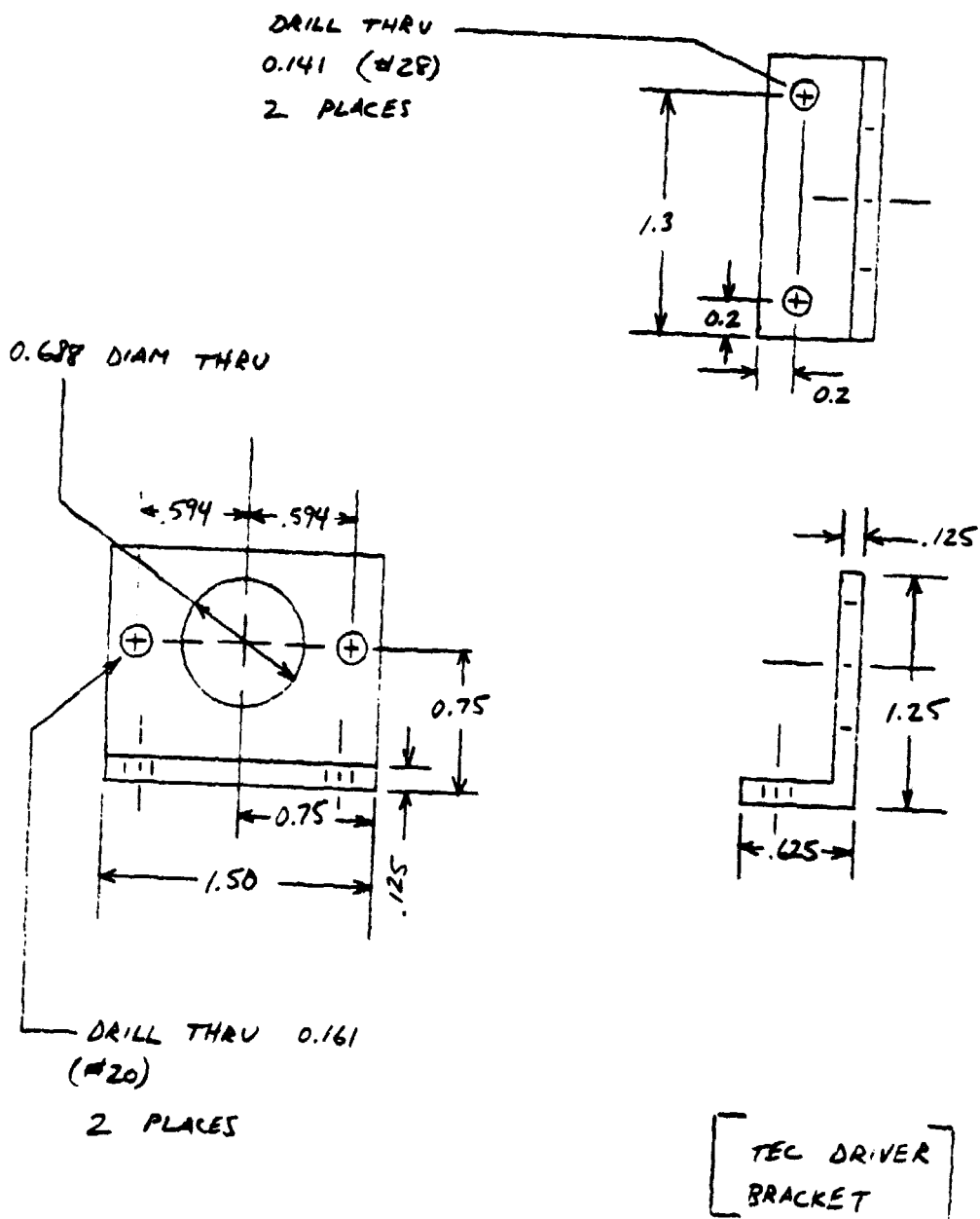
[EMITTER MODULE  
ENCLOSURE]

1. CUT BOX @ CUT LINE
2. HOLE DIMENSIONS ARE TO BE TAKEN  
AFTER CUT
3. FAR SIDE IDENTICAL TO NEAR SIDE  
8 HOLES TOTAL

ORIGINAL PAGE IS  
OF POOR QUALITY

C-2

QTY: 2  
MATERIAL:  
ALUMINUM  
SCALE: 1X

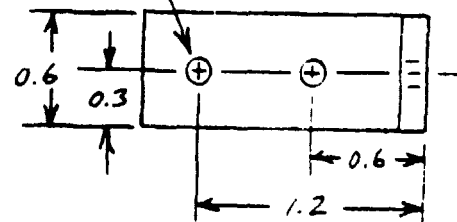


MATERIAL:  
ALUM. NUM

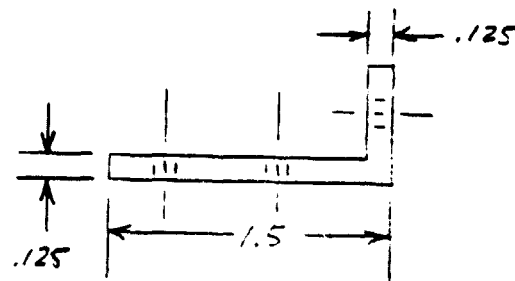
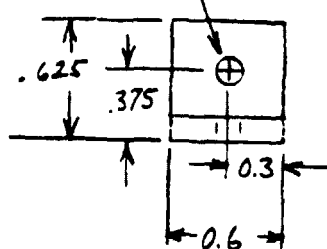
QTY: 4

SCALE: 1X

TAP THRU FOR  
6-32 THD  
2 PLACES



DRILL THRU  
0.141 (#2P)  
1 PLACE



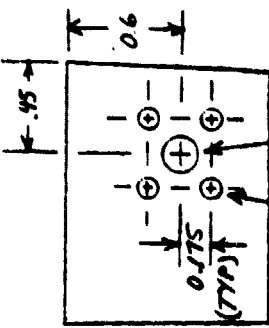
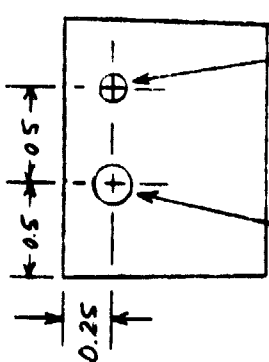
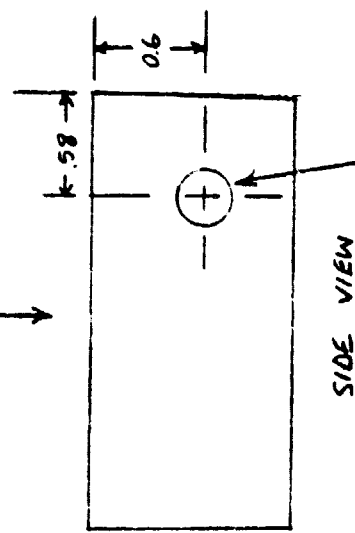
[  
EMITTER MODULE  
ANGLE BRACKETS  
]

EXTRAS PAGE  
NO FRESH QUALITY

D180-25888-1

Qty. 2  
Scale : 1x

TOP (OPEN)



II-6

TAP THRU FOR  
12-32 THD  
DRILL THRU  
0.141 (#28)

TAP THRU  
FOR 4-40 THD  
FOUR PLACES

DRILL THRU  
0.281 (#K)

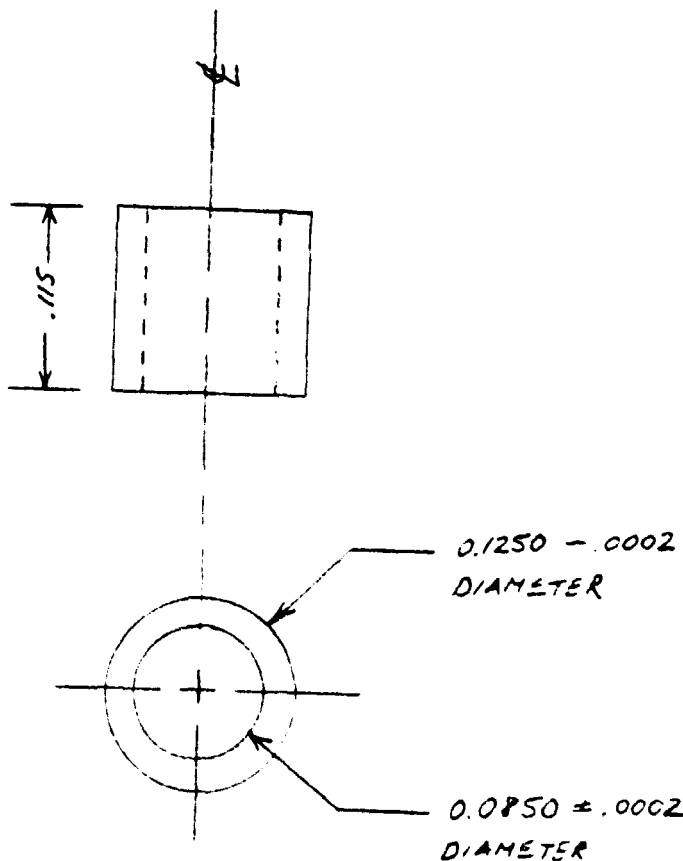
DRILL THRU  
0.180 (#15)

ALL DIMENSIONS TO BE MEASURED  
FROM OUTSIDE OF BOX.

[  
DETECTOR  
MODULE BOX  
]

MATERIAL: NYLON  
QTY: 3

DIMENSIONS IN INCHES. HOLD CONCENTRICITY  
TO BEST OF CAPABILITIES



RCA 30908E/AMPHENOL CONNECTOR  
ADAPTER BUSHING